Atlas of Model Currents and Variability in Maritime Canadian Waters

D. Brickman and A. Drozdowski

Ocean and Ecosystem Sciences Division
Maritimes Region
Fisheries and Oceans Canada

Bedford Institute of Oceanography
P.O. Box 1006
Dartmouth, Nova Scotia
Canada B2Y 4A2

2012

Canadian Technical Report of Hydrography and Ocean Sciences 277

Fisheries and Oceans Canada | Pêches et Océans Canada

Canada

Canadian Technical Report of Hydrography and Ocean Sciences

Technical reports contain scientific and technical information of a type that represents a contribution to existing knowledge but which is not normally found in the primary literature. The subject matter is generally related to programs and interests of the Oceans and Science sectors of Fisheries and Oceans Canada.

Technical reports may be cited as full publications. The correct citation appears above the abstract of each report. Each report is abstracted in the data base *Aquatic Sciences and Fisheries Abstracts*.

Technical reports are produced regionally but are numbered nationally. Requests for individual reports will be filled by the issuing establishment listed on the front cover and title page.

Regional and headquarters establishments of Ocean Science and Surveys ceased publication of their various report series as of December 1981. A complete listing of these publications and the last number issued under each title are published in the *Canadian Journal of Fisheries and Aquatic Sciences*, Volume 38: Index to Publications 1981. The current series began with Report Number 1 in January 1982.

Rapport technique canadien sur l'hydrographie et les sciences océaniques

Les rapports techniques contiennent des renseignements scientifiques et techniques qui constituent une contribution aux connaissances actuelles mais que l'on ne trouve pas normalement dans les revues scientifiques. Le sujet est généralement rattaché aux programmes et intérêts des secteurs des Océans et des Sciences de Pêches et Océans Canada.

Les rapports techniques peuvent être cités comme des publications à part entière. Le titre exact figure au-dessus du résumé de chaque rapport. Les rapports techniques sont résumés dans la base de données *Résumés des sciences aquatiques et halieutiques*.

Les rapports techniques sont produits à l'échelon régional, mais numérotés à l'échelon national. Les demandes de rapports seront satisfaites par l'établissement auteur dont le nom figure sur la couverture et la page de titre.

Les établissements de l'ancien secteur des Sciences et Levés océaniques dans les régions et à l'administration centrale ont cessé de publier leurs diverses séries de rapports en décembre 1981. Vous trouverez dans l'index des publications du volume 38 du *Journal canadien des sciences halieutiques et aquatiques*, la liste de ces publications ainsi que le dernier numéro paru dans chaque catégorie. La nouvelle série a commencé avec la publication du rapport numéro 1 en janvier 1982.

Canadian Technical Report of
Hydrography and Ocean Sciences

2012

Atlas of Model Currents and Variability in Maritime Canadian Waters

by

David Brickman
and Adam Drozdowski

david.brickman@dfo-mpo.gc.ca
adam.drozdowski@dfo-mpo.gc.ca

Ocean and Ecosystem Sciences Division
Maritimes Region
Fisheries and Oceans Canada

Bedford Institute of Oceanography
P.O. Box 1006
Dartmouth, N.S.
Canada B2Y 4A2

©Her Majesty the Queen in Right of Canada 2012
Cat. No. Fs 97-18/277E ISSN 0711-6764

Correct citation for this publication:

Brickman. D.. and A. Drozdowski 2012. Atlas of Model Currents and Variability in Maritime Canadian Waters . Can. Tech. Rep. Hydrogr. Ocean Sci. 277: vii + 64 pp.

Table of Contents

List of Figures v

1 Introduction 1

2 Model setup and simulation 1

3 Acknowledgements 2

4 References 2

List of Figures

1 Atlantic Canada region showing Maritime Canada domain. Contour colors on this and subsequent figures are: 50m = blue, 100m = magenta, 200m = brown, 1000m = red. 4

Annual Fields

2 Annual depth-averaged velocity for the entire model domain. The annual average is over the 365 daily model outputs. 6
3 Annual depth-averaged velocity in the Gulf of Maine region. 7
4 Annual depth-averaged velocity on the Scotian Shelf. 8
5 Annual depth-averaged velocity in the Cabot Strait region. 9
6 Annual depth-averaged velocity in the St. Lawrence Estuary and Gulf of St. Lawrence region. 10
7 Sea surface height (m) averaged over the 365 daily fields. The offshelf region (> 2000m) is masked for clarity. Note that on colour image plots the standard contours are p.tted in white. 11
8 Standard deviation (m) of SSH derived from the 365 daily fields. Note that the std is due to the effects of surface forcing, not tides. 12

Seasonal Fields – depth-averaged

9 Winter depth-averaged velocity. 14
10 Spring depth-averaged velocity. 15
11 Summer depth-averaged velocity. 16
12 Fall depth-averaged velocity. 17
13 Winter perturbation log(kinetic energy (cm^2/s^2)) for the depth-averaged velocity. 18
14 Spring perturbation log(kinetic energy (cm^2/s^2)) for the depth-averaged velocity. 19
15 Summer perturbation log(kinetic energy (cm^2/s^2)) for the depth-averaged velocity. 20
16 Fall perturbation log(kinetic energy (cm^2/s^2)) for the depth-averaged velocity. 21
17 Winter major axes of variation (cm^2/s^2, top) and log{(energy in major axis) / (energy in minor axis)} (btm), for the depth-averaged velocity. . . 22
18 Spring major axes of variation (cm^2/s^2, top) and log{(energy in major axis) / (energy in minor axis)} (btm), for the depth-averaged velocity. . . 23
19 Summer major axes of variation (cm^2/s^2, top) and log{(energy in major axis) / (energy in minor axis)} (btm), for the depth-averaged velocity. . . 24
20 Fall major axes of variation (cm^2/s^2, top) and log{(energy in major axis) / (energy in minor axis)} (btm), for the depth-averaged velocity. 25

Seasonal Fields – surface layer

21 Winter surface layer velocity. 27
22 Spring surface layer velocity. 28
23 Summer surface layer velocity. 29
24 Fall surface layer velocity. 30
25 Winter perturbation log(kinetic energy (cm^2/s^2)) for the surface layer velocity. 31
26 Spring perturbation log(kinetic energy (cm^2/s^2)) for the surface layer velocity. 32
27 Summer perturbation log(kinetic energy (cm^2/s^2)) for the surface layer velocity. 33
28 Fall perturbation log(kinetic energy (cm^2/s^2)) for the surface layer velocity. 34
29 Winter major axes of variation (cm^2/s^2, top) and log{(energy in major axis) / (energy in minor axis)} (btm), for the surface layer velocity. . . . 35
30 Spring major axes of variation (cm^2/s^2, top) and log{(energy in major axis) / (energy in minor axis)} (btm), for the surface layer velocity. . . . 36
31 Summer major axes of variation (cm^2/s^2, top) and log{(energy in major axis) / (energy in minor axis)} (btm), for the surface layer velocity. . . . 37
32 Fall major axes of variation (cm^2/s^2, top) and log{(energy in major axis) / (energy in minor axis)} (btm), for the surface layer velocity. 38

Seasonal Fields – middle layer

33 Winter mid-layer velocity. 40
34 Spring mid-layer velocity. 41
35 Summer mid-layer velocity. 42
36 Fall mid-layer velocity. 43
37 Winter perturbation log(kinetic energy (cm^2/s^2)) for the mid-layer velocity. 44
38 Spring perturbation log(kinetic energy (cm^2/s^2)) for the mid-layer velocity. 45
39 Summer perturbation log(kinetic energy (cm^2/s^2)) for the mid-layer velocity. 46
40 Fall perturbation log(kinetic energy (cm^2/s^2)) for the mid-layer velocity. . 47
41 Winter major axes of variation (cm^2/s^2, top) and log{(energy in major axis) / (energy in minor axis)} (btm), for the mid-layer layer velocity. . . 48
42 Spring major axes of variation (cm^2/s^2, top) and log{(energy in major axis) / (energy in minor axis)} (btm), for the mid-layer layer velocity. . . 49
43 Summer major axes of variation (cm^2/s^2, top) and log{(energy in major axis) / (energy in minor axis)} (btm), for the mid-layer layer velocity. . . 50
44 Fall major axes of variation (cm^2/s^2, top) and log{(energy in major axis) / (energy in minor axis)} (btm), for the mid-layer layer velocity. 51

45 Winter bottom layer velocity. 53
46 Spring bottom layer velocity. 54
47 Summer bottom layer velocity. 55
48 Fall bottom layer velocity. 56
49 Winter perturbation log(kinetic energy (cm^2/s^2)) for the bottom layer velocity. 57
50 Spring perturbation log(kinetic energy (cm^2/s^2)) for the bottom layer velocity. 58
51 Summer perturbation log(kinetic energy (cm^2/s^2)) for the bottom layer velocity. 59
52 Fall perturbation log(kinetic energy (cm^2/s^2)) for the bottom layer velocity. 60
53 Winter major axes of variation (cm^2/s^2, top) and log{(energy in major axis) / (energy in minor axis)} (btm), for the bottom layer velocity. . . . 61
54 Spring major axes of variation (cm^2/s^2, top) and log{(energy in major axis) / (energy in minor axis)} (btm), for the bottom layer velocity. . . . 62
55 Summer major axes of variation (cm^2/s^2, top) and log{(energy in major axis) / (energy in minor axis)} (btm), for the bottom layer velocity. . . . 63
56 Fall major axes of variation (cm^2/s^2, top) and log{(energy in major axis) / (energy in minor axis)} (btm), for the bottom layer velocity. 64

Abstract

Brickman, D., and A. Drozdowski 2012. Atlas of Model Currents and Variability in Maritime Canadian Waters Can. Tech. Rep. Hydrogr. Ocean Sci. 277: vii + 64 pp.

An atlas of currents and current variability for the Gulf of St. Lawrence, Scotian Shelf and Gulf of Maine, is derived from output of the CANOPA numerical circulation model. The model is forced by a 365 day "cyclical year" dataset designed to represent the climatological atmospheric forcing with its climatological variability. Model output is 365 daily-averaged fields which are analyzed to produce annual and seasonal circulations plus metrics of variability on these timescales. Plots include: the annual mean sea surface height and its standard deviation; annual and seasonal mean horizontal velocity fields for 4 representative velocities – depth-averaged, surface (0-20m average), mid-depth (20-50m average), and bottom (averaged over the bottom 2 layers of the water column); seasonal major and minor axes of velocity variation; and seasonal spatial patterns of perturbation kinetic energy. The spatial maps created for this atlas are designed to provide qualitative/quantitative details of the circulation of relevance to the numerous clients interested in processes in the regional shelf seas of Maritime Canada.

Résumé

Brickman, D., et A. Drozdowski, 2012. Atlas des courants et de la variabilité du modèle dans les eaux Canadiennes de la région des Maritimes. Rapp. tech. can. hydrogr. sci. océan. 277 :vii + 64 p.

L'atlas portant sur les courants et la variabilité actuelle du golfe du Saint-Laurent, du plateau néo-écossais et du golfe du Maine découle de la rétroaction reçue au sujet du modèle numérique de la circulation CANOPA. Le modèle est forcé par un ensemble de données d'une ≪année cyclique≫ de 365 jours conçu pour représenter le forçage atmosphérique météorologique et la variabilité météorologique correspondante. Le résultat découlant du modèle correspond à 365 secteurs en moyenne au quotidien, qui sont analysés de sorte à produire des circulations saisonnière et annuelle et des paramètres de variabilité dans les délais établis. Parmi les secteurs, on retrouve : la hauteur moyenne annuelle de la surface de la mer et son écart-type, les secteurs de vitesse horizontale moyenne saisonnière pour quatre vitesses représentatives (moyenne de profondeur, surface [moyenne de 0 à 20 mètres], mi- profondeur [moyenne de 20 à 50 mètres] et fond [moyenne des deux dernières couches de la colonne d'eau]), les axes principaux et secondaires saisonniers de la variation de la vitesse et les tendances spatiales saisonnières de l'énergie cinétique turbulente. Les cartes spatiales créées dans le cadre de cet atlas sont conçues pour fournir des détails quantitatifs et qualitatifs au sujet de la circulation pertinente aux nombreux clients démontrant un intérêt envers les processus liés aux plateaux régionaux de la mer du Canada atlantique.

1 Introduction

This report is an atlas of currents and current variability for the Gulf of St. Lawrence, Scotian Shelf and Gulf of Maine, derived from the CANOPA numerical circulation model. The model is forced by the Common Ocean-ice Reference Experiments (CORE) normal year (NY) atmospheric forcing dataset (Large and Yeager, 2004) – a 365 day "cyclical year" dataset designed to represent the climatological atmospheric forcing with its climatological variability. Model output is 365 daily-averaged fields which are analyzed to produce annual and seasonal circulations plus metrics of variability on these timescales. For more details on the CANOPA circulation model see the companion report: *Development and Validation of a Regional Shelf Model for Maritime Canada based on the NEMO-OPA Circulation Model* (Brickman and Drozdowski, 2012).

The motivation for this atlas is to provide qualitative/quantitative details of the circulation of relevance to the numerous clients interested in processes in the regional shelf seas of Maritime Canada. For example, an MPA planner may want to know if their area of interest has any special circulation features or whether open ocean vessel ballast water exchange could affect an existing MPA, or a fisheries scientist may need an estimate of the bottom velocity at a particular location and its variability. The spatial maps created for this atlas are designed to provide first order "at-a-glance" answers to questions such as the above.

2 Model setup and simulation

This section provides an overview of CANOPA modeling system. For more details of the model setup and validation the reader is directed to Brickman and Drozdowski (2012).

The Nucleus for European Modelling of the Ocean – Ocean Parallisé (NEMO-OPA) ocean model is a 3D, non-linear, hydrostatic, C-grid, primitive equation numerical ocean model written in parallelized fortran 90 (Madec, 2008). The CANOPA circulation model is a version of the NEMO-OPA model adapted (originally) for use on the shelf regions of Maritime Canada (Gulf of St. Lawrence, Scotian Shelf and Gulf of Maine, figure 1). The CANOPA model includes a coupled sea ice model and the ability to run a full suite of tidal constituents.

The horizontal grid resolution for the Maritime Canada ("MC") domain is $1/12 \times 1/12$ degrees which translates into (nominally) 6km grid cells (~5-7km range). The run reported herein used surface forcing derived from the CORE-NY dataset. Atmospheric wind velocity, surface temperature, precipitation (rain and snow), specific humidity and cloud coverage were rendered onto a daily timebase and spatially interpolated onto the MC grid. Monthly climatological temperature and salinity fields, derived from the BIO climate database, are used for initialization and open boundary fields. Velocities on the open boundaries are calculated using the thermal wind relation, with the barotropic

transport adjusted at the Strait of Belle Isle and the Newfoundland shelfbreak in order to improve model-data transport comparisons in the interior of the domain. Open boundary tidal forcing included the M2 constituent only, as this is the major component in this region. A major addition to the CANOPA model is a river module that accounts for the freshwater inputs that are important in the shelf environment. This run includes climatological monthly freshwater fluxes from 78 rivers in Maritime Canadian waters.

An interior restoring timescale of 900 days is used to allow the model to respond freely to the cyclical surface and open boundary forcing. The model is run for 6 years in order to allow it to equilibrate to the applied forcing. The equilibration is measured by the repeatability of the domain-averaged seasonal cycle of temperature and salinity. Results reported herein are daily averages from year 6 of the model run, averaged over the last M2 tidal period of each day.

Historically, climatologies are computed as single realizations of model output based on *averaged* forcing. The 365 daily-averaged model outputs allow computation of mean fields averaged over a set of time-dependent realizations, arguably a more stringent test of model performance. An added benefit of using a cyclical climatology of forcing is that one can compute deviations from the mean (and statistics thereof).

In this document we present annual and seasonal mean horizontal velocity fields for 4 representative velocities: depth-averaged, surface (0-20m average), mid-depth (20-50m average), and bottom (averaged over the bottom 2 layers of the water column). Major and minor axes of velocity variation are computed for the seasonal fields, as well as seasonal spatial patterns of perturbation kinetic energy (KE). The latter is defined for each grid cell as

$$KE = < \{(U')^2 + (V')^2\} >$$

where $U' = U(day) - U(seas)$ etc., and $< \ldots >$ denotes average over a season.

The layout of the document is the following: To get a sense of the mean circulation, figures 2-6 show the annual average depth-averaged velocity fields for the entire domain, plus zooms of various subregions. Figures 7 and 8 show the annual mean sea surface height (SSH) and its standard deviation (std). Because the tides are removed from the signal, the std represents the expected variation in SSH due to wind and buoyancy forcing.

The rest of the document presents the seasonal fields for each of the 4 representative velocities. Each velocity section contains the velocity for the four seasons, the perturbation KE for the four seasons, and major and minor axes of variation. Because the axes of variation are perpendicular to each other, the minor axes are plotted as the ratio of the energy in the major axis divided by the energy in the minor axis. For many plots the offshelf part of the fields have been masked-out as this not-relevant region of the domain often dominated the figure. Note that the plot scales for the surface fields may be different from the other levels, in order to more clearly present the information.

3 Acknowledgements

The authors would like to thank Dr. Z. Wang (BIO) and B. deTracey (BIO) for their reviews of this document. The DFO Aquatic Invasive Species program and the DFO Centre for Ocean Model Development for Applications (COMDA) provided support for model development.

4 References

Brickman, D. and A. Drozdowski, 2012. Development and Validation of a Regional Shelf Model for Maritime Canada based on the NEMO-OPA Circulation Model. Can. Tech. Rep. Hydrogr. Ocean Sci. 278: vii + 57 pp.

Large, W. and S. Yeager. 2004. Diurnal to decadal global forcing for ocean and sea-ice models: the data sets and flux climatologies. CGD Division of the National Center for Atmospheric Research, NCAR Technical Note: NCAR/TN-460+STR.

Madec G. 2008. "NEMO ocean engine". Note du Pole de modlisation, Institut Pierre-Simon Laplace (IPSL), France, No 27 ISSN No 1288-1619.

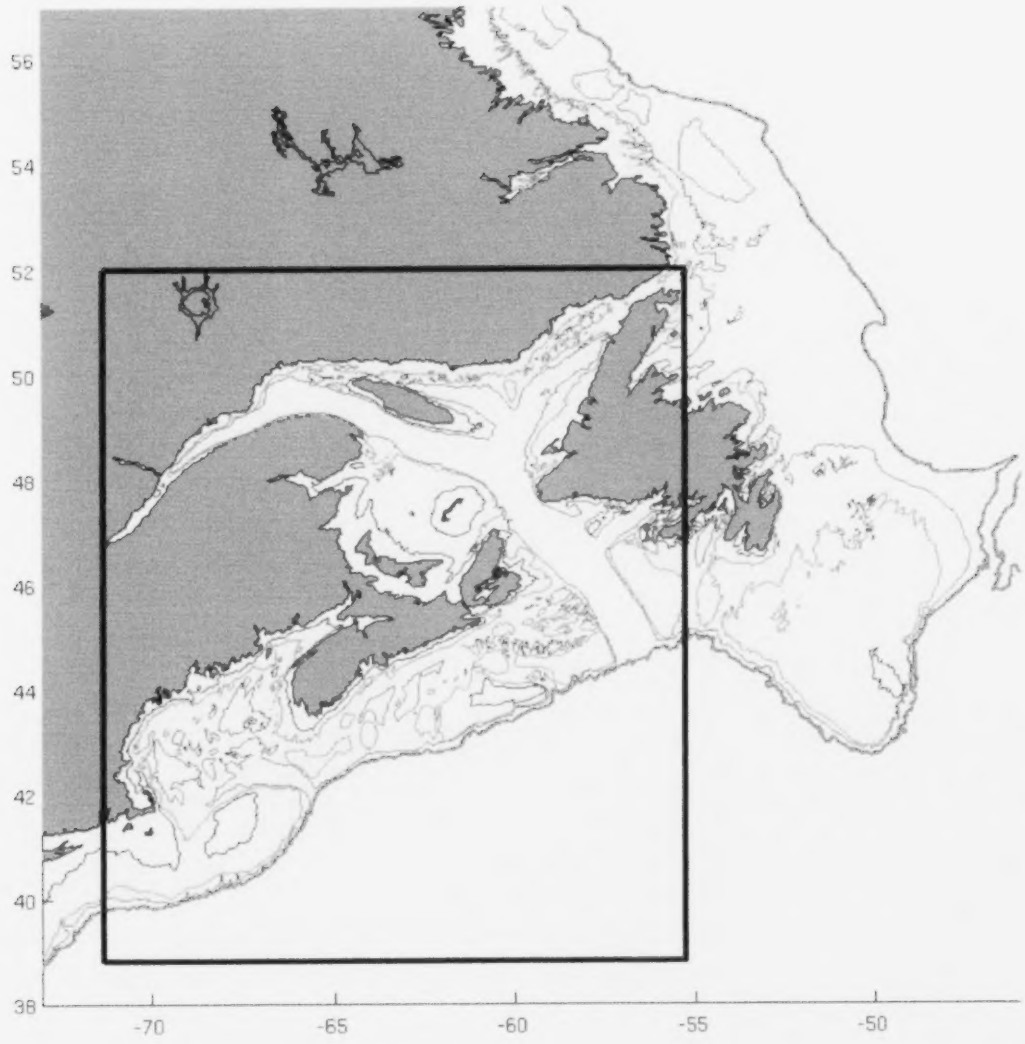

Figure 1: Atlantic Canada region showing Maritime Canada domain. Contour colors on this and subsequent figures are: 50m = blue, 100m = magenta, 200m = brown, 1000m = red.

ANNUALLY AVERAGED FIELDS

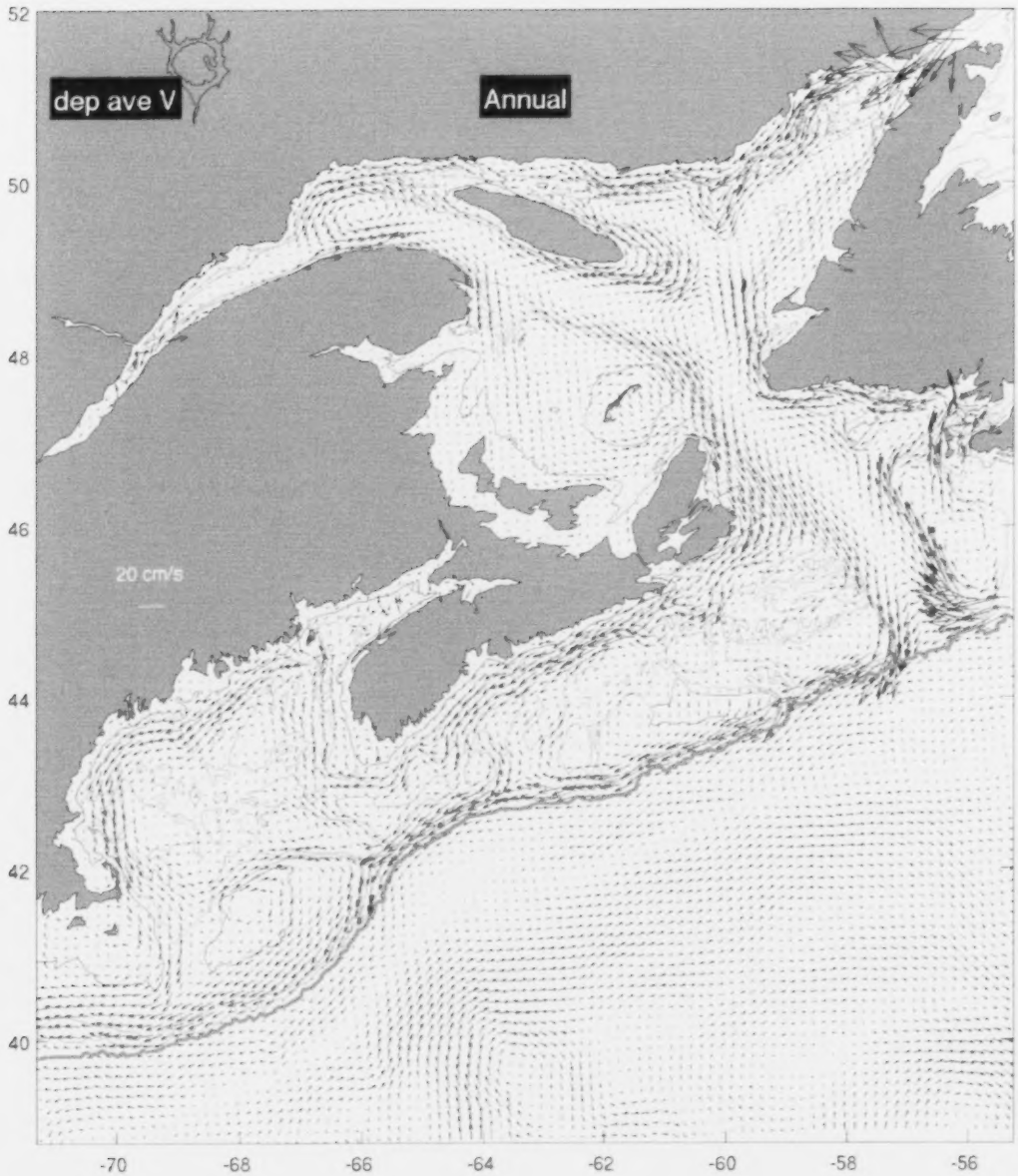

Figure 2: Annual depth-averaged velocity for the entire model domain. The annual average is over the 365 daily model outputs.

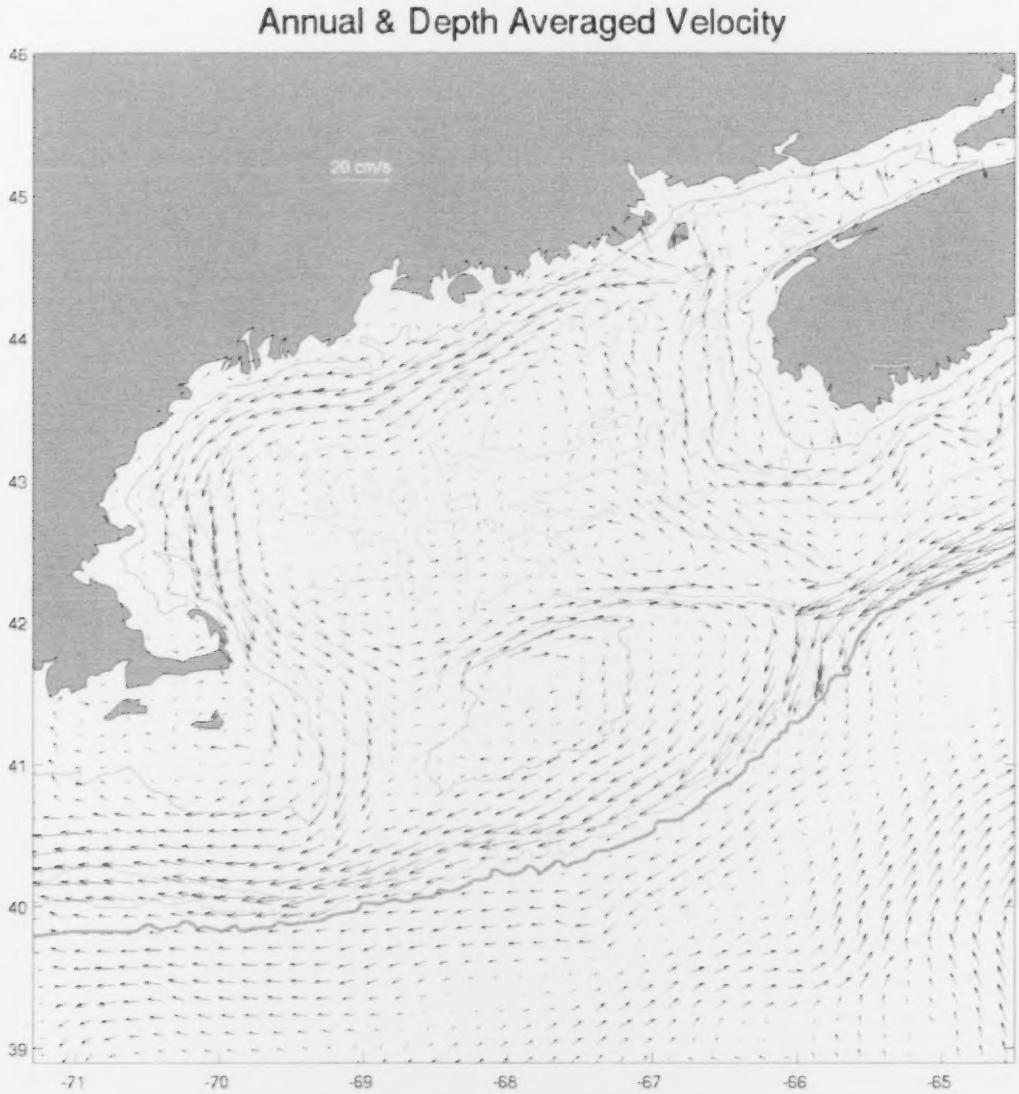

Figure 3: Annual depth-averaged velocity in the Gulf of Maine region.

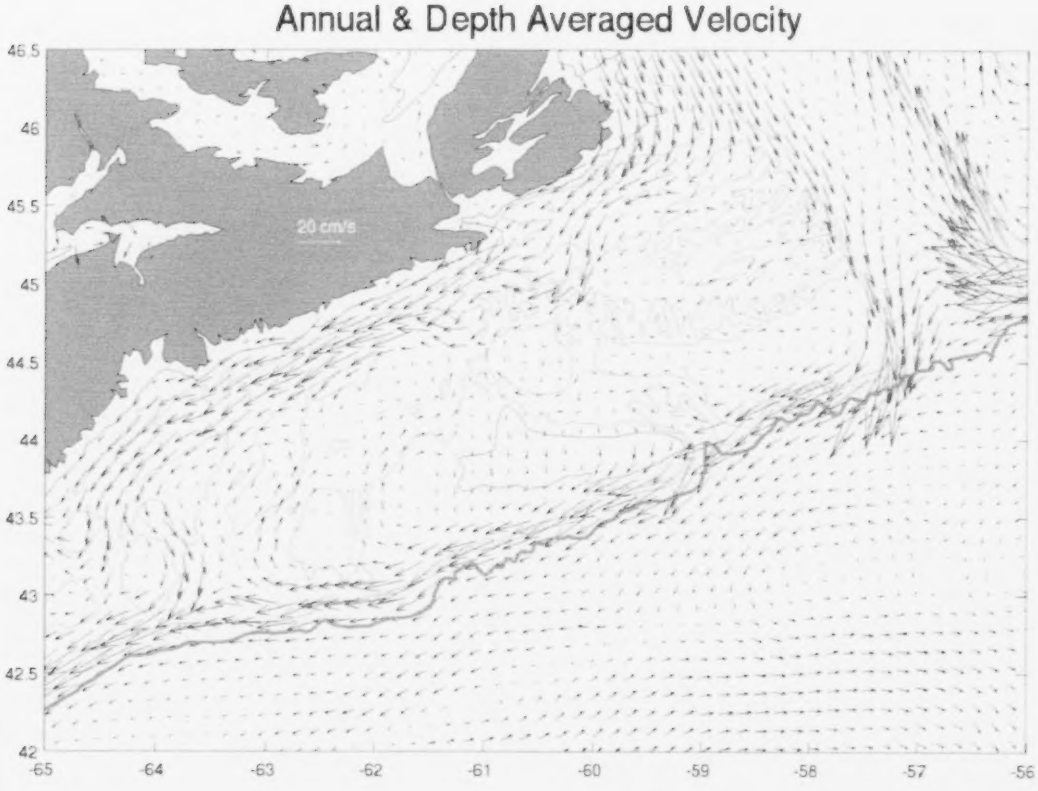

Figure 4: Annual depth-averaged velocity on the Scotian Shelf.

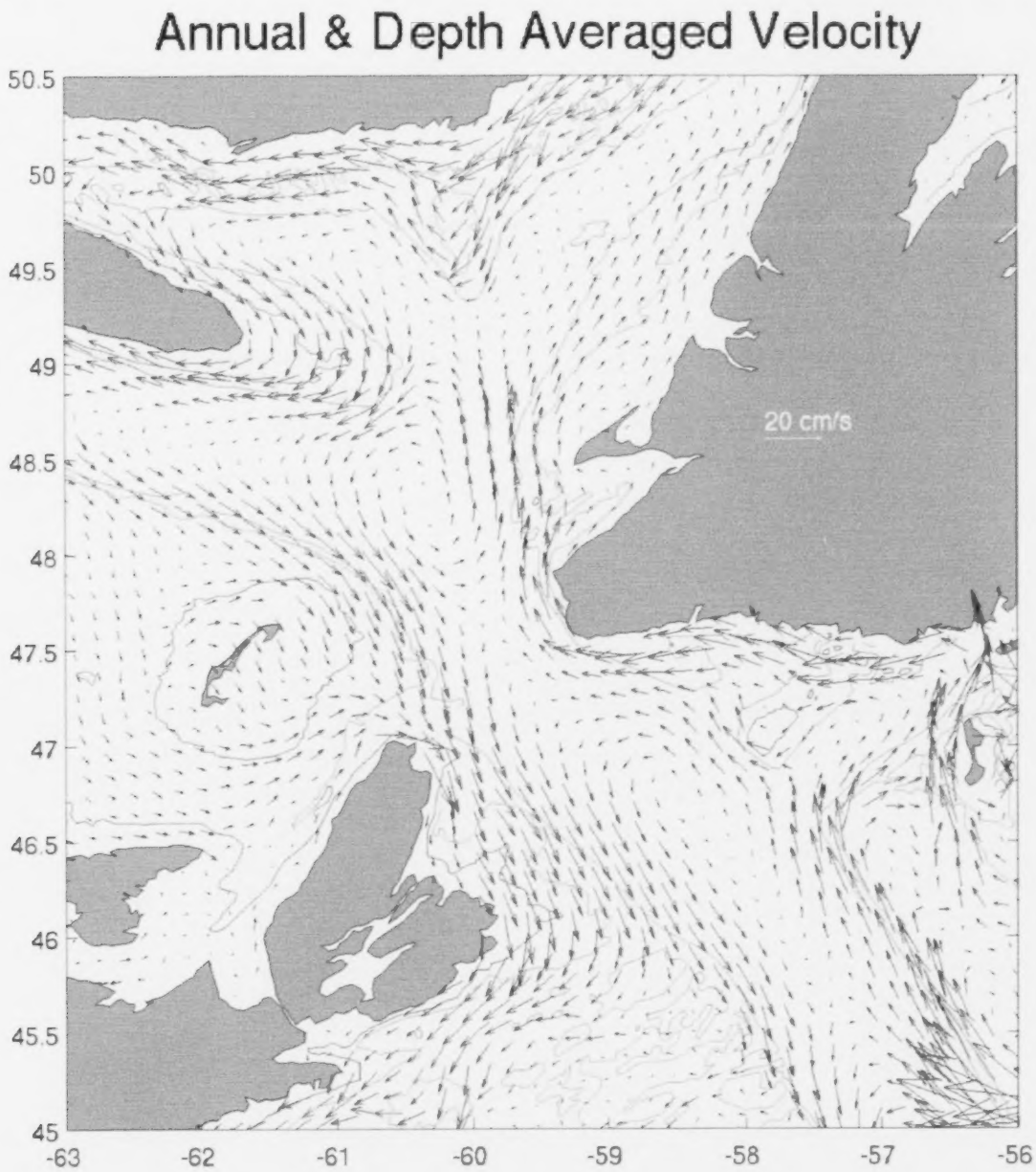

Figure 5: Annual depth-averaged velocity in the Cabot Strait region.

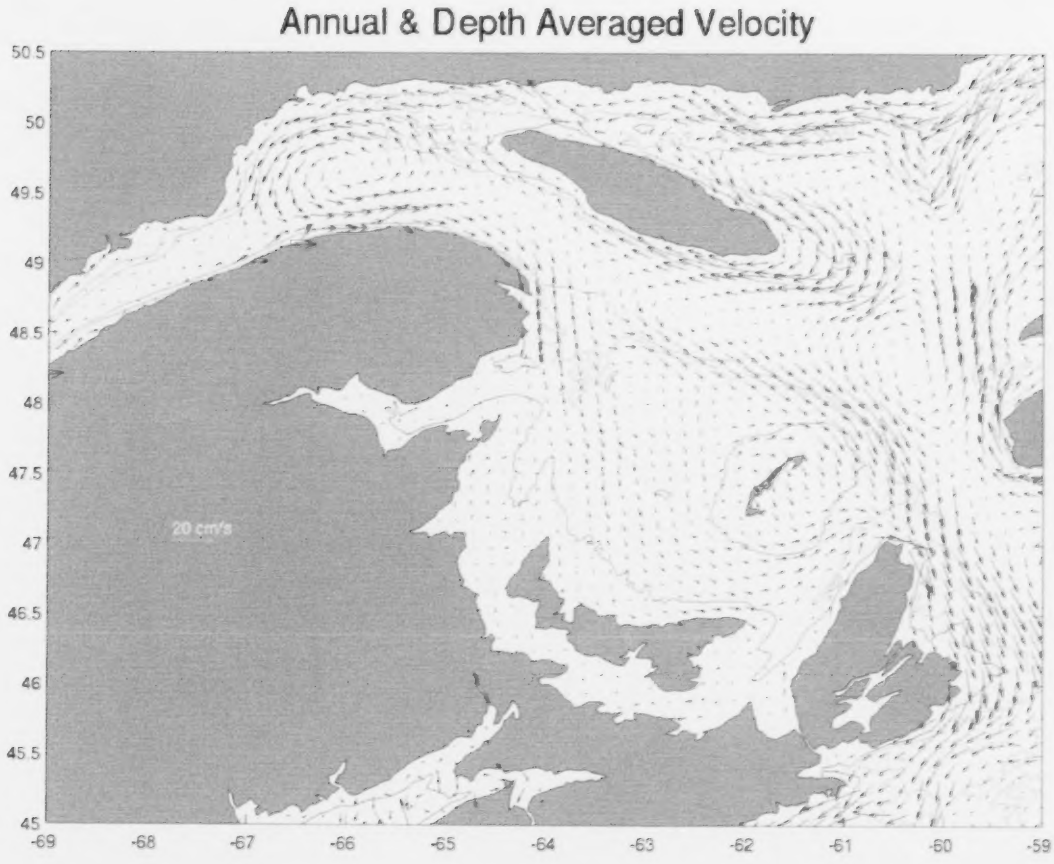

Figure 6: Annual depth-averaged velocity in the St. Lawrence Estuary and Gulf of St. Lawrence region.

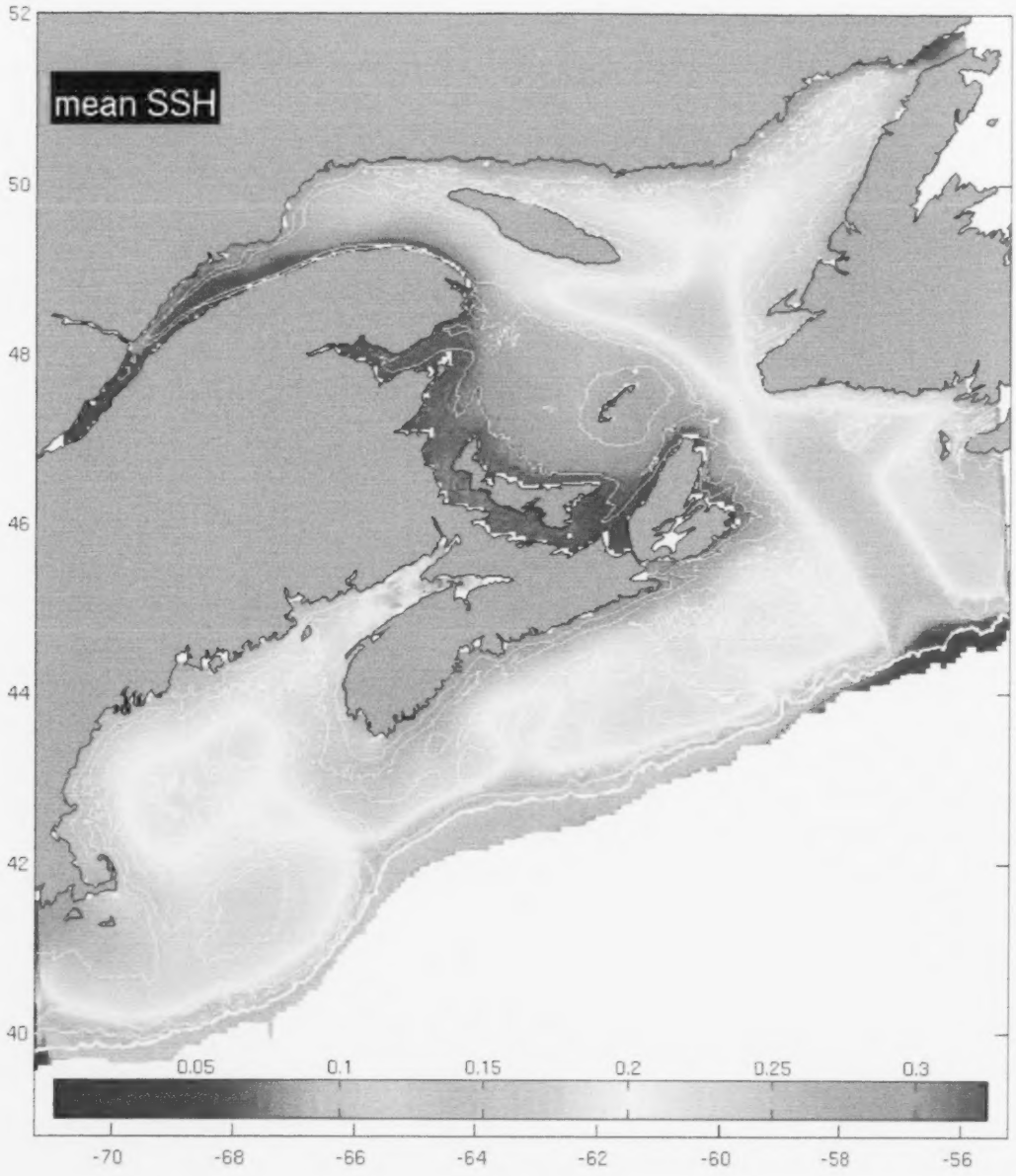

Figure 7: Sea surface height (m) averaged over the 365 daily fields. The offshelf region (> 2000m) is masked for clarity. Note that on colour image plots the standard contours are plotted in white.

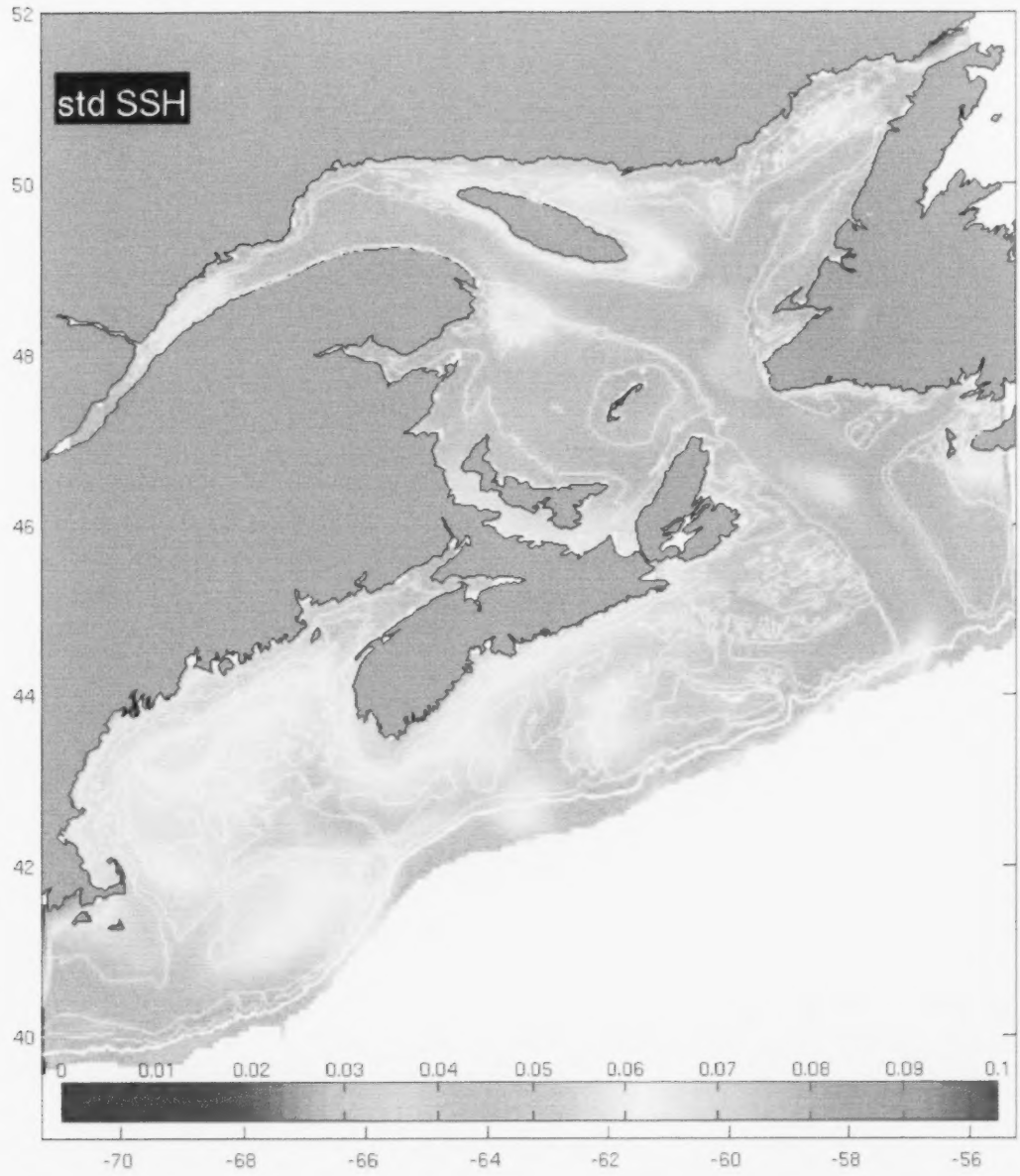

Figure 8: Standard deviation (m) of SSH derived from the 365 daily fields. Note that the std is due to the effects of surface forcing, not tides.

SEASONALLY AVERAGED FIELDS

Depth-Averaged

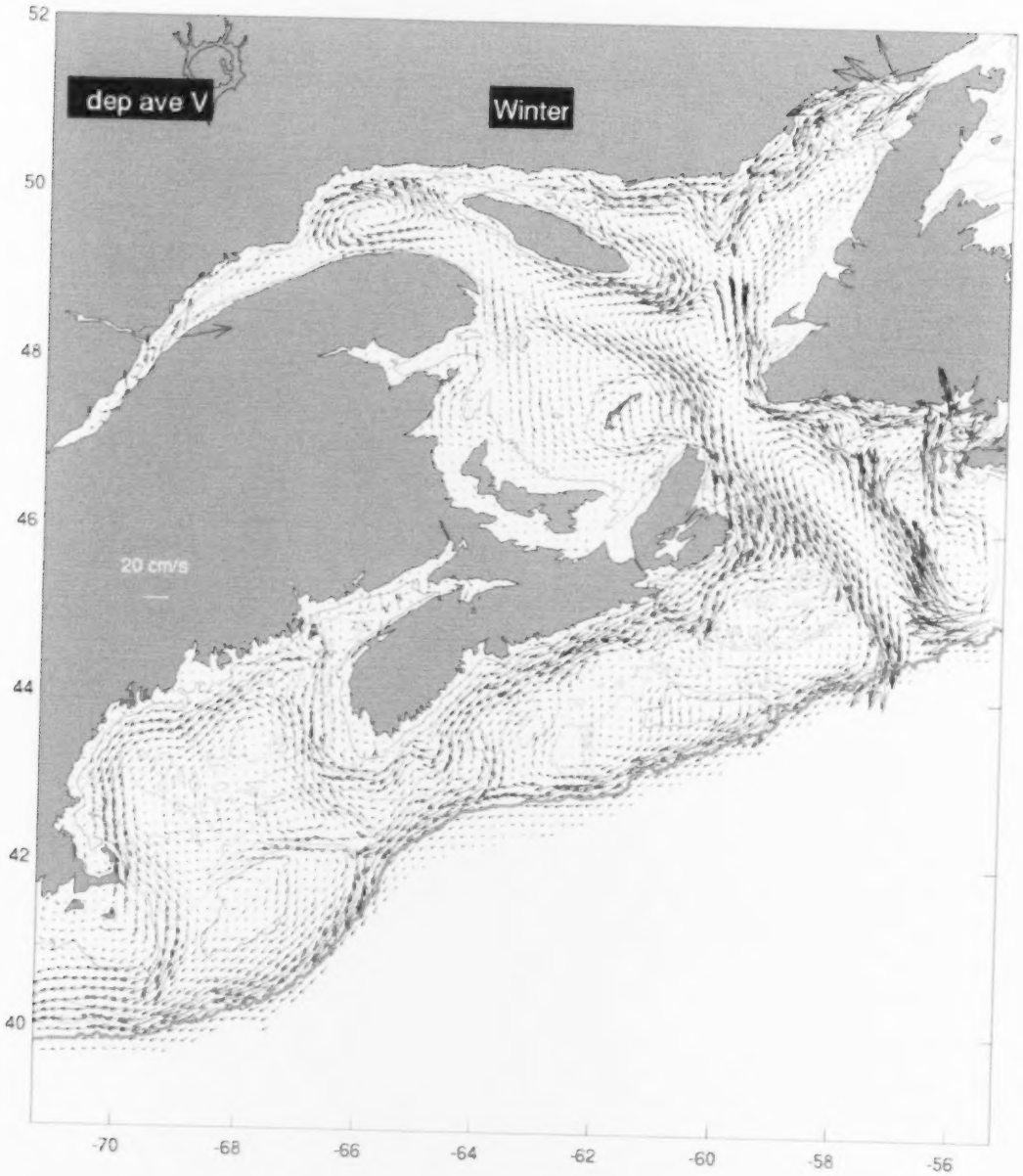

Figure 9: Winter depth-averaged velocity.

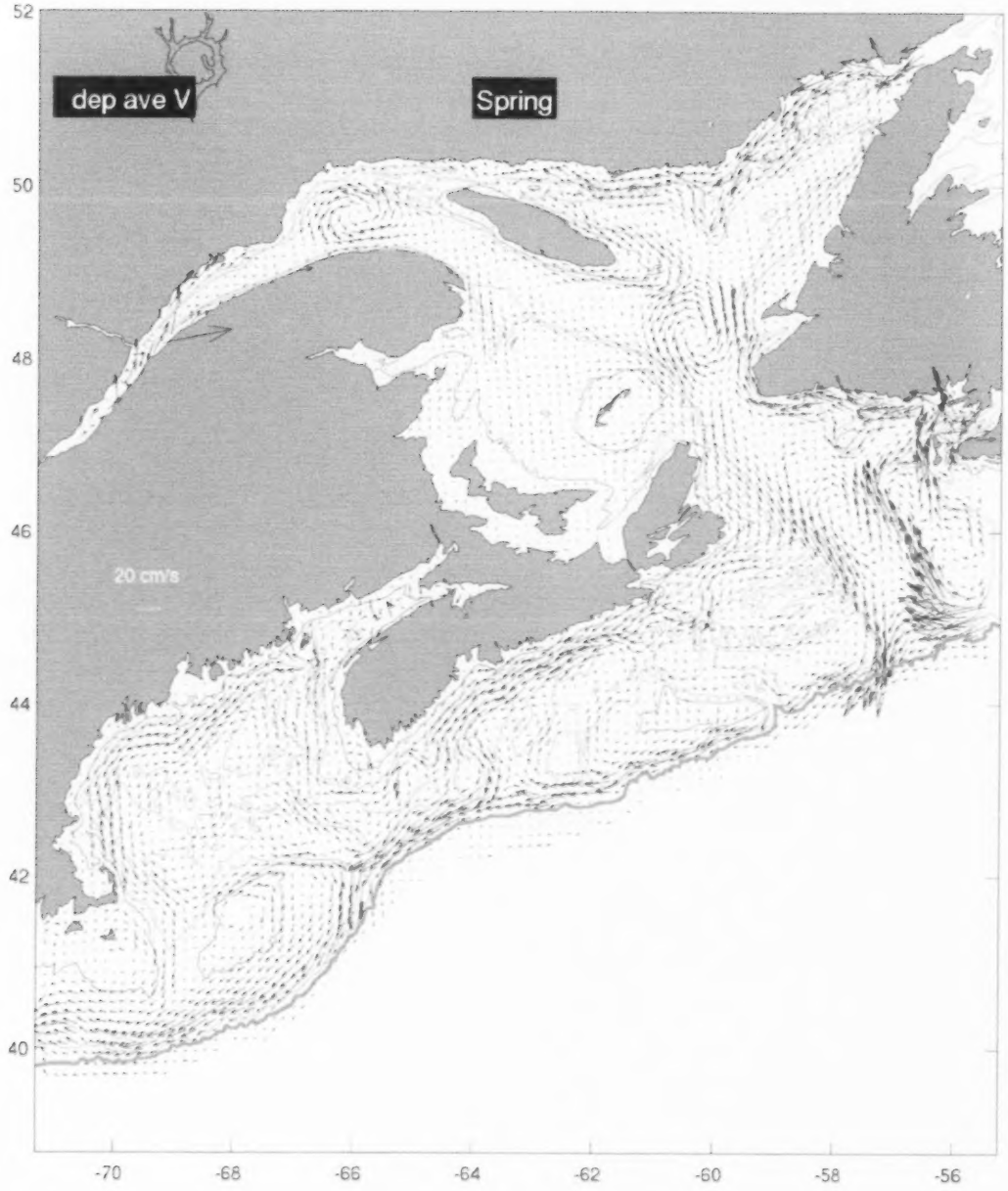

Figure 10: Spring depth-averaged velocity.

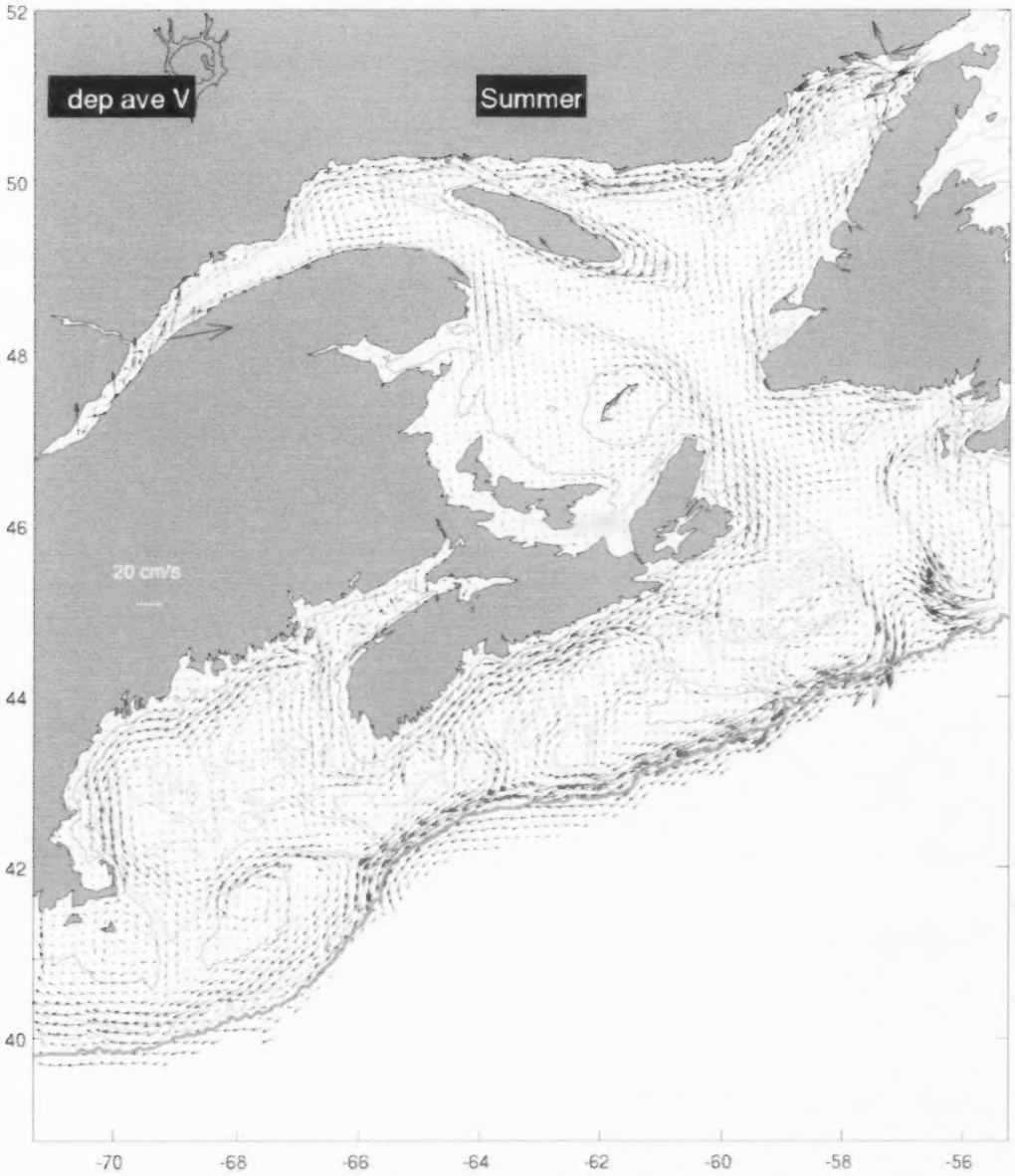

Figure 11: Summer depth-averaged velocity.

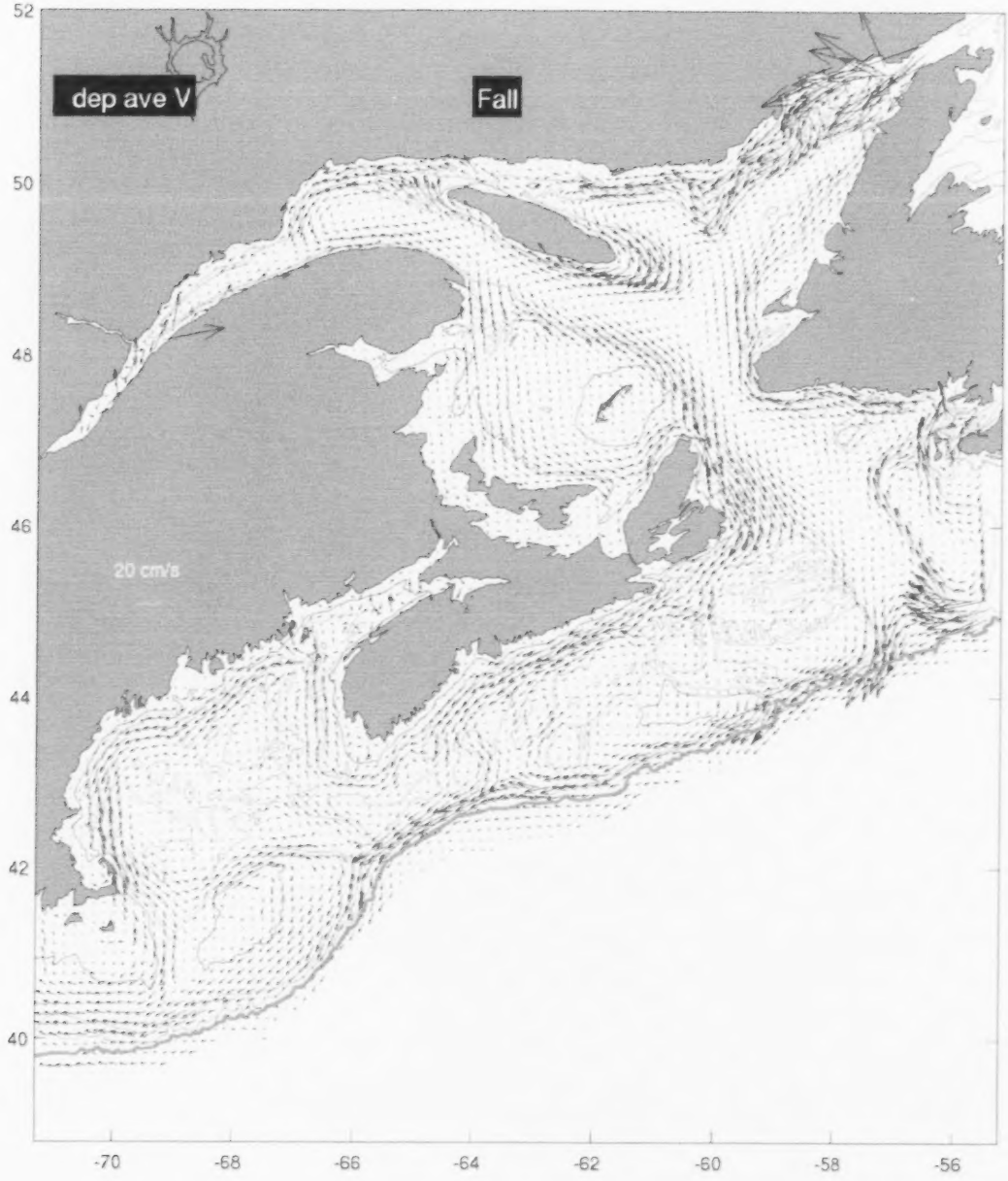

Figure 12: Fall depth-averaged velocity.

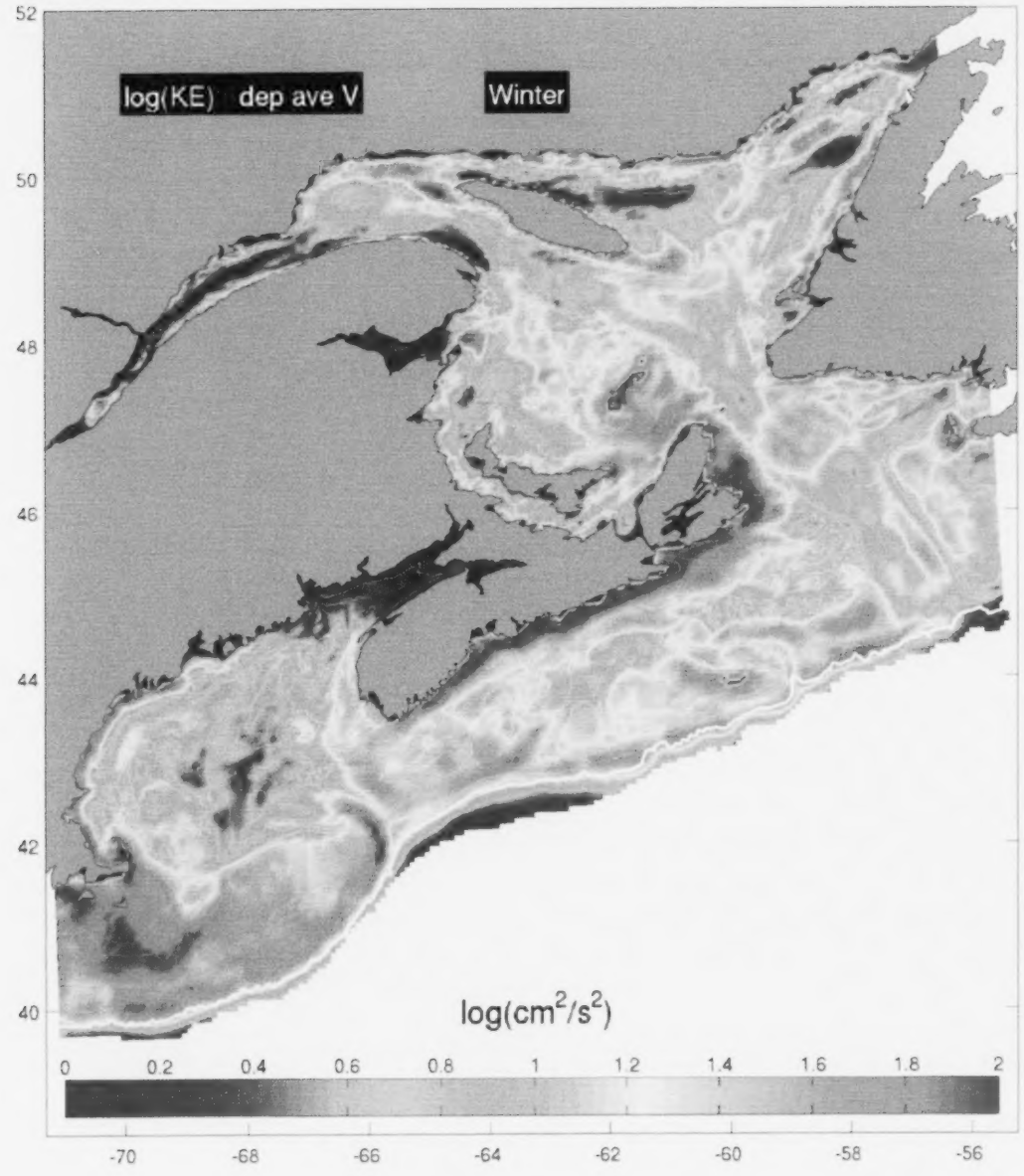

Figure 13: Winter perturbation log(kinetic energy (cm^2/s^2)) for the depth-averaged velocity.

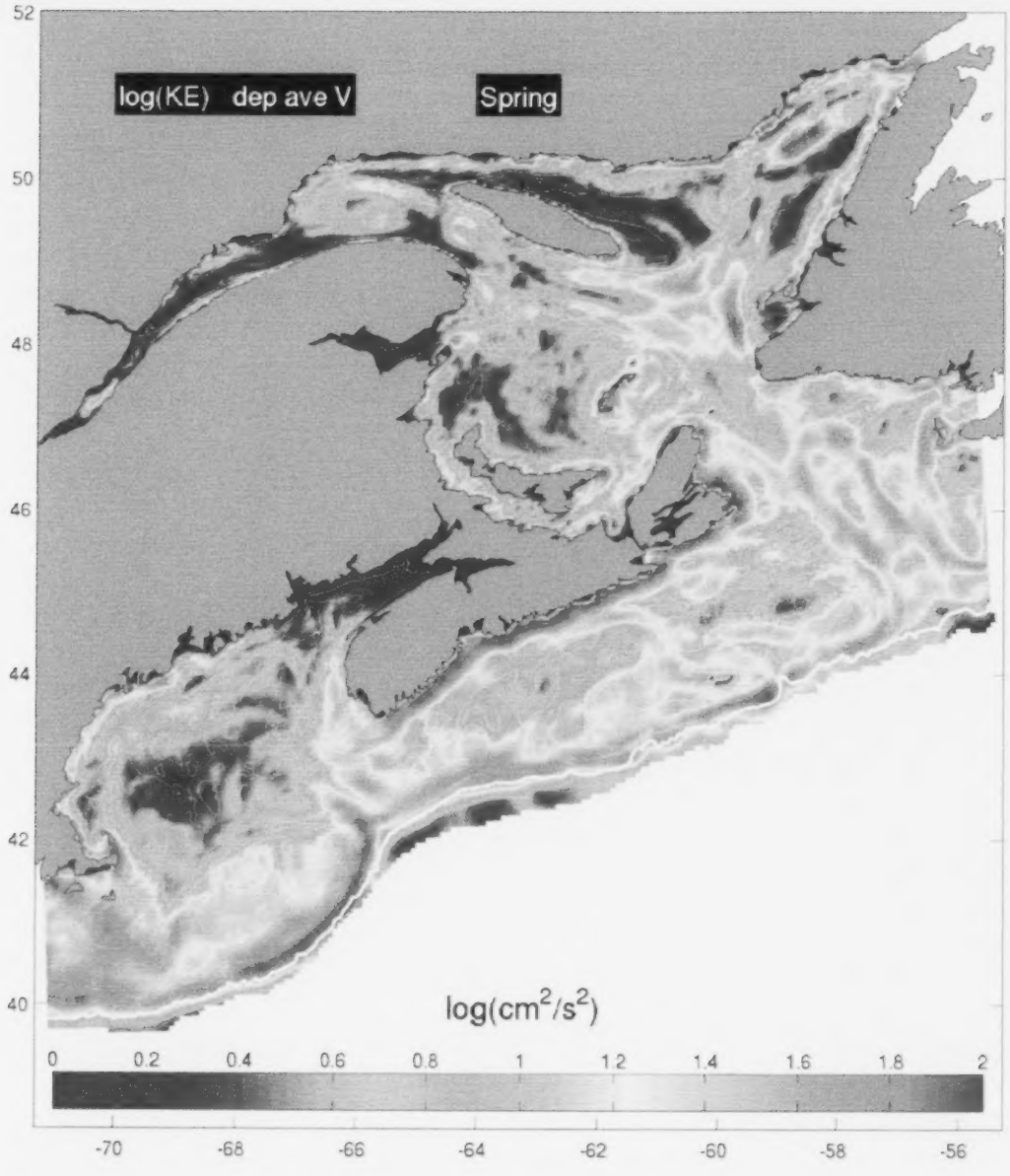

Figure 14: Spring perturbation log(kinetic energy (cm^2/s^2)) for the depth-averaged velocity.

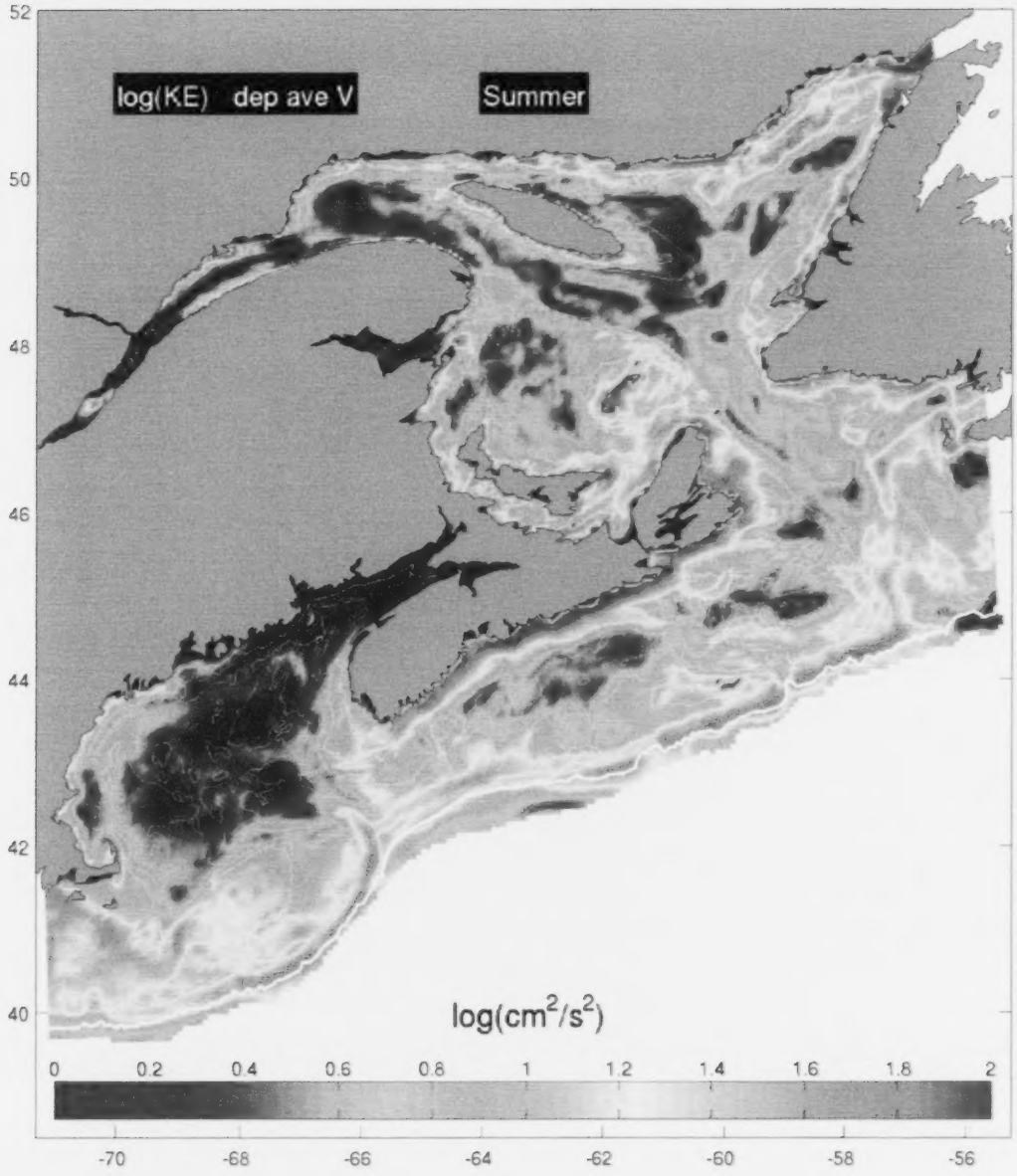

Figure 15: Summer perturbation log(kinetic energy (cm^2/s^2)) for the depth-averaged velocity.

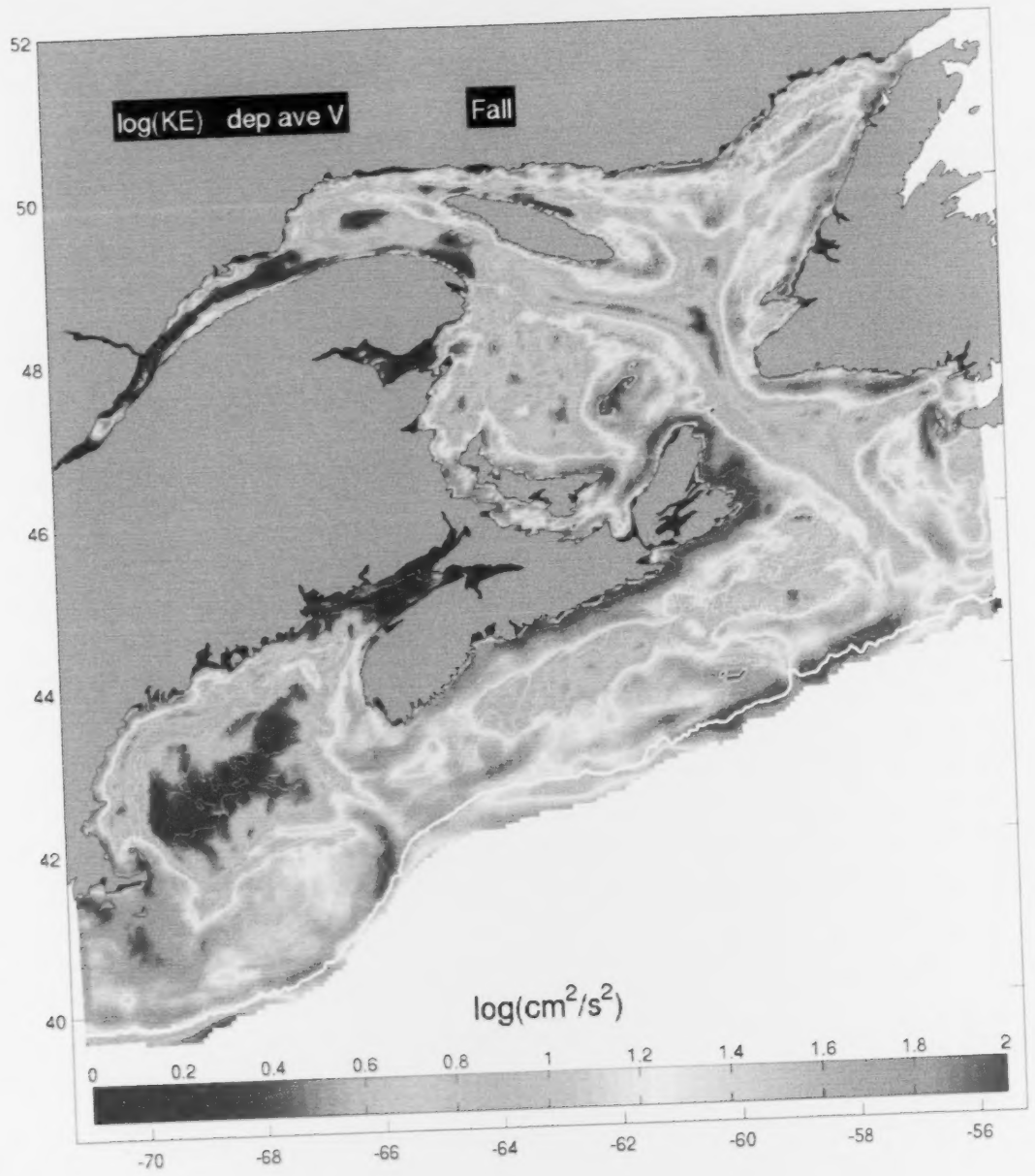

Figure 16: Fall perturbation log(kinetic energy (cm^2/s^2)) for the depth-averaged velocity.

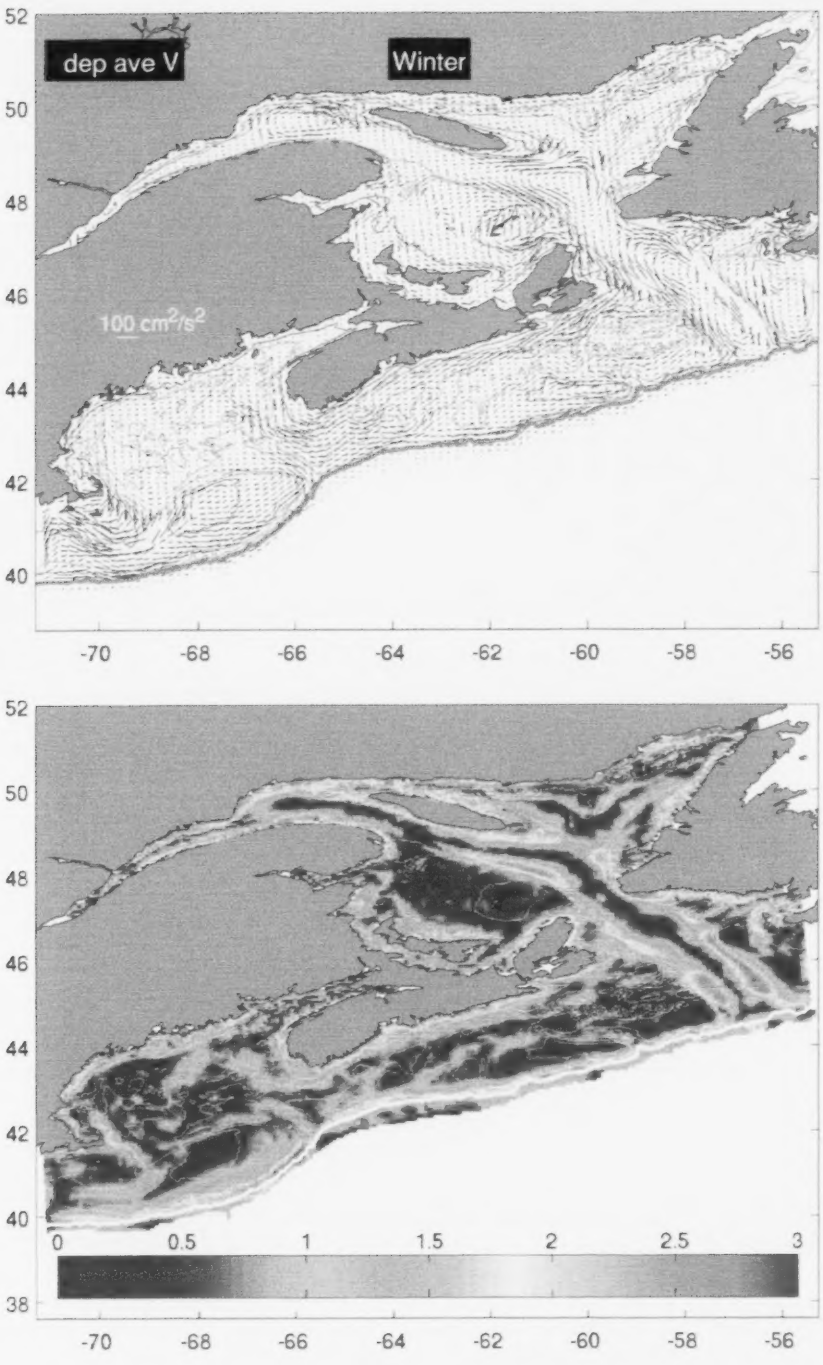

Figure 17: Winter major axes of variation (cm^2/s^2, top) and log{(energy in major axis) / (energy in minor axis)} (btm), for the depth-averaged velocity.

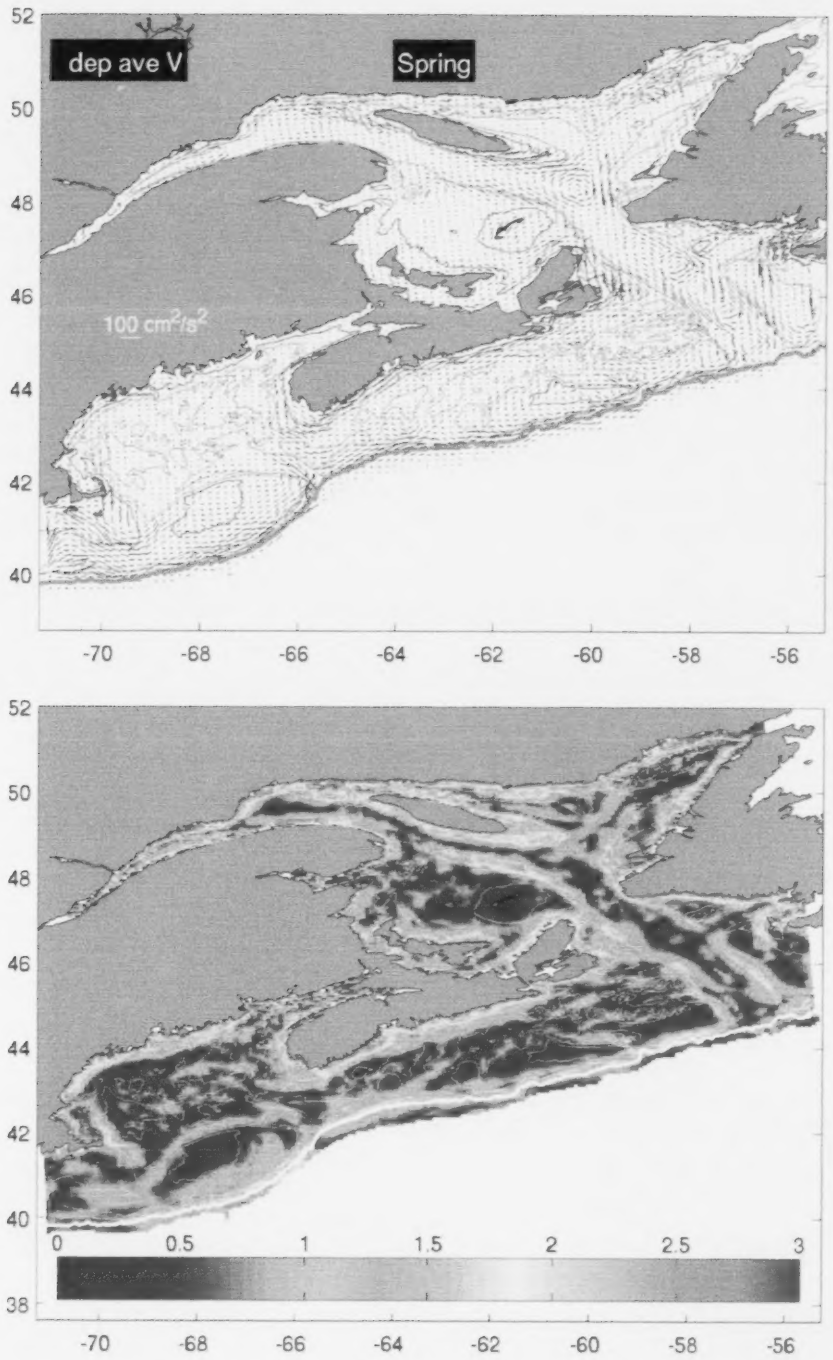

Figure 18: Spring major axes of variation (cm^2/s^2, top) and log{(energy in major axis) / (energy in minor axis)} (btm), for the depth-averaged velocity.

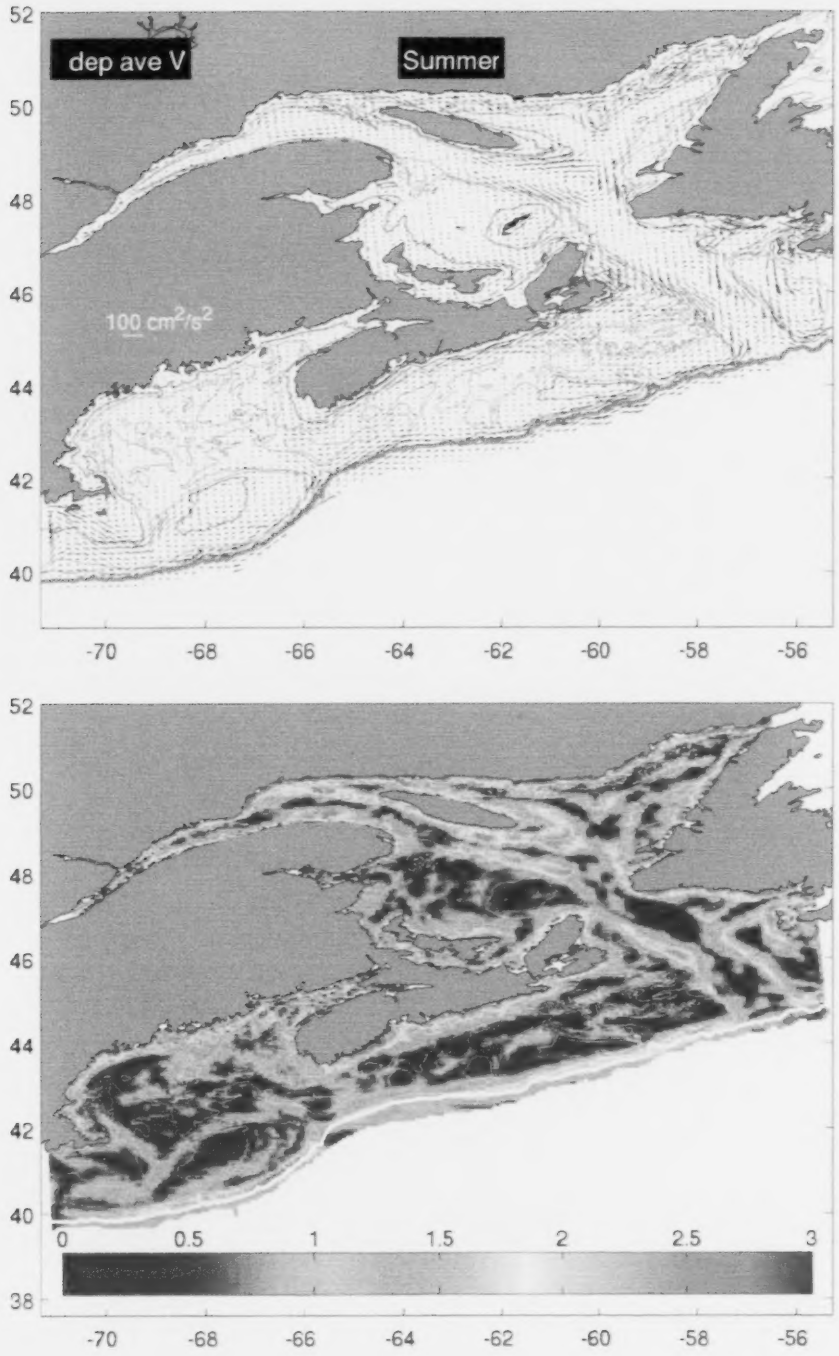

Figure 19: Summer major axes of variation (cm^2/s^2, top) and log{(energy in major axis) / (energy in minor axis)} (btm), for the depth-averaged velocity.

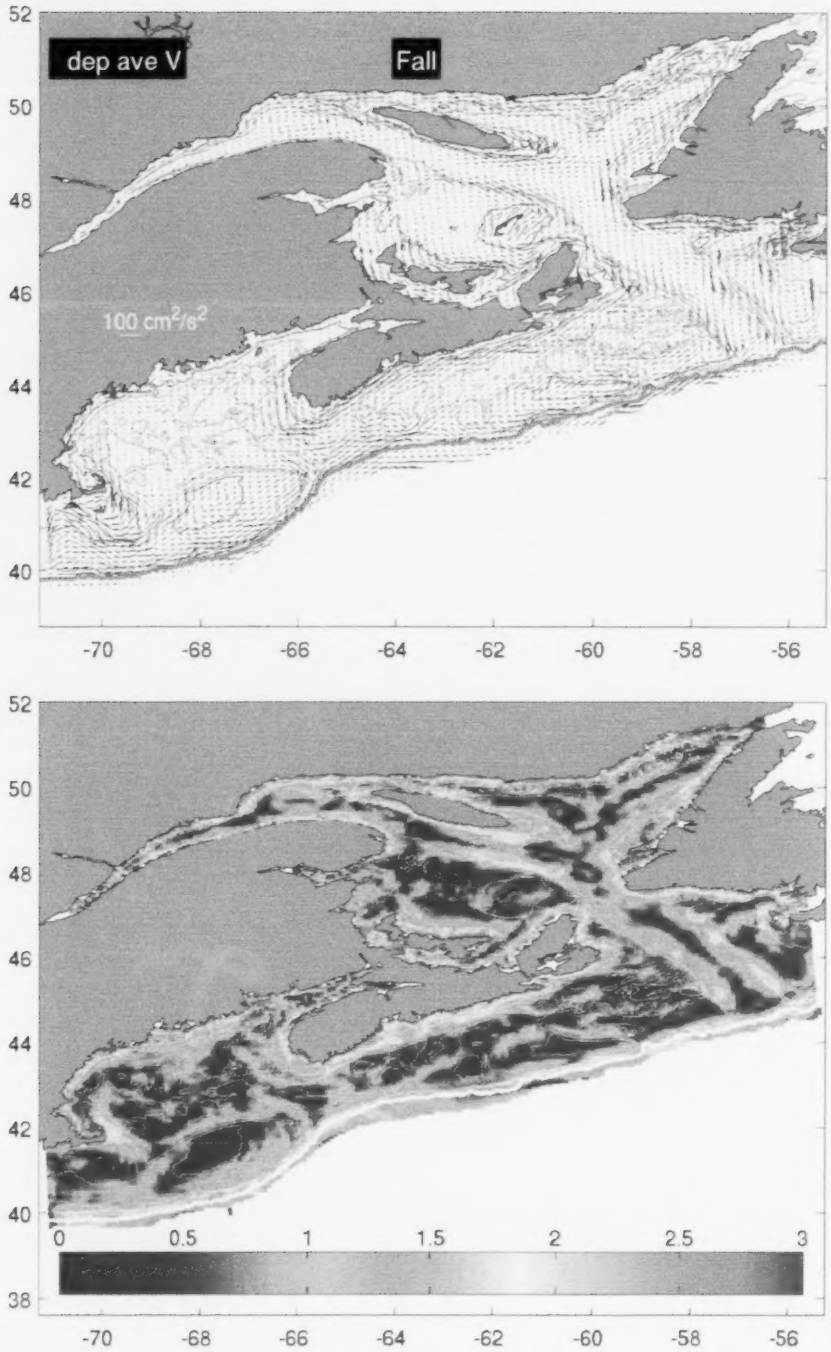

Figure 20: Fall major axes of variation (cm^2/s^2, top) and log{(energy in major axis) / (energy in minor axis)} (btm), for the depth-averaged velocity.

SEASONALLY AVERAGED FIELDS

Surface Layer (0-20m)

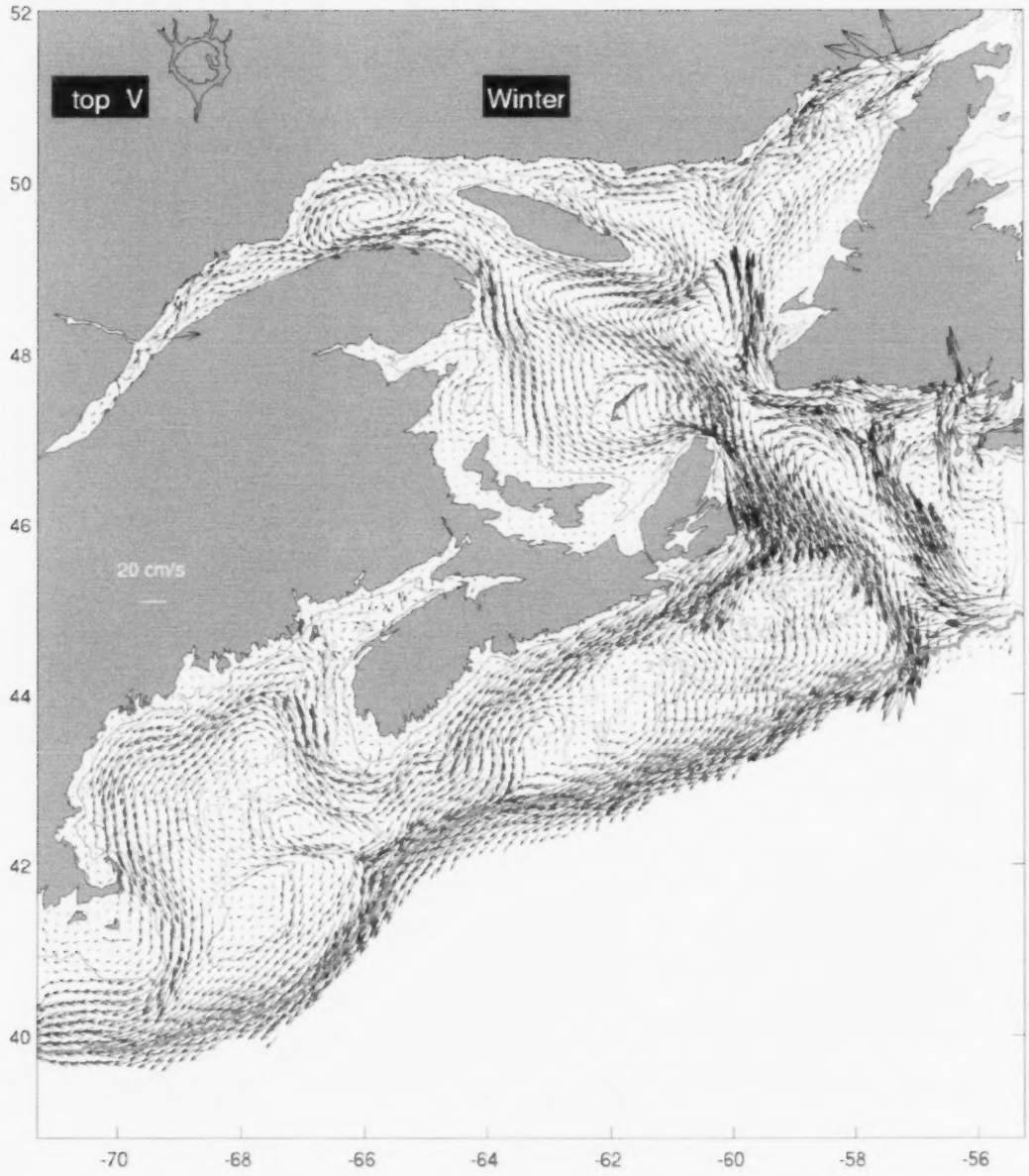

Figure 21: Winter surface layer velocity.

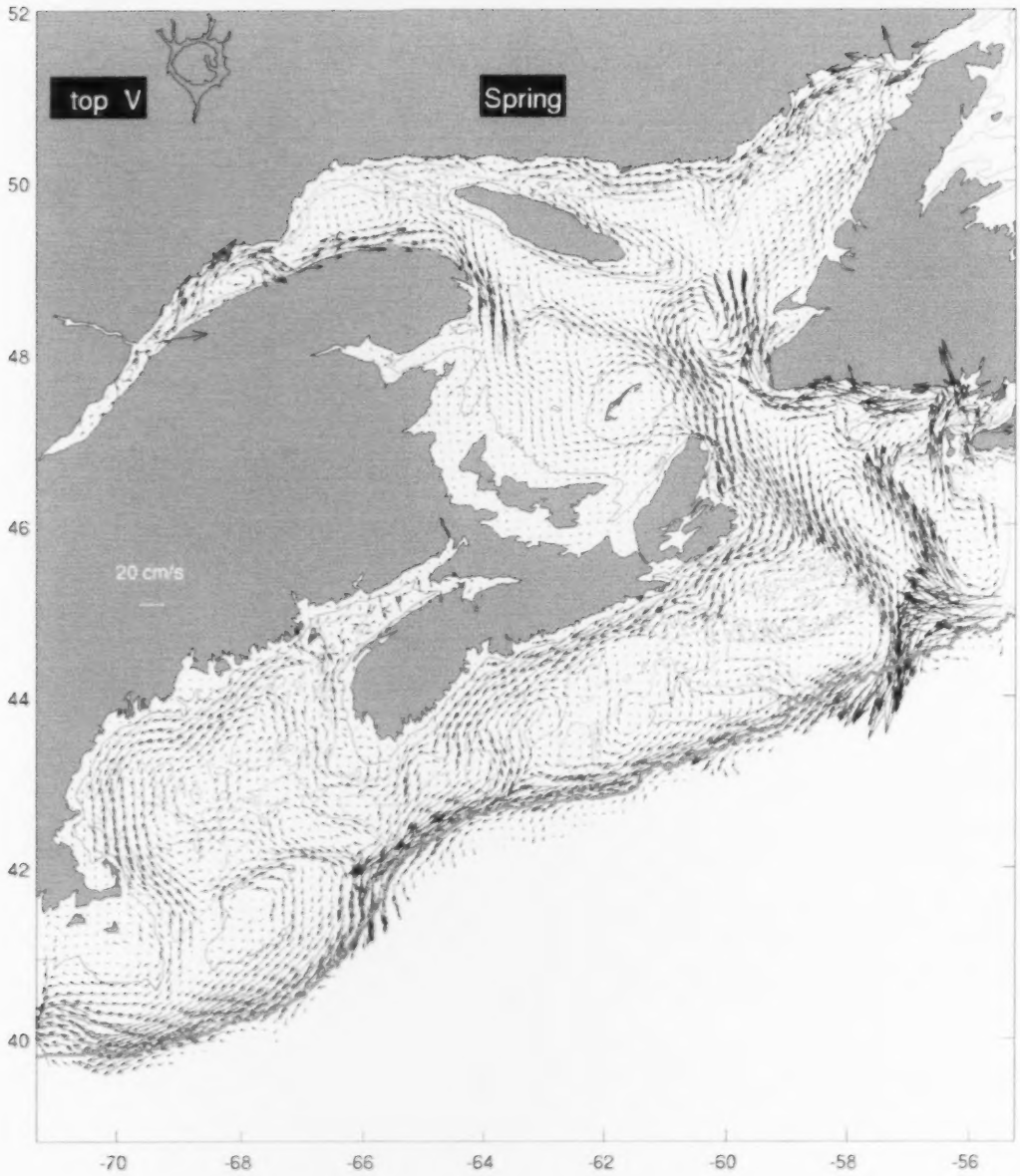

Figure 22: Spring surface layer velocity.

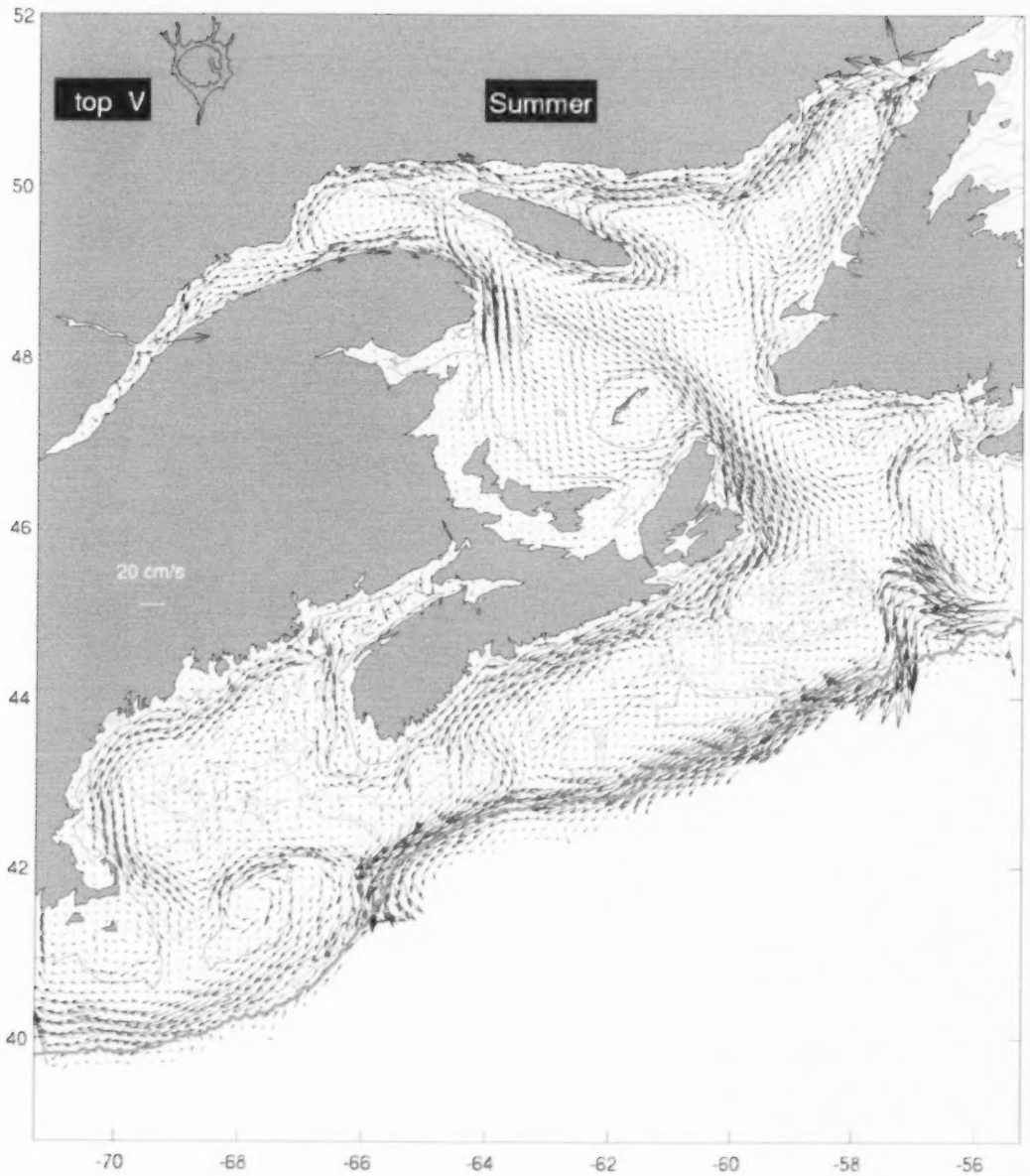

Figure 23: Summer surface layer velocity.

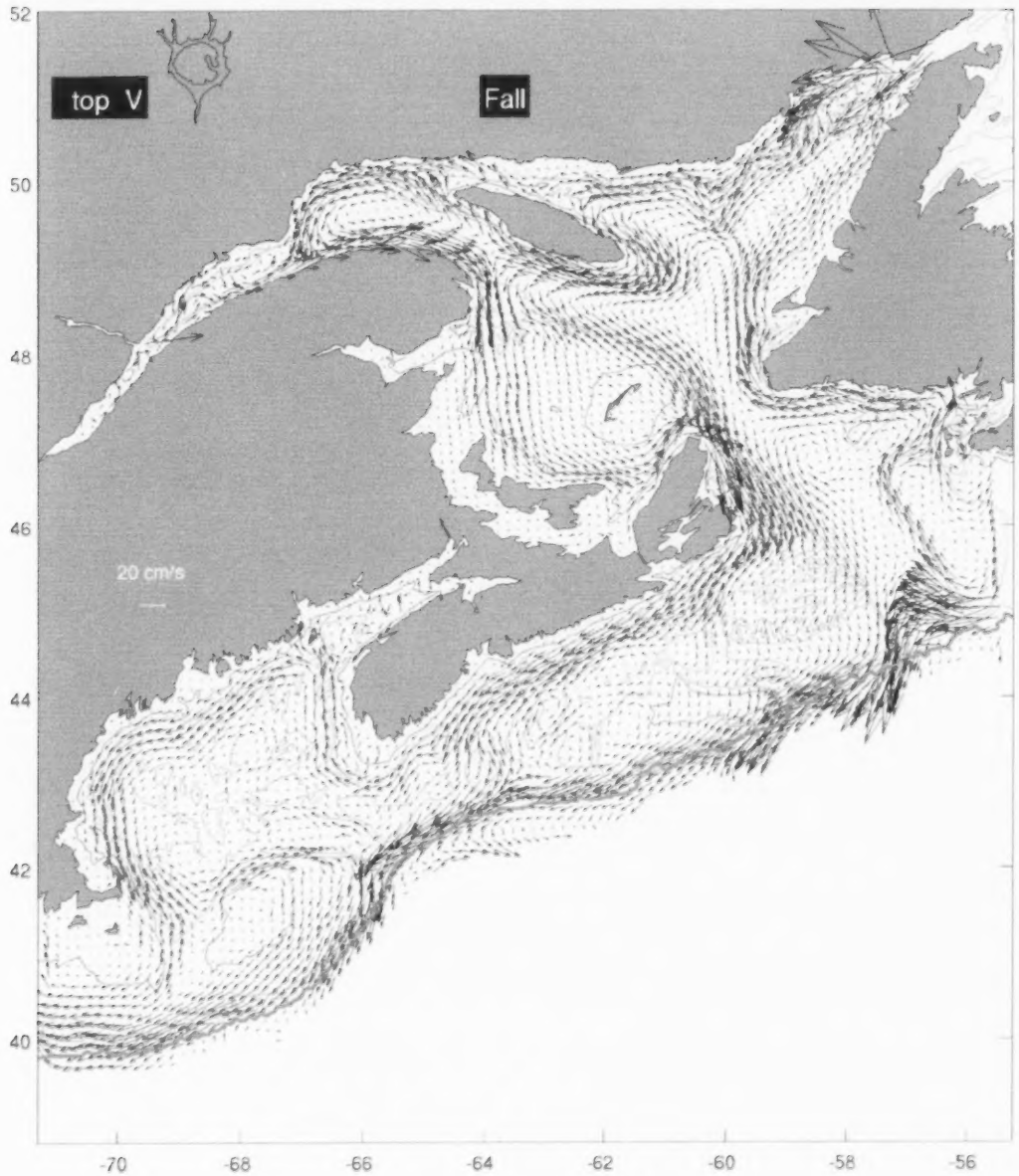

Figure 24: Fall surface layer velocity.

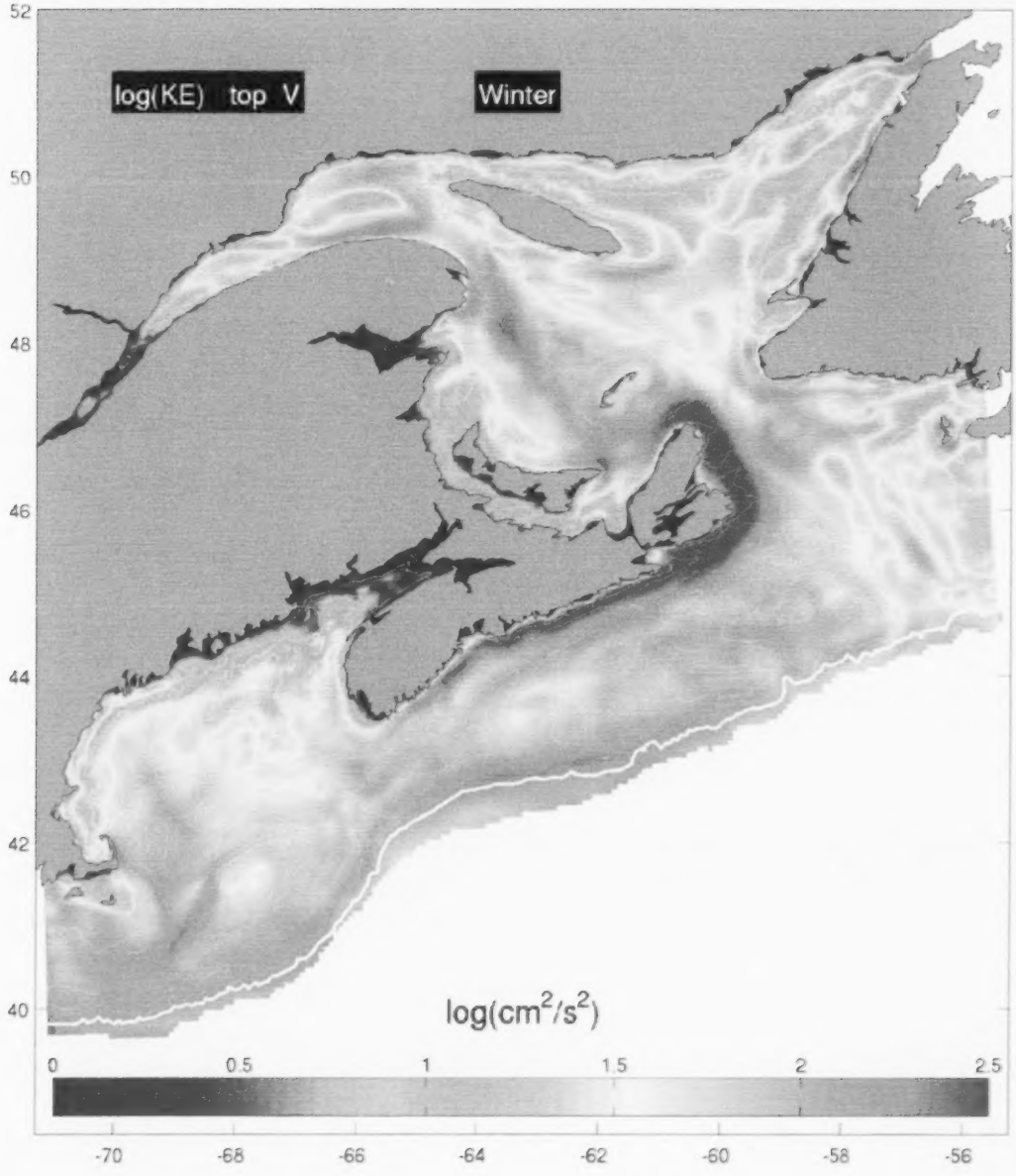

Figure 25: Winter perturbation log(kinetic energy (cm^2/s^2)) for the surface layer velocity.

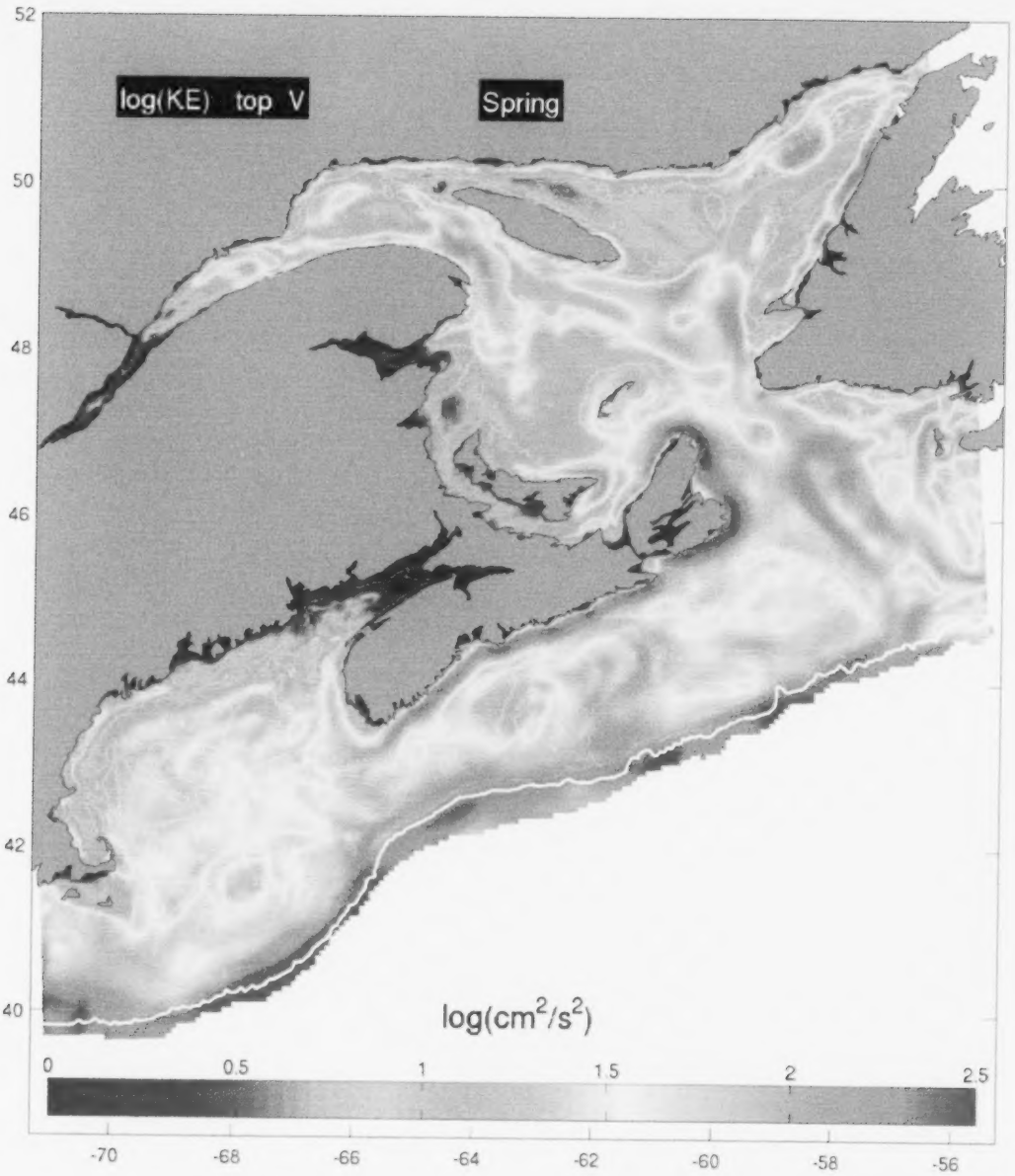

Figure 26: Spring perturbation log(kinetic energy (cm^2/s^2)) for the surface layer velocity.

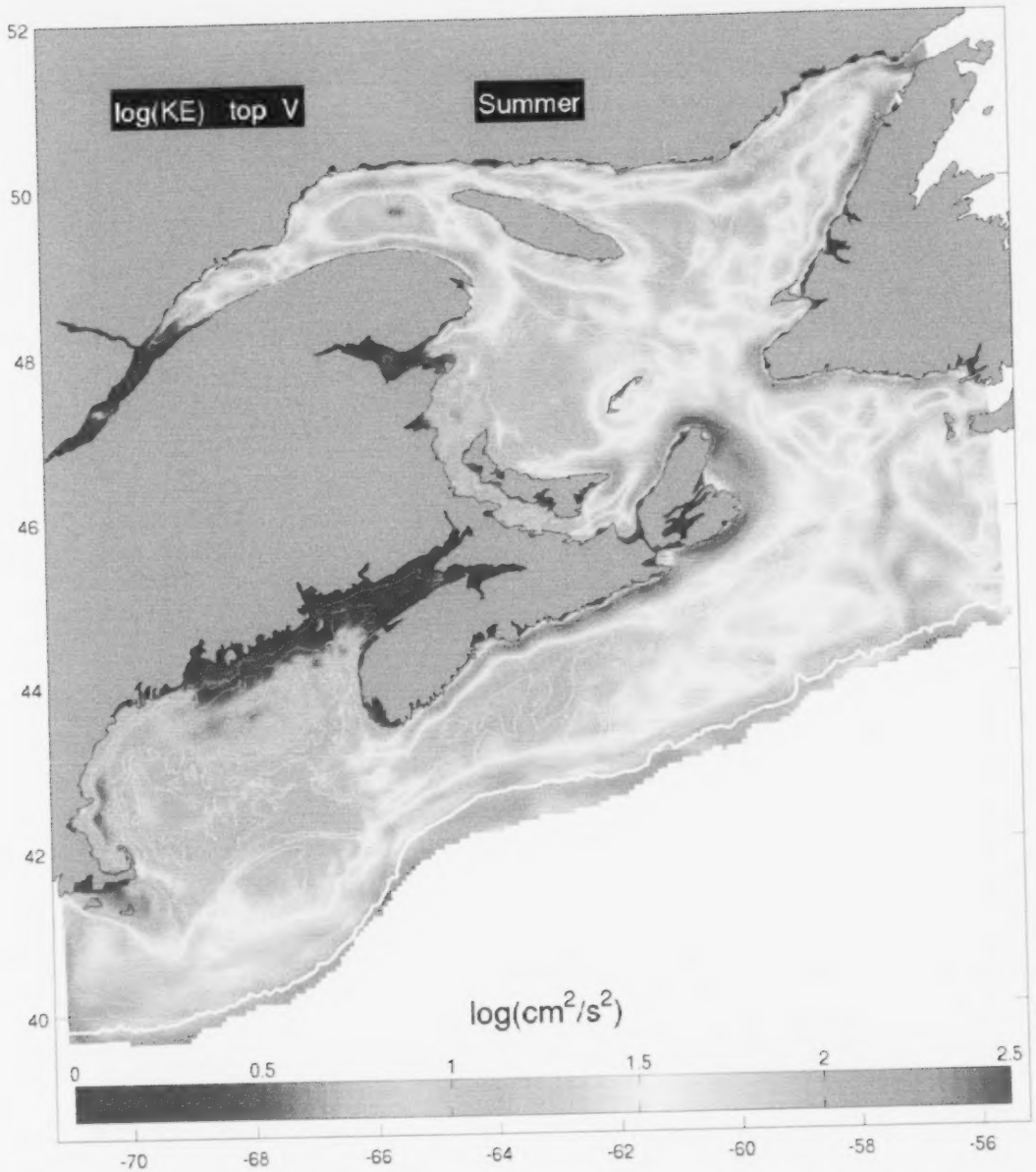

Figure 27: Summer perturbation log(kinetic energy (cm^2/s^2)) for the surface layer velocity.

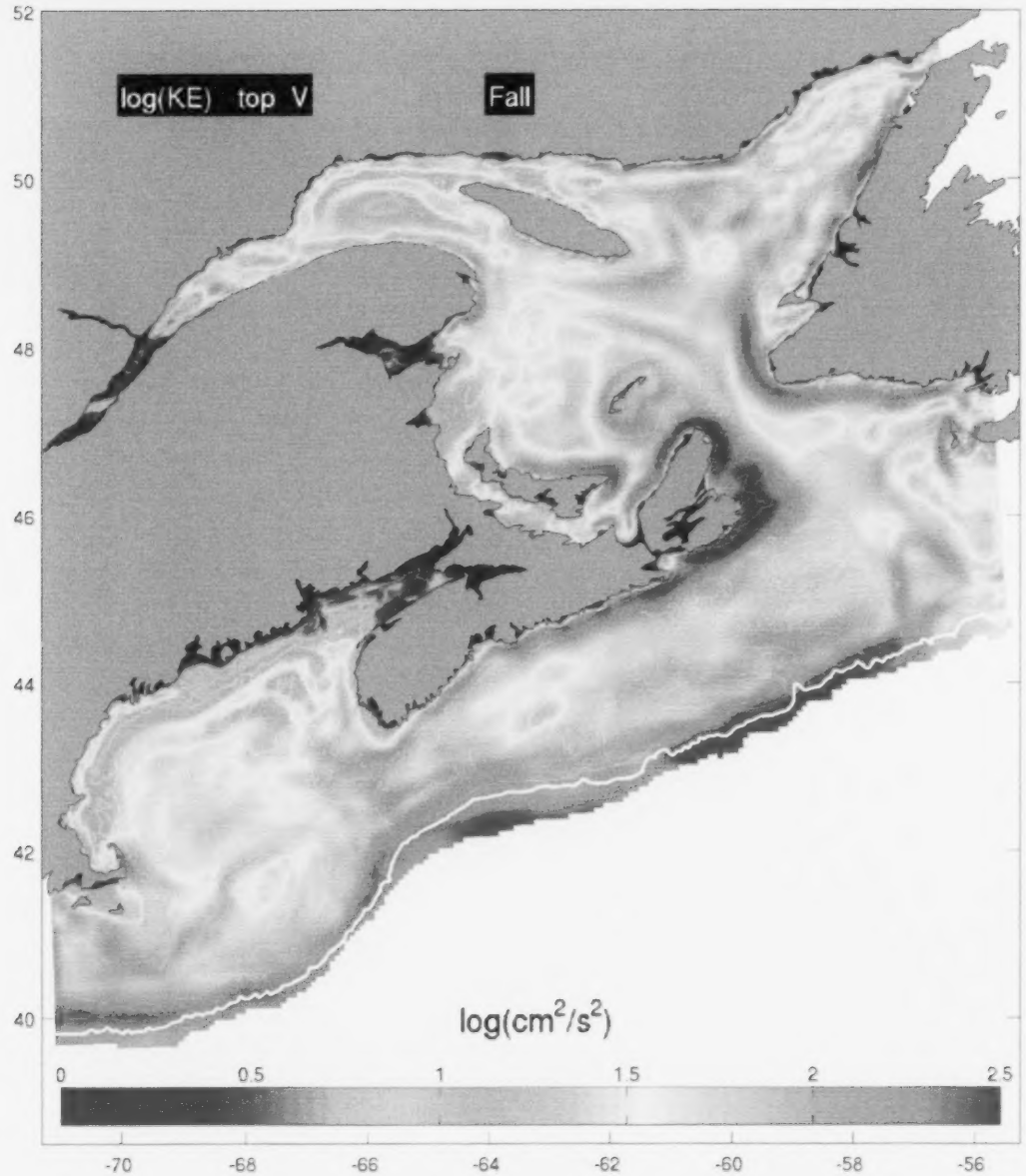

Figure 28: Fall perturbation log(kinetic energy (cm^2/s^2)) for the surface layer velocity.

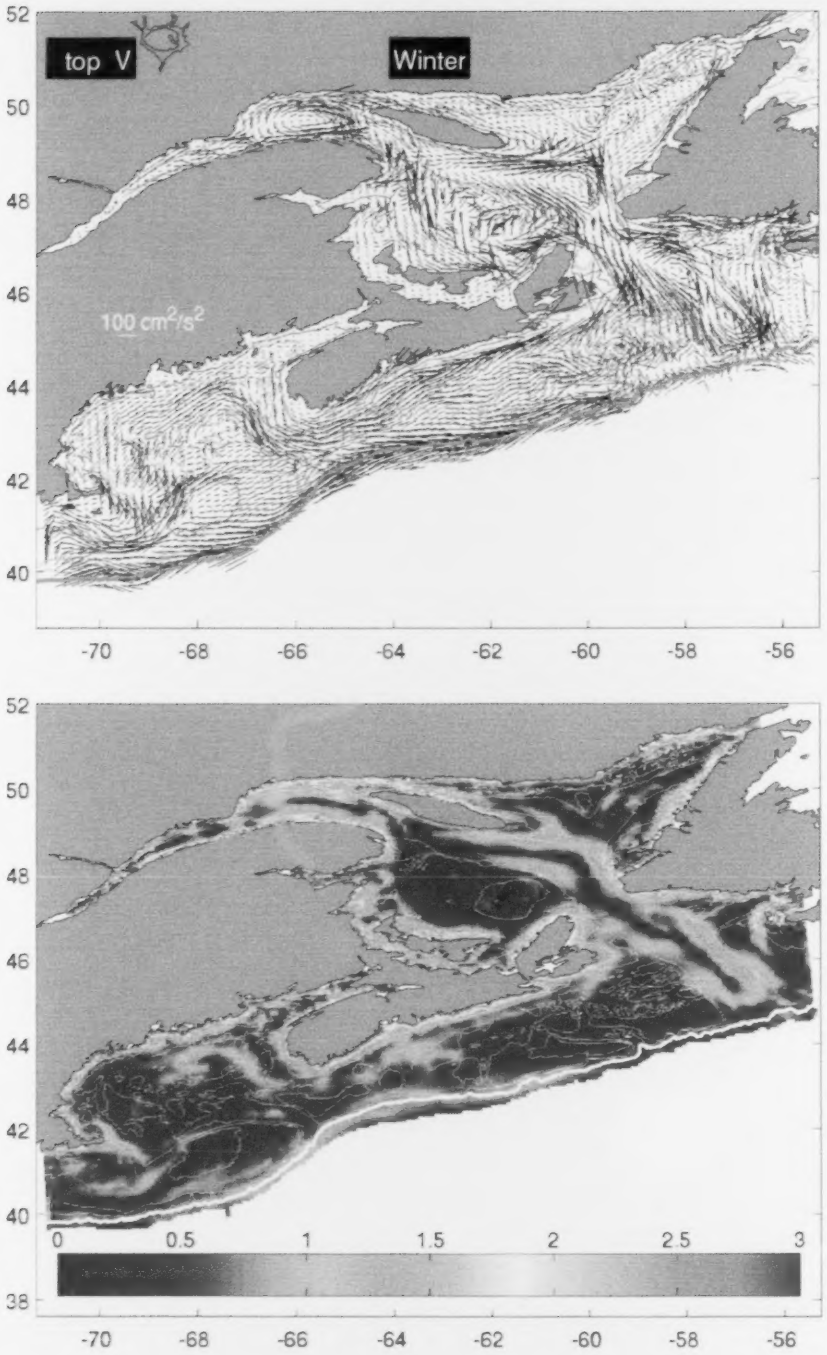

Figure 29: Winter major axes of variation (cm^2/s^2, top) and log{(energy in major axis) / (energy in minor axis)} (btm), for the surface layer velocity.

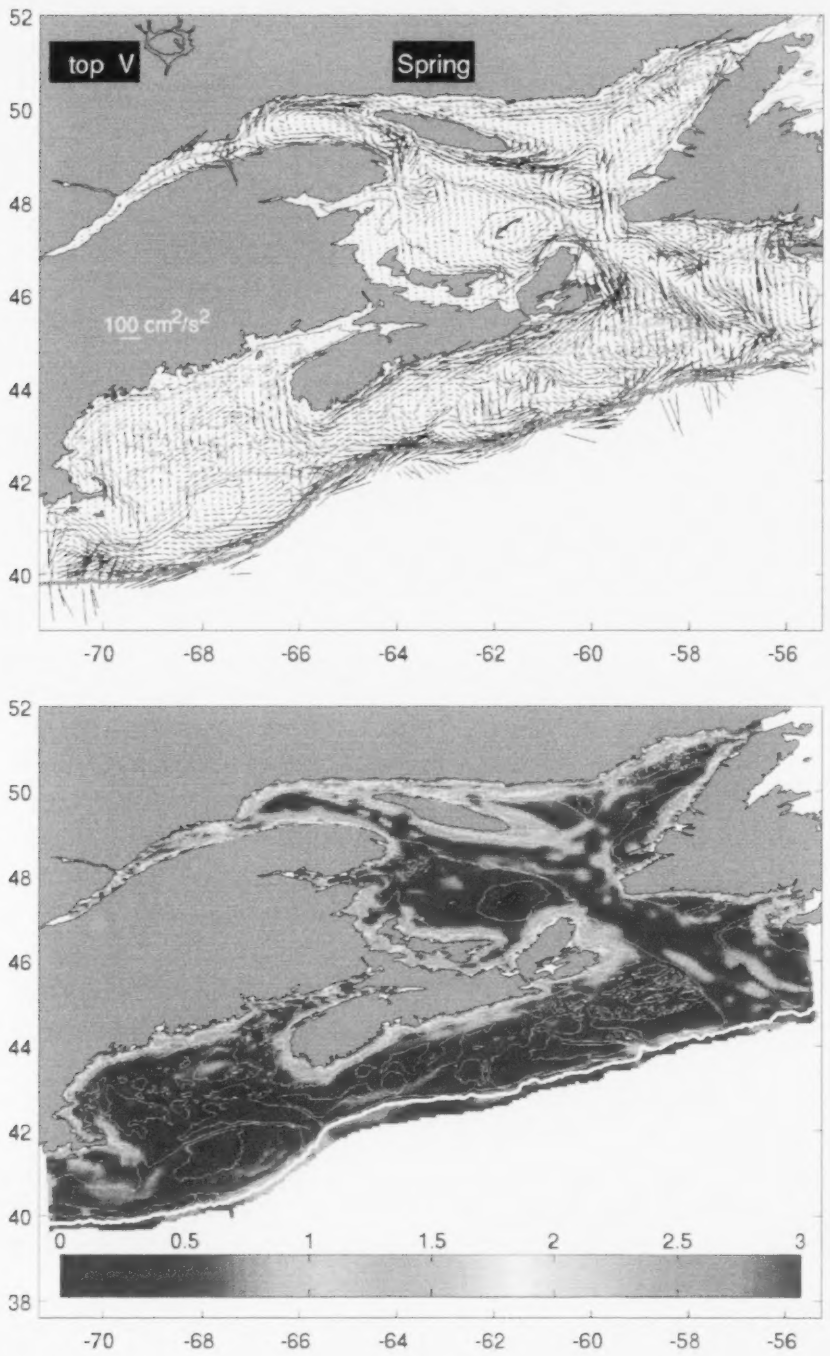

Figure 30: Spring major axes of variation (cm^2/s^2, top) and log{(energy in major axis) / (energy in minor axis)} (btm), for the surface layer velocity.

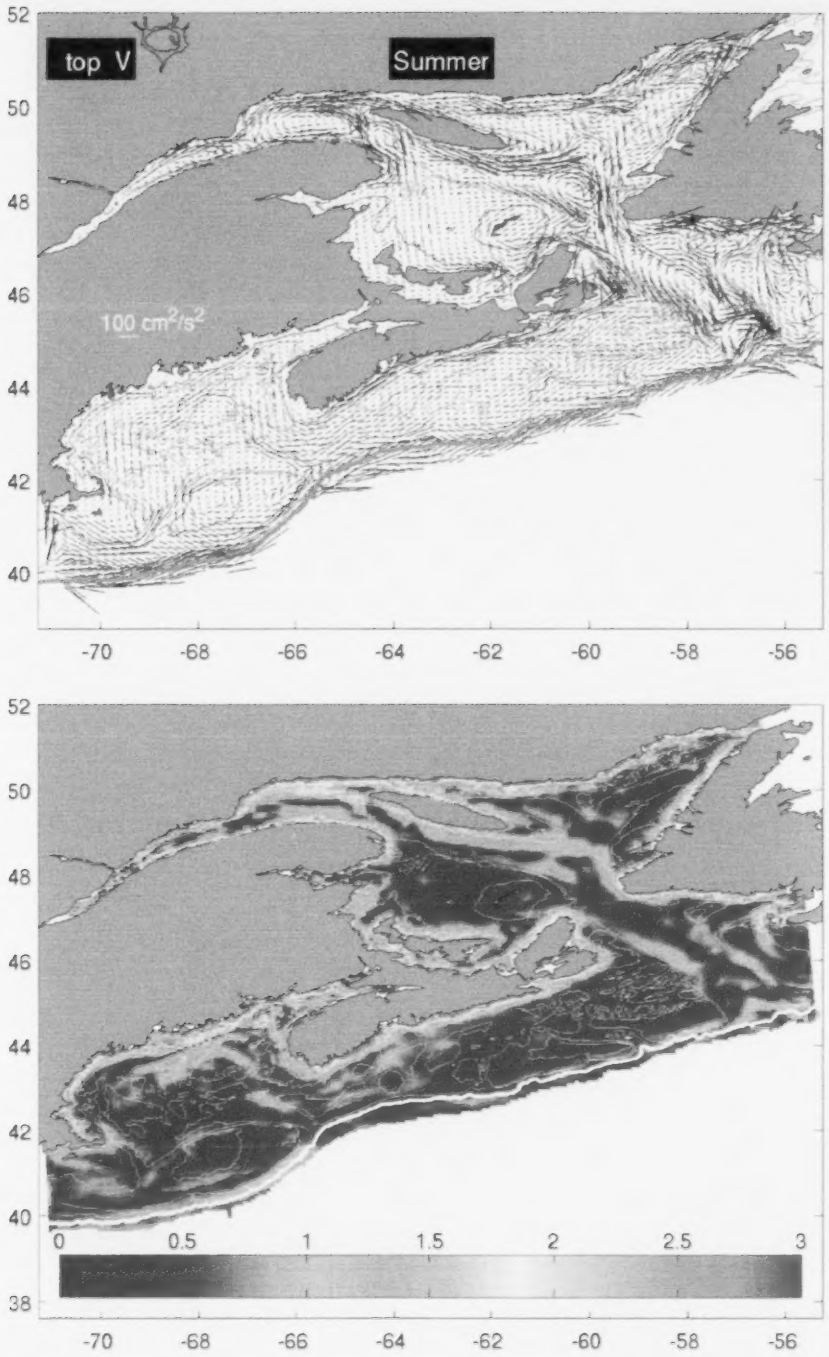

Figure 31: Summer major axes of variation (cm^2/s^2, top) and log{(energy in major axis) / (energy in minor axis)} (btm), for the surface layer velocity.

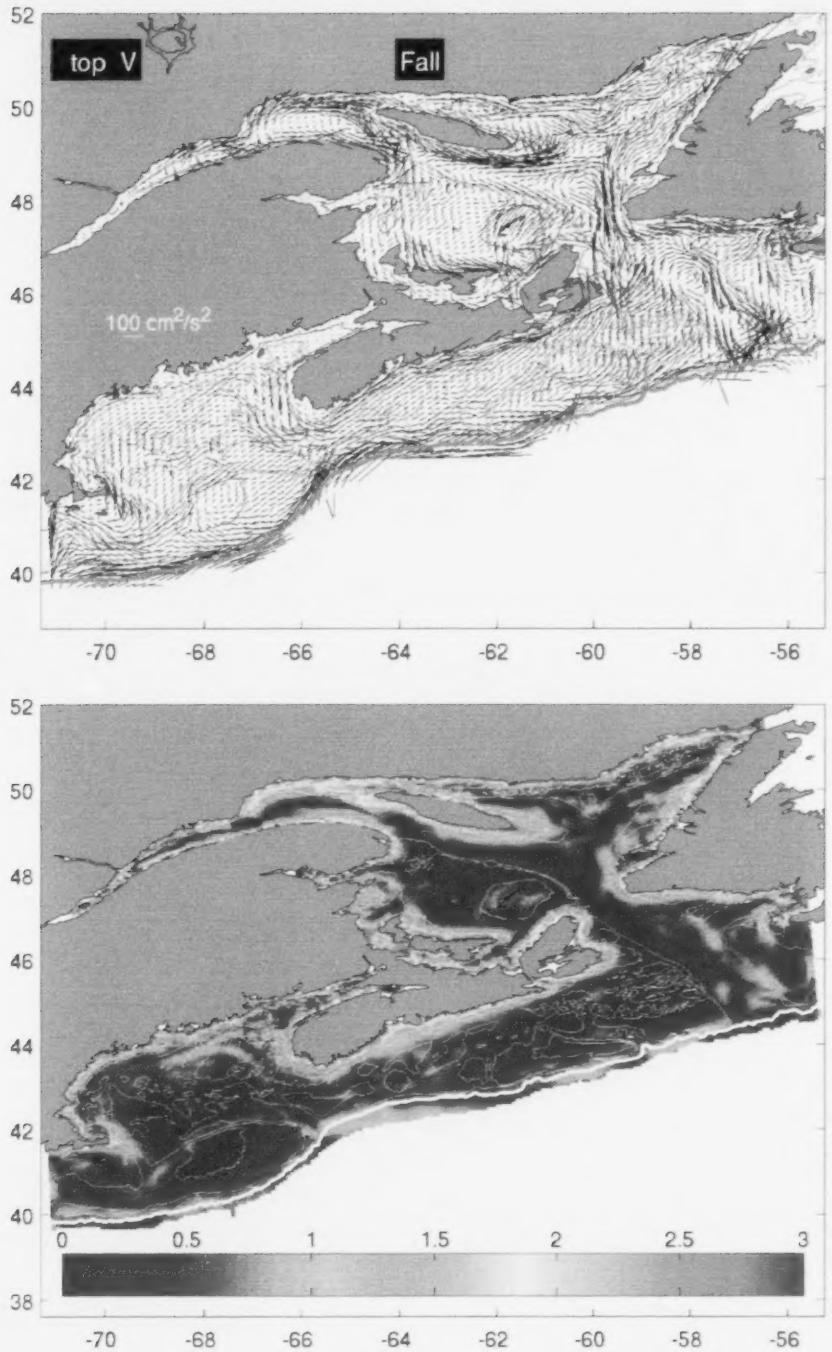

Figure 32: Fall major axes of variation (cm^2/s^2, top) and log{(energy in major axis) / (energy in minor axis)} (btm), for the surface layer velocity.

SEASONALLY AVERAGED FIELDS

Mid Water Column (20-50m)

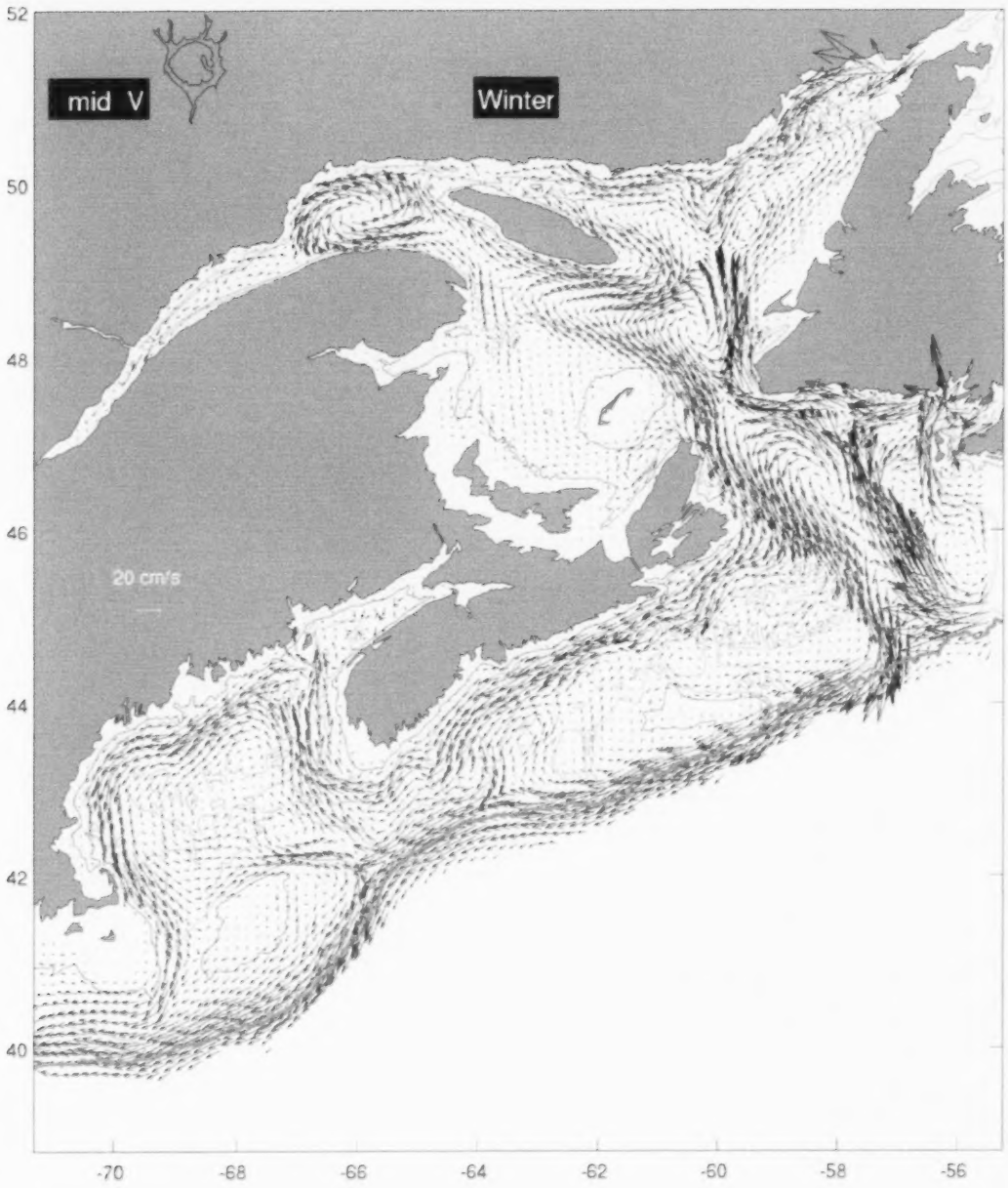

Figure 33: Winter mid-layer velocity.

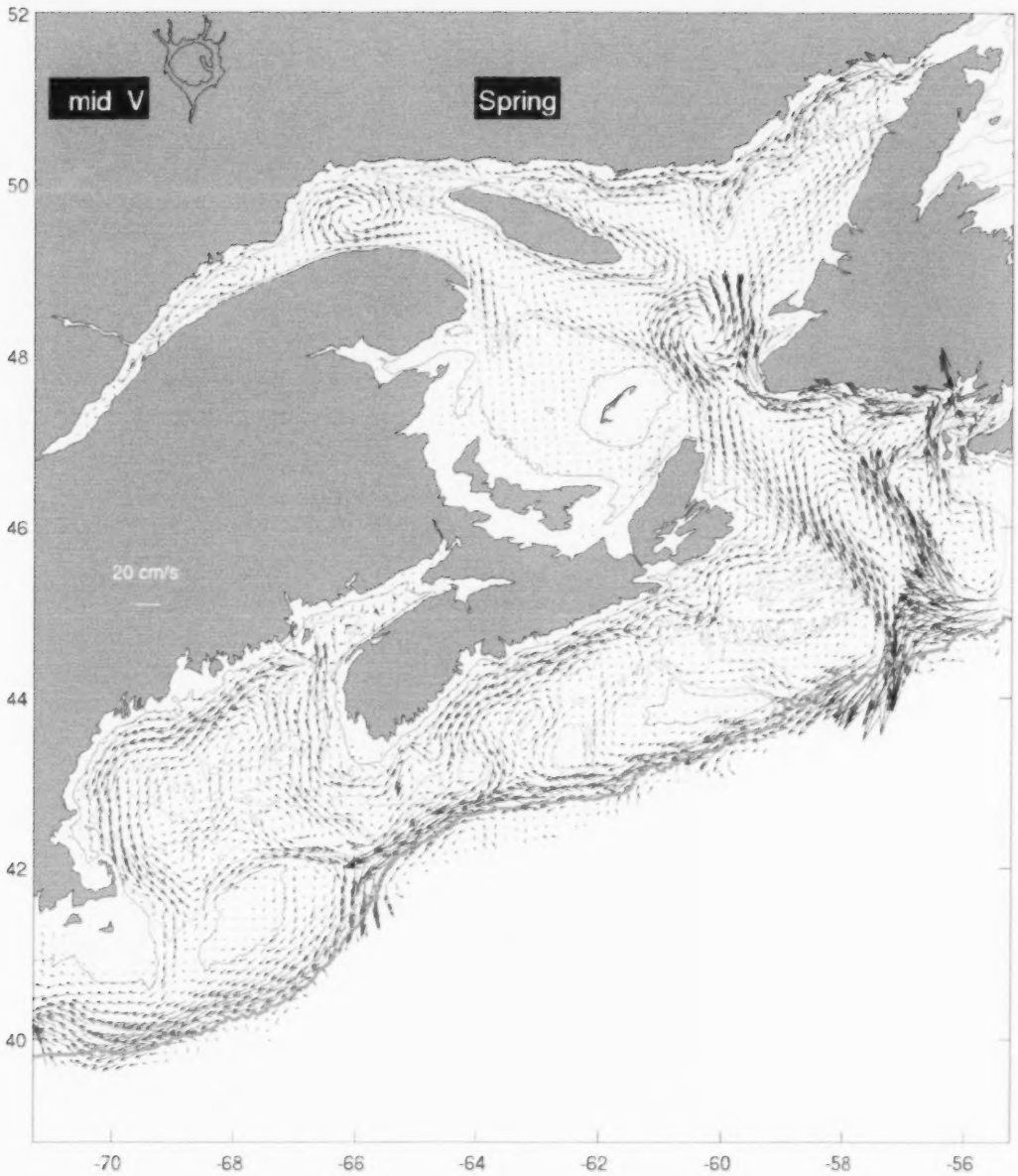

Figure 34: Spring mid-layer velocity.

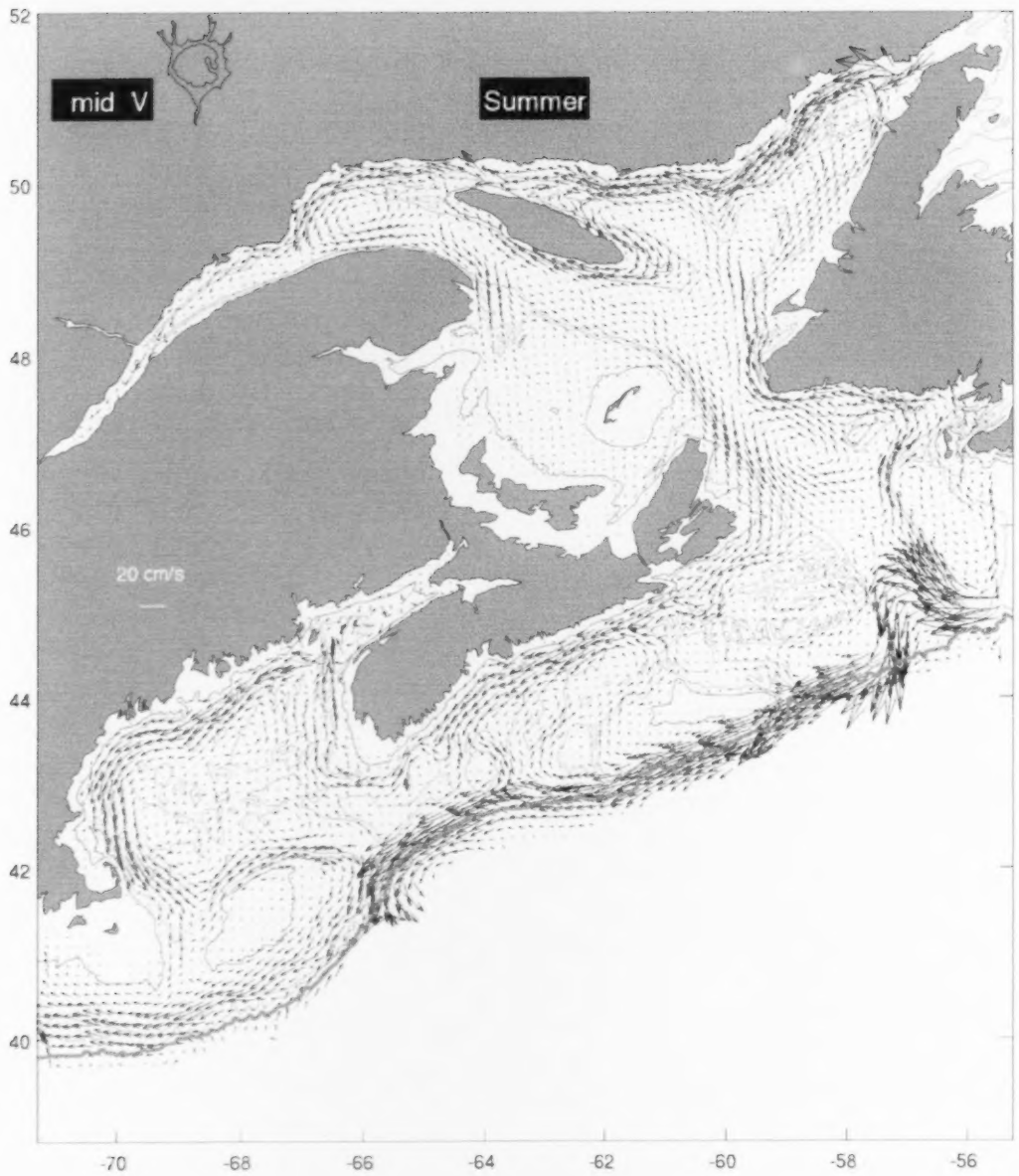

Figure 35: Summer mid-layer velocity.

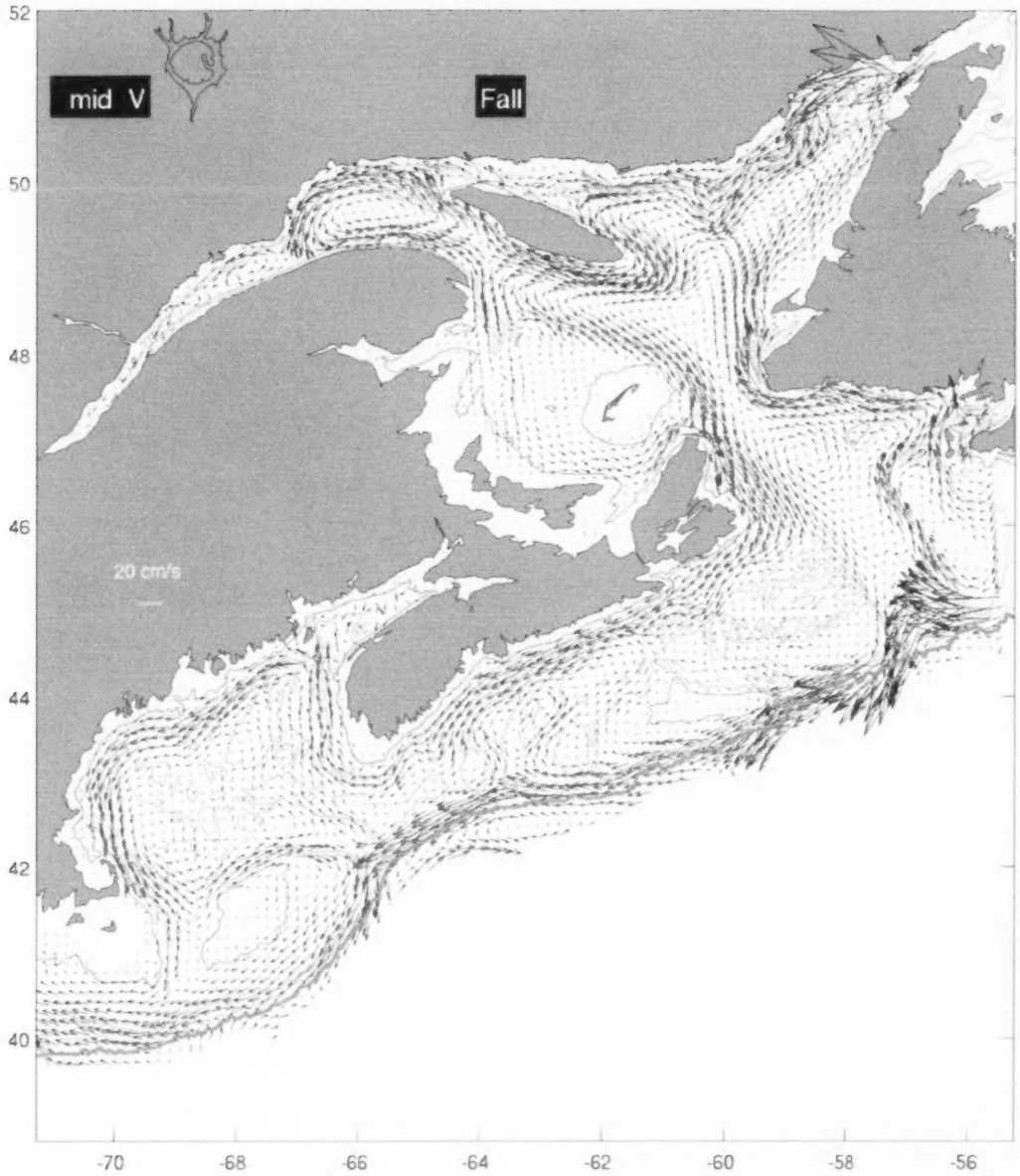

Figure 36: Fall mid-layer velocity.

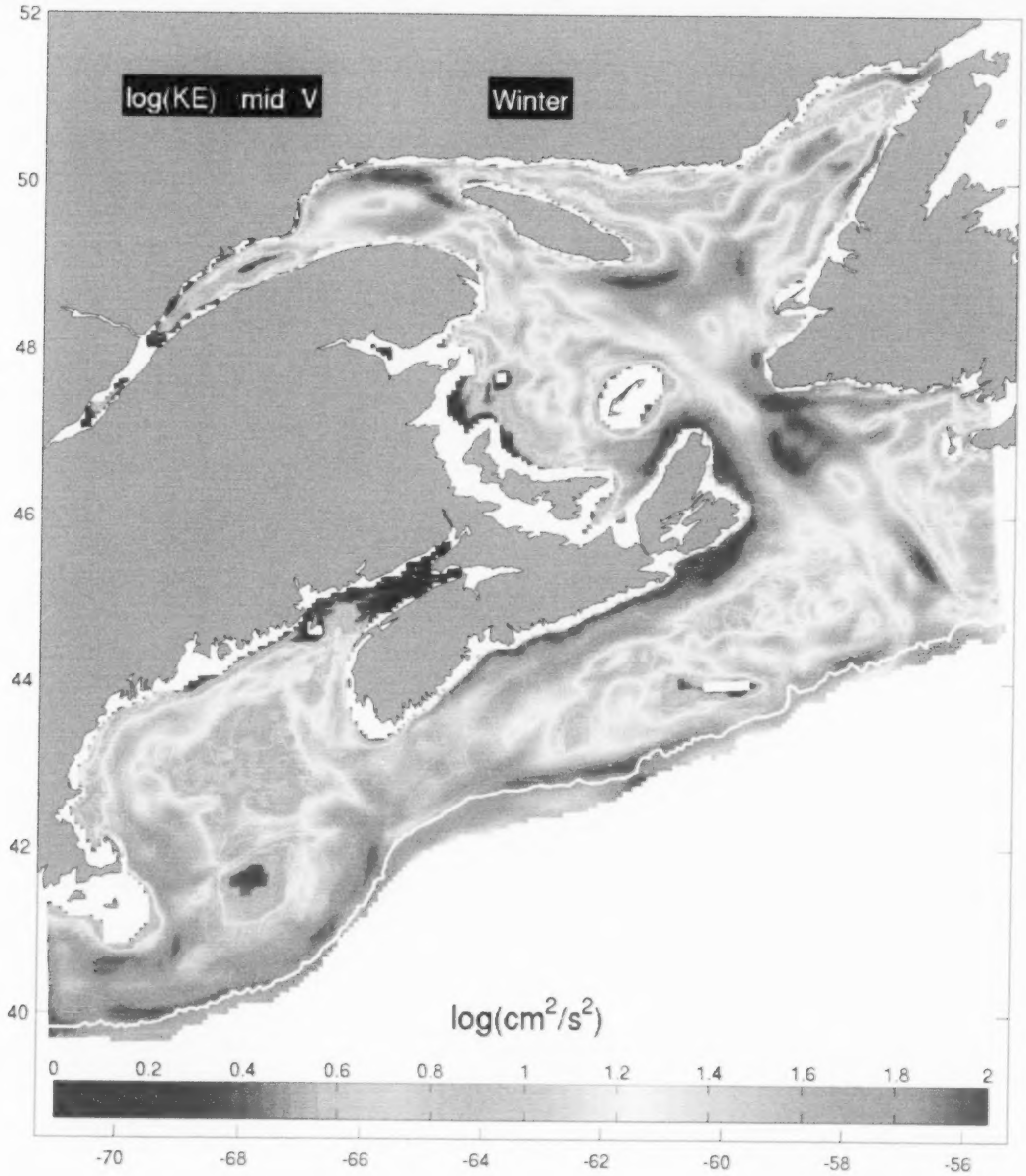

Figure 37: Winter perturbation log(kinetic energy (cm^2/s^2)) for the mid-layer velocity.

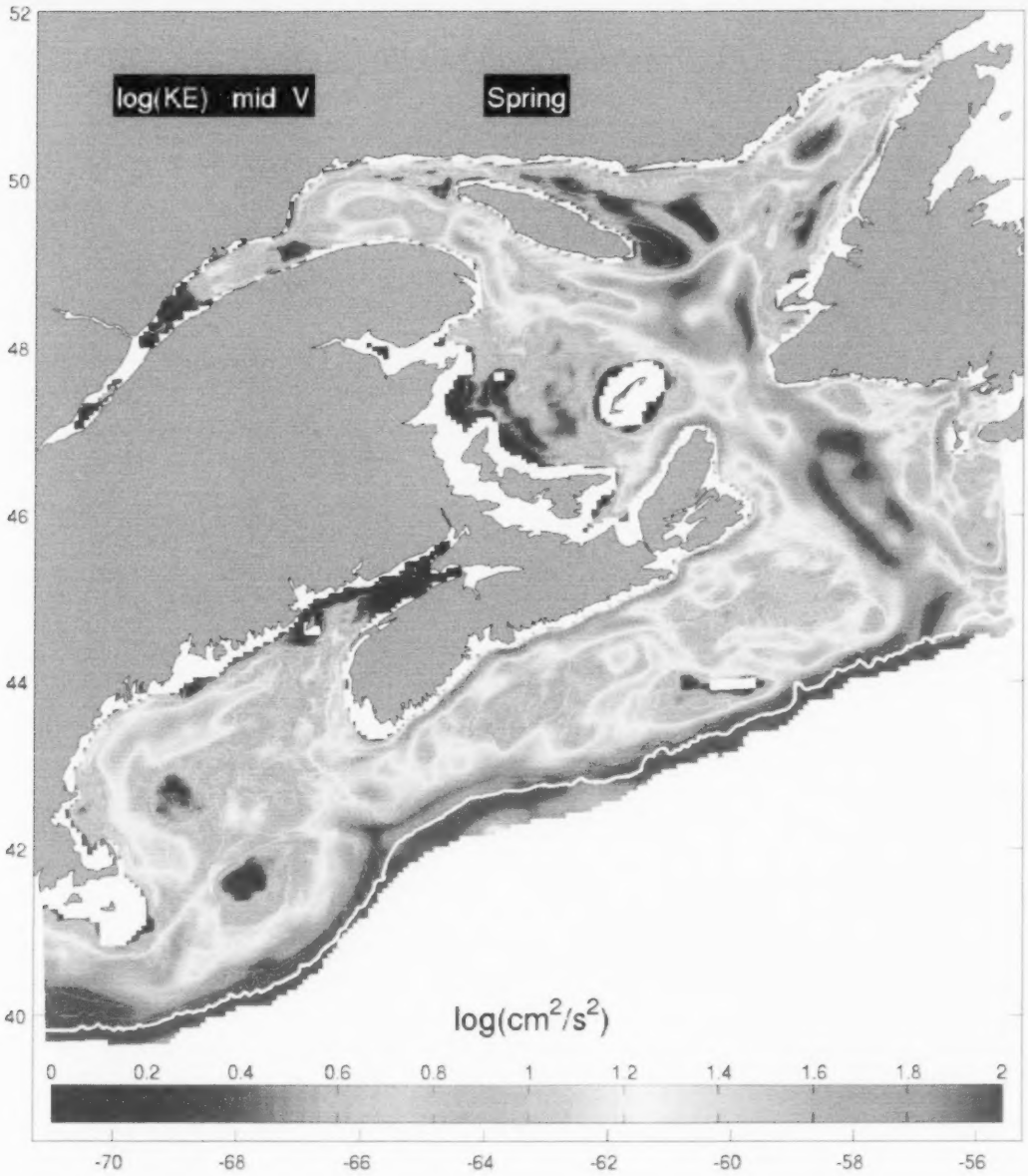

Figure 38: Spring perturbation log(kinetic energy (cm^2/s^2)) for the mid-layer velocity.

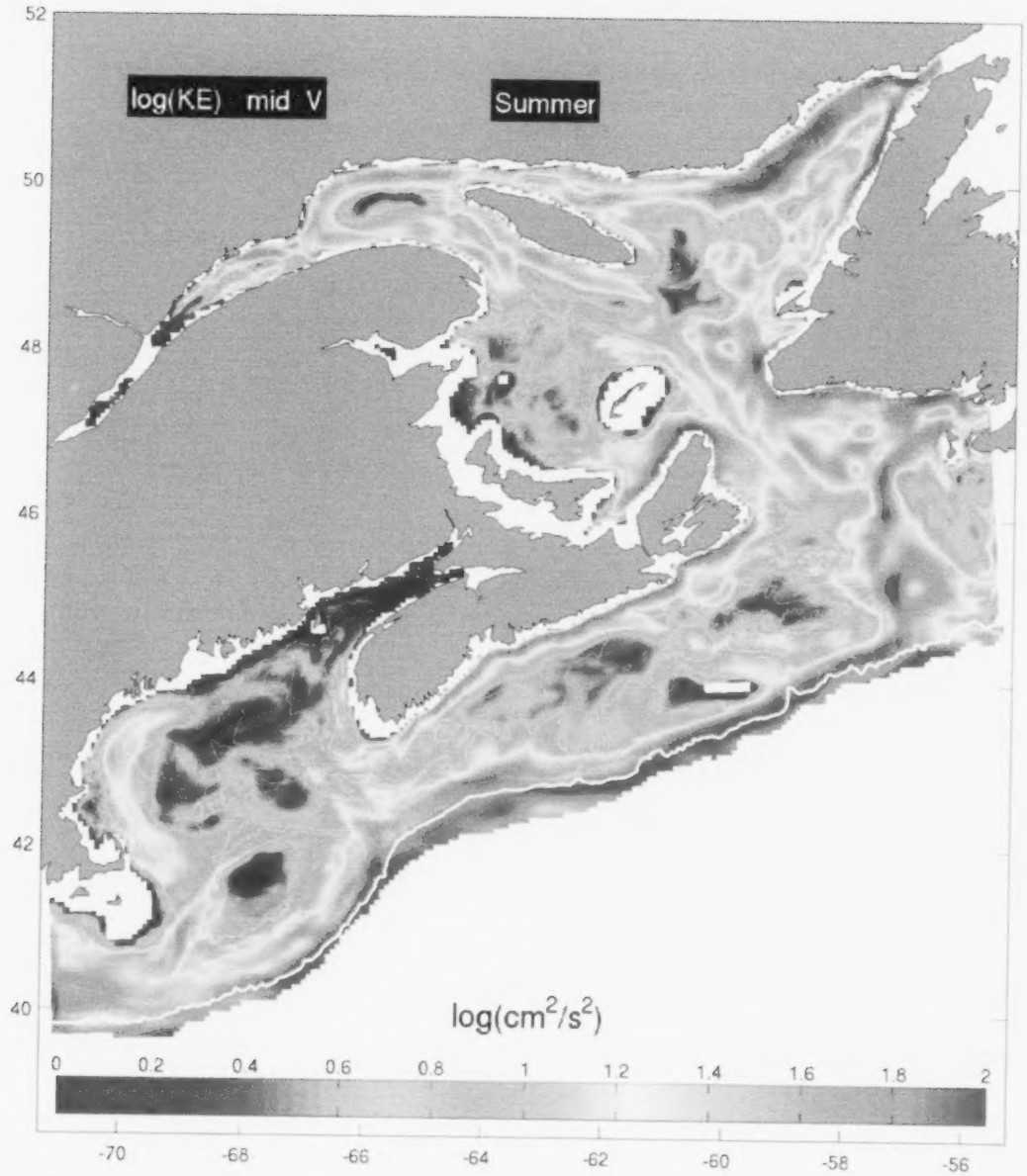

Figure 39: Summer perturbation log(kinetic energy (cm^2/s^2)) for the mid-layer velocity.

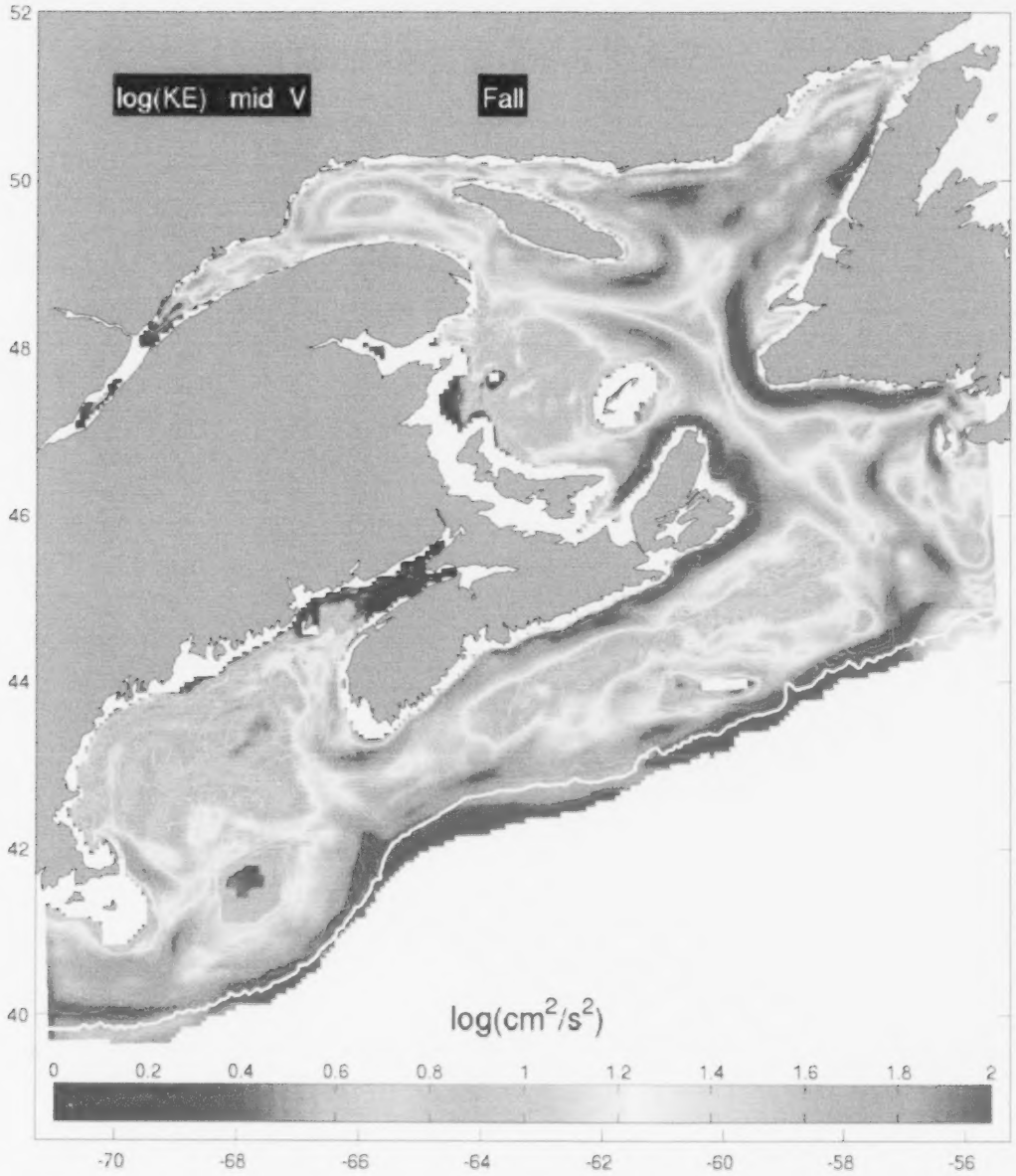

Figure 40: Fall perturbation log(kinetic energy (cm^2/s^2)) for the mid-layer velocity.

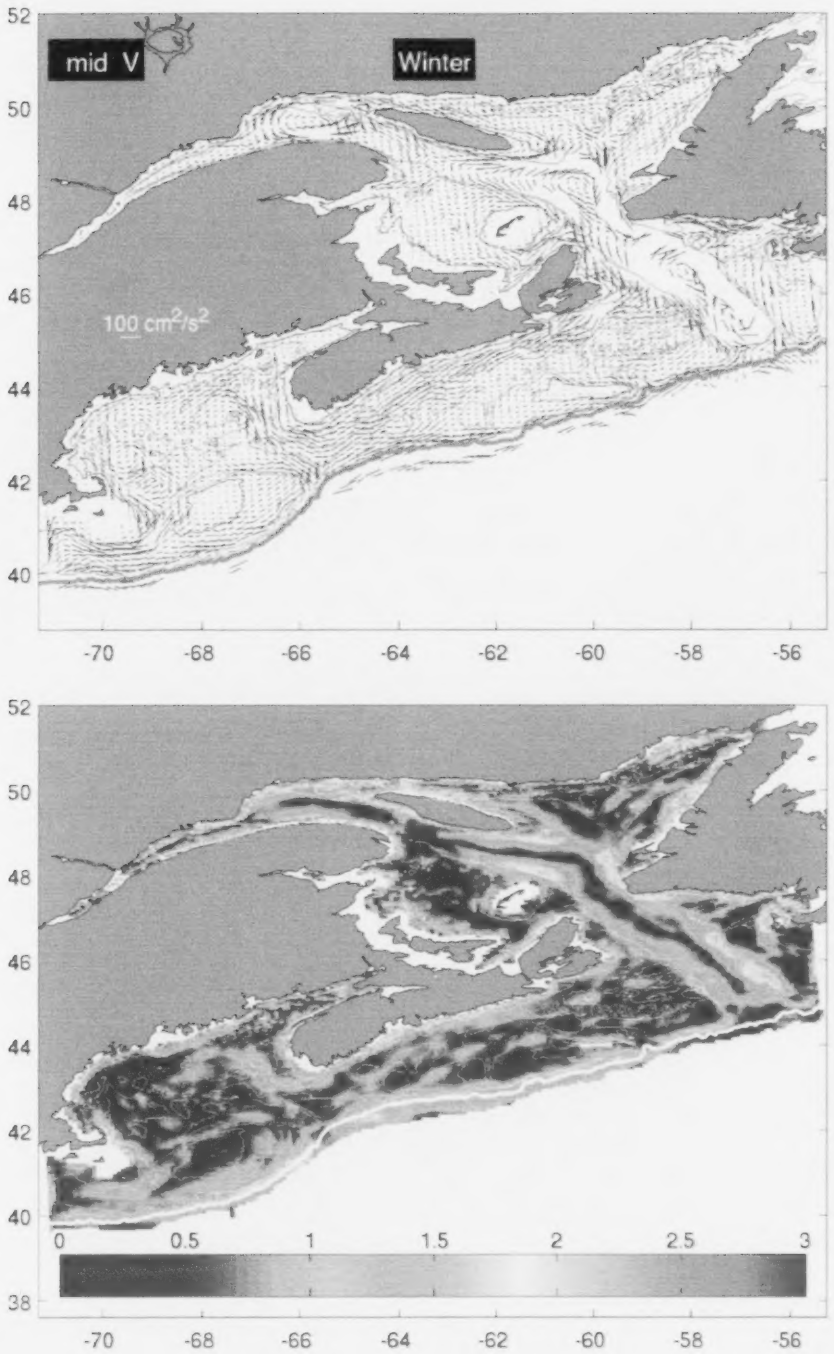

Figure 41: Winter major axes of variation (cm^2/s^2, top) and log{(energy in major axis) / (energy in minor axis)} (btm), for the mid-layer layer velocity.

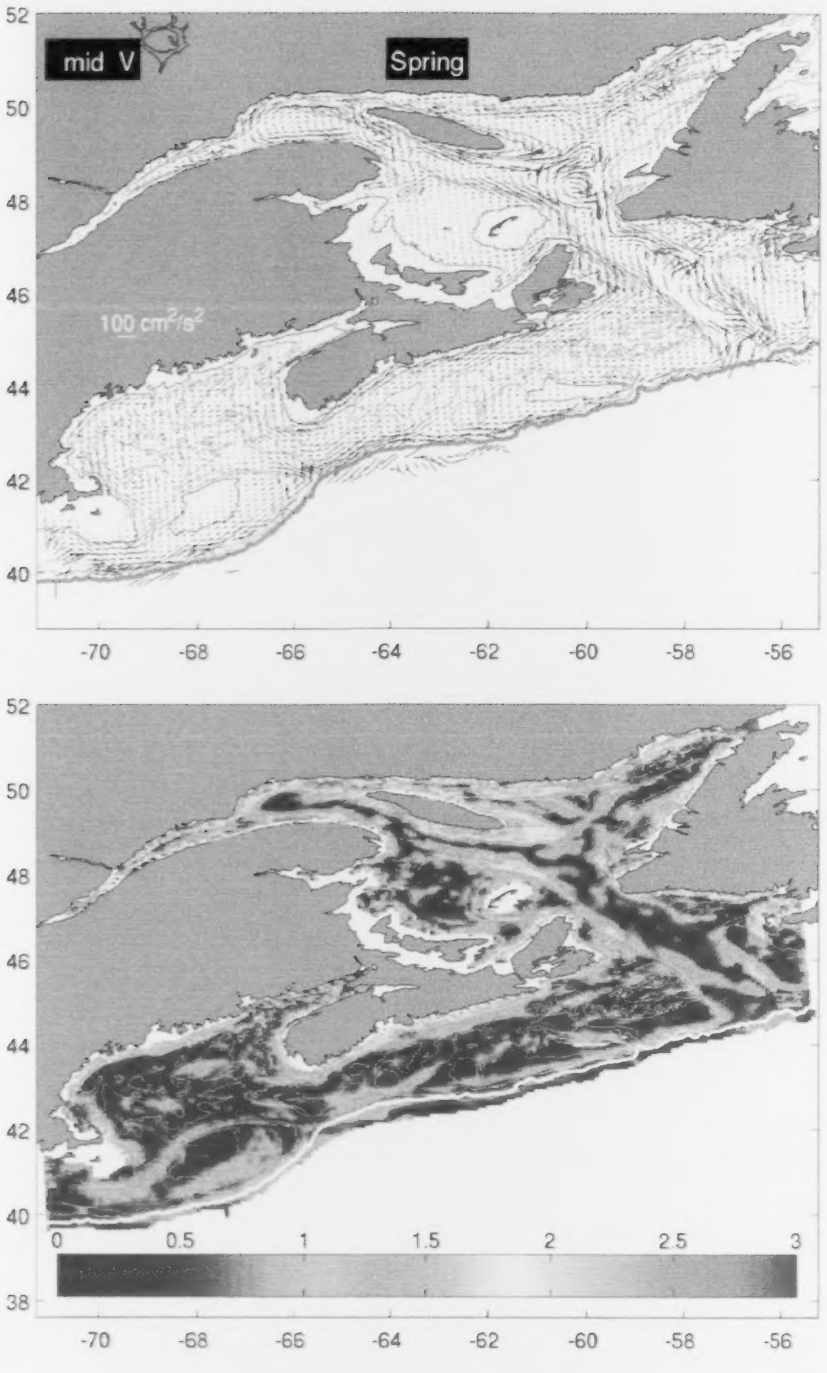

Figure 42: Spring major axes of variation (cm^2/s^2, top) and log{(energy in major axis) / (energy in minor axis)} (btm), for the mid-layer layer velocity.

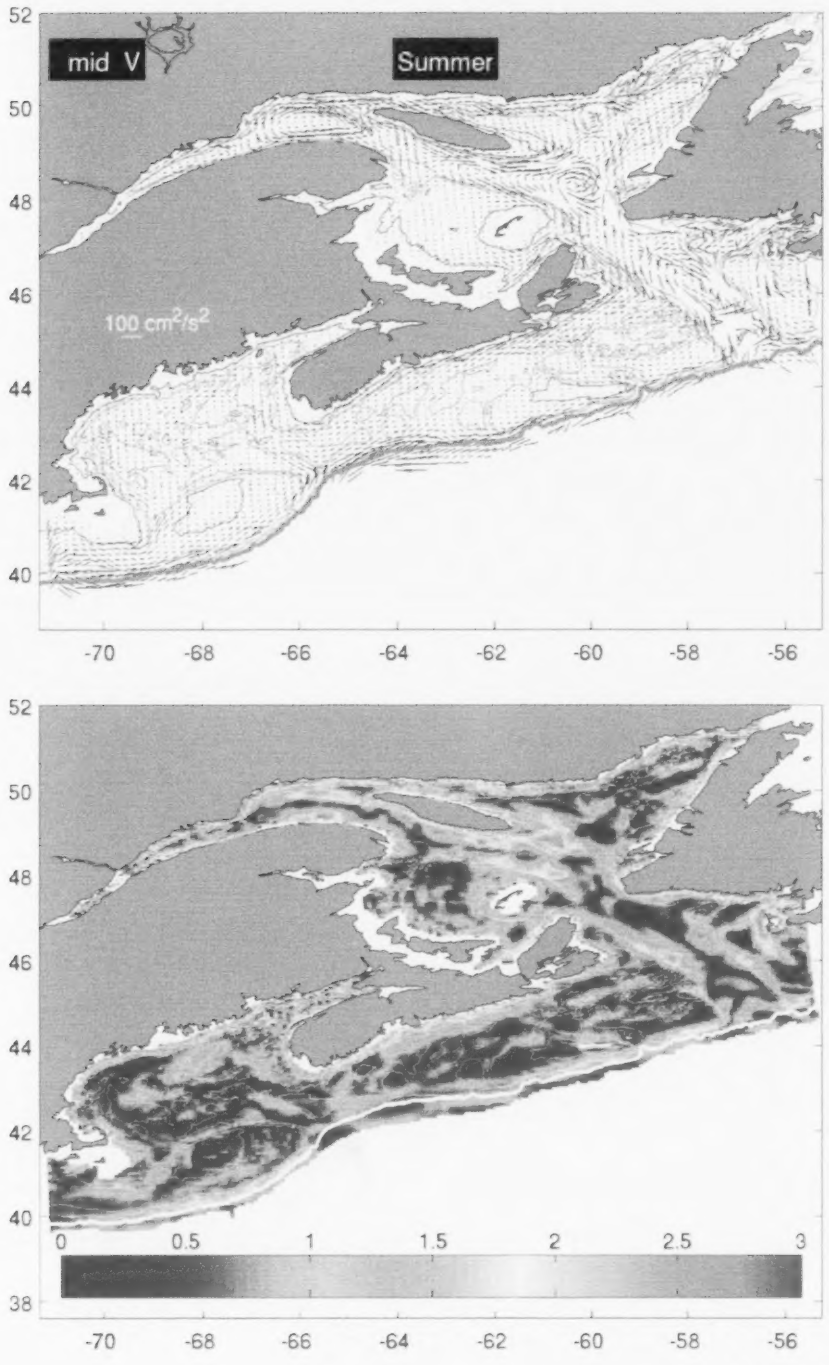

Figure 43: Summer major axes of variation (cm^2/s^2, top) and log{(energy in major axis) / (energy in minor axis)} (btm), for the mid-layer layer velocity.

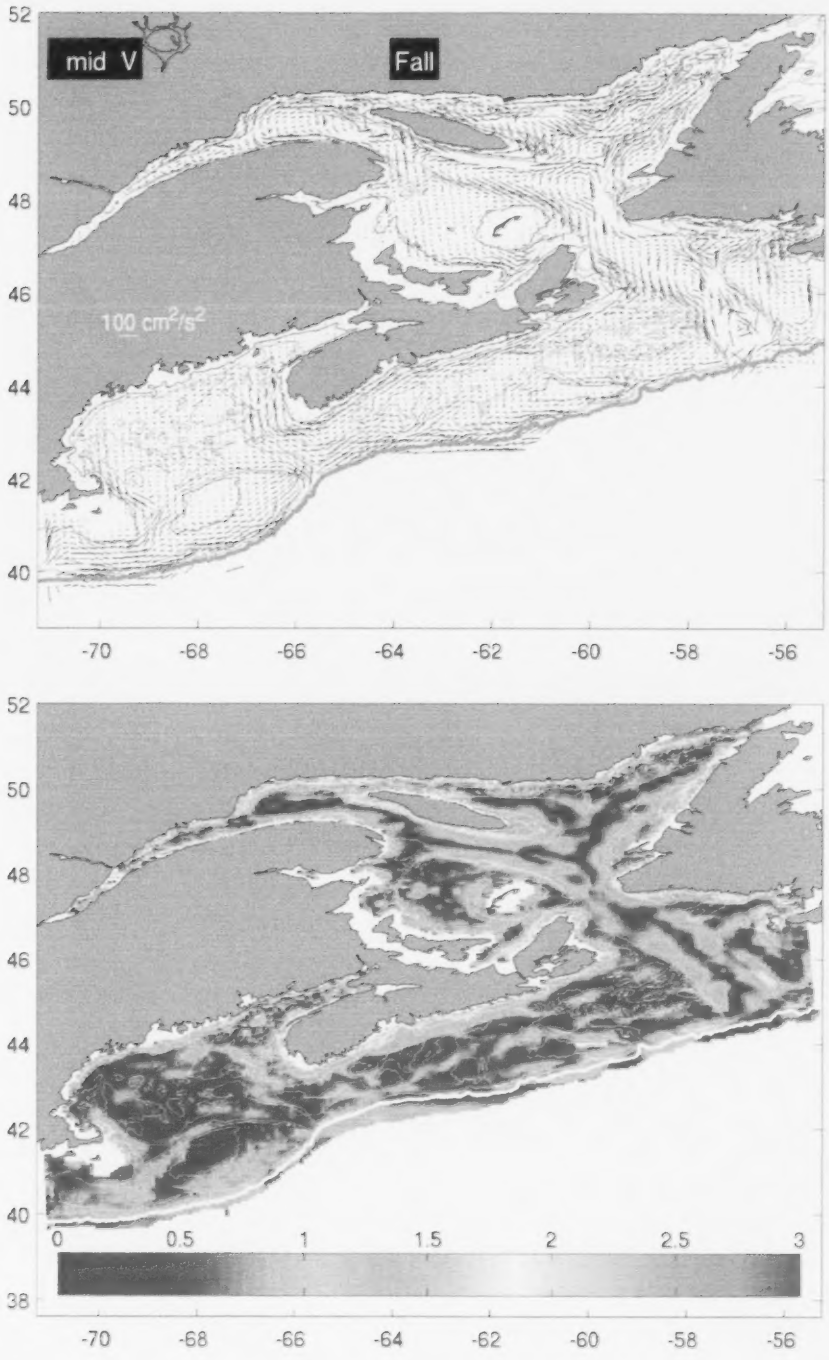

Figure 44: Fall major axes of variation (cm^2/s^2, top) and log{(energy in major axis) / (energy in minor axis)} (btm), for the mid-layer layer velocity.

SEASONALLY AVERAGED FIELDS

Bottom Velocity

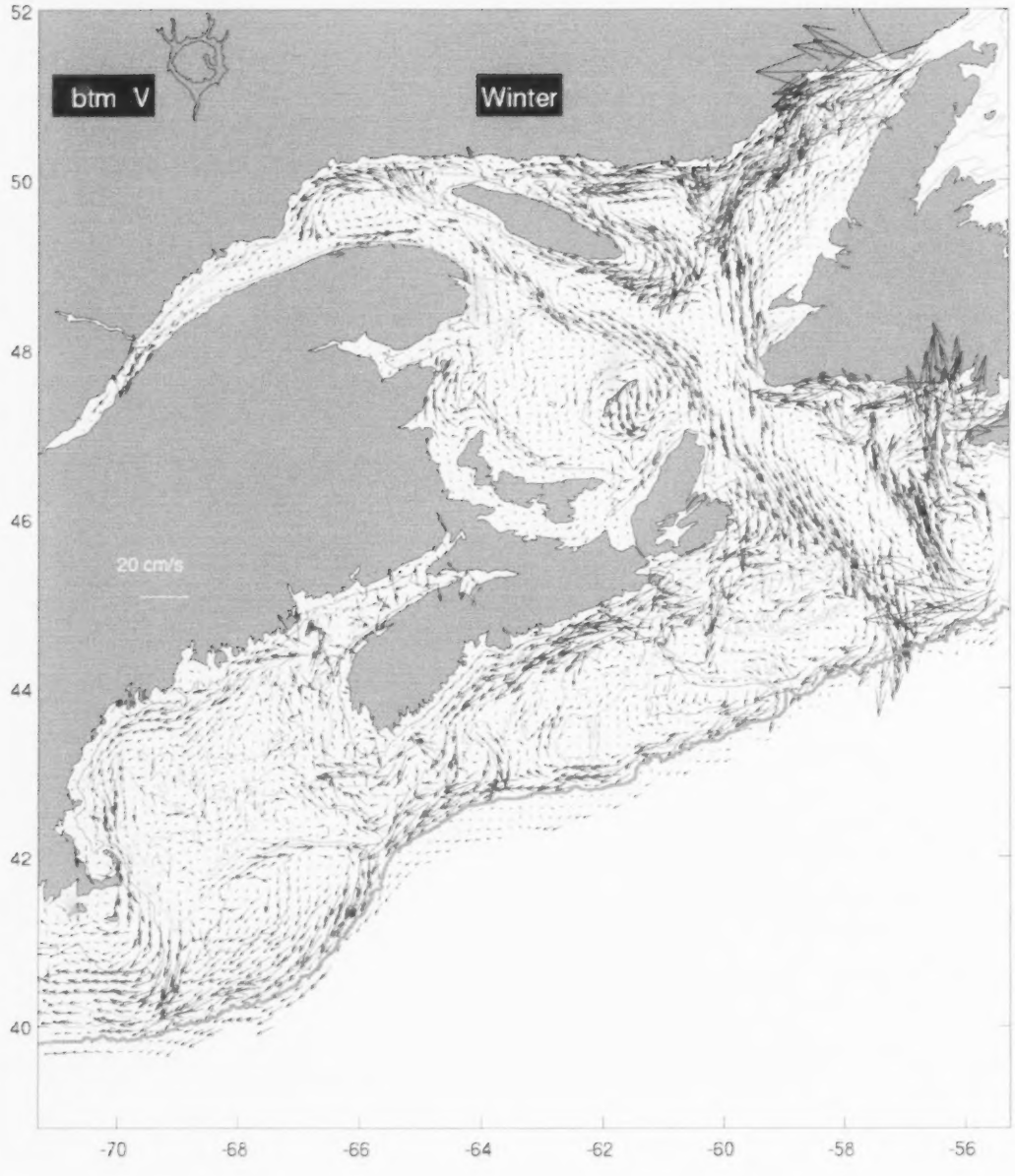

Figure 45: Winter bottom layer velocity.

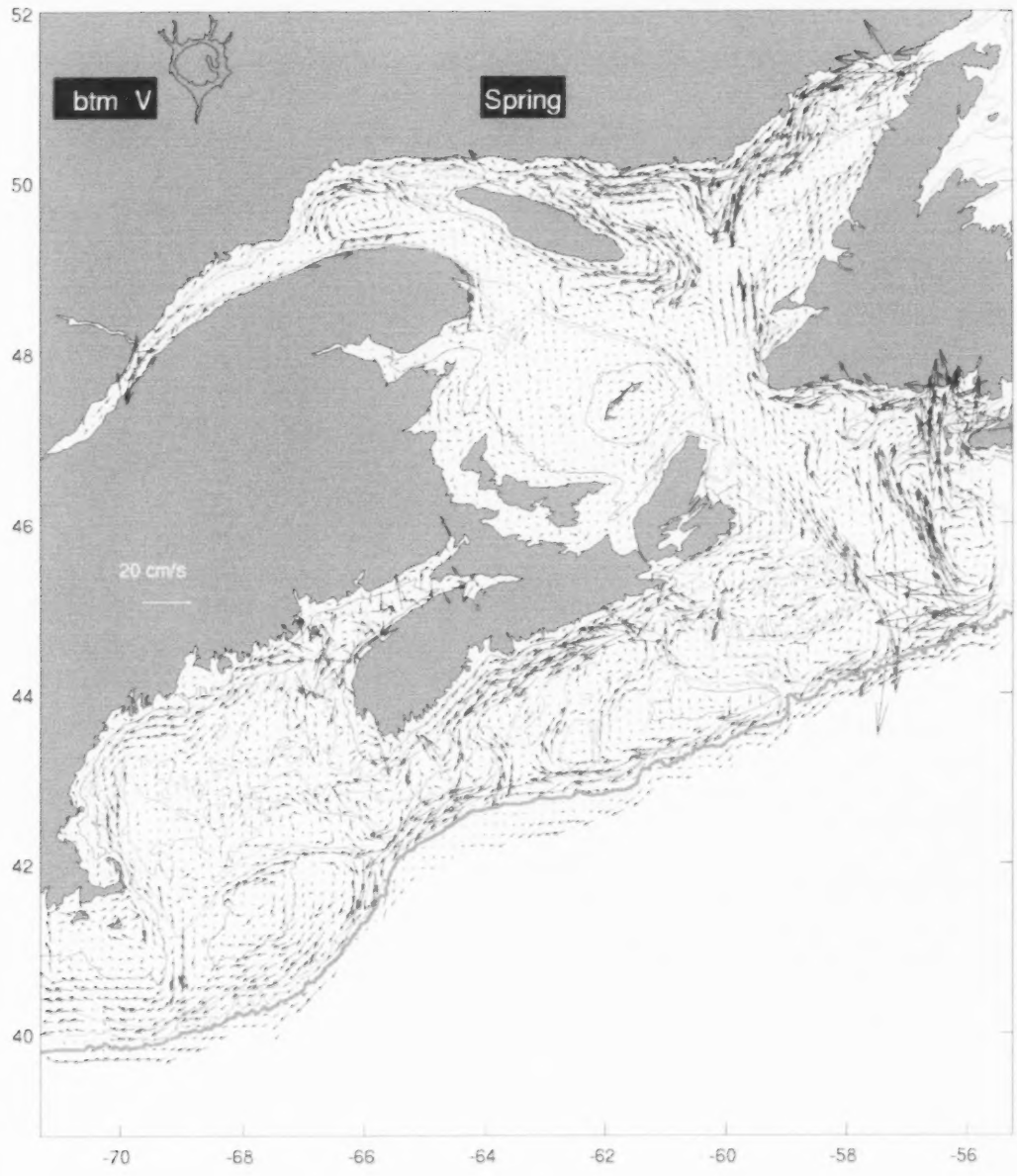

Figure 46: Spring bottom layer velocity.

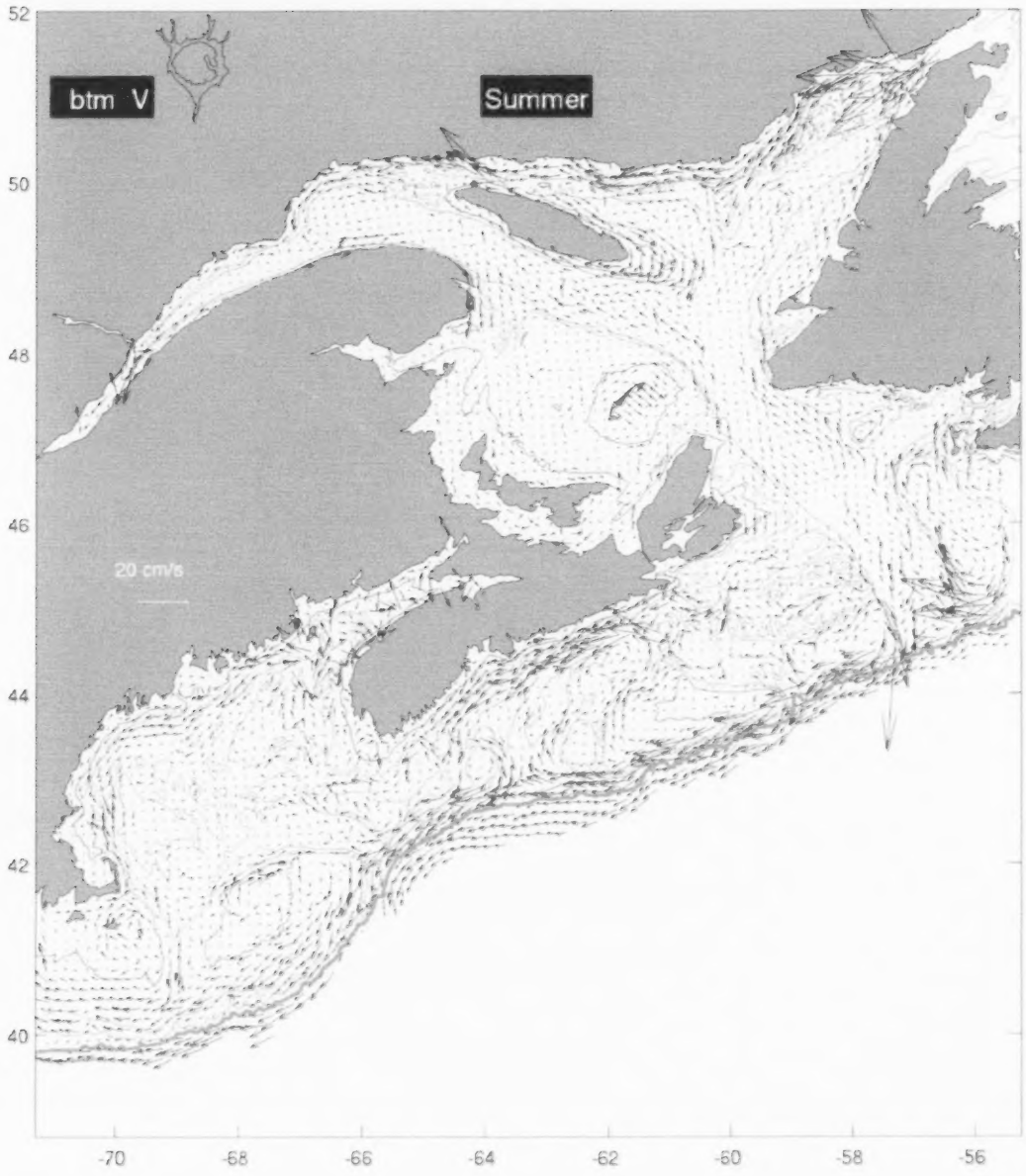

Figure 47: Summer bottom layer velocity.

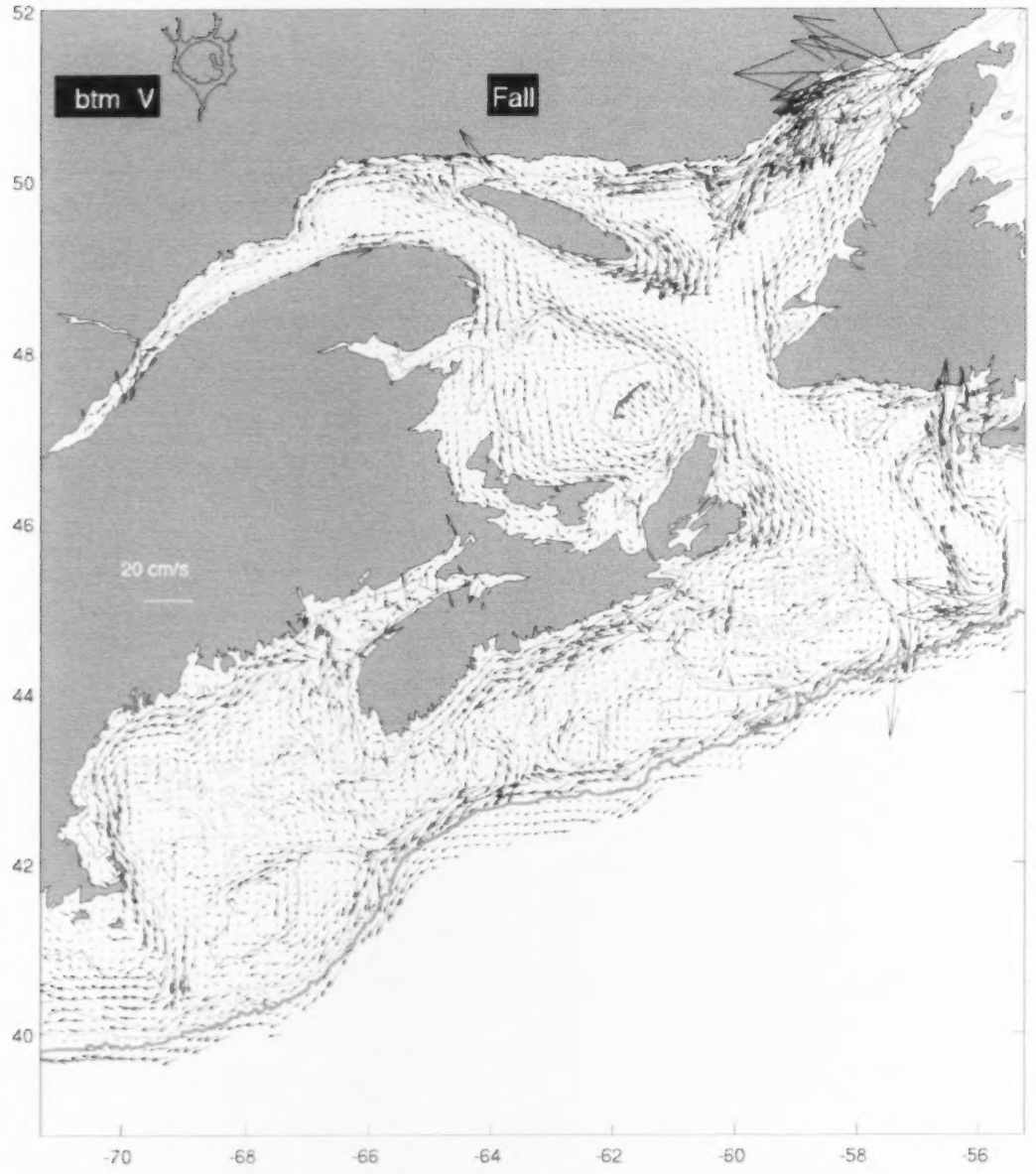

Figure 48: Fall bottom layer velocity.

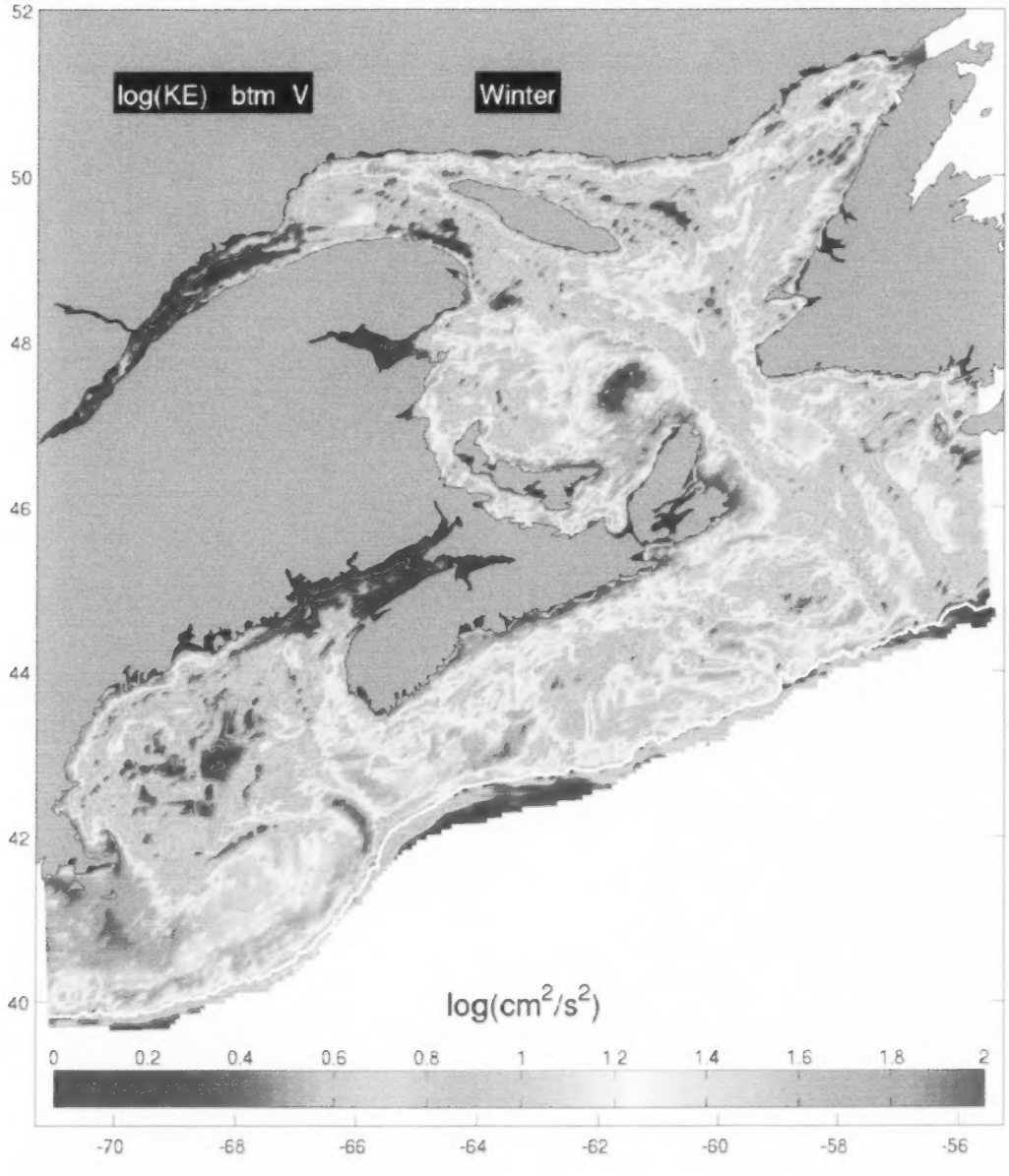

Figure 49: Winter perturbation log(kinetic energy (cm^2/s^2)) for the bottom layer velocity.

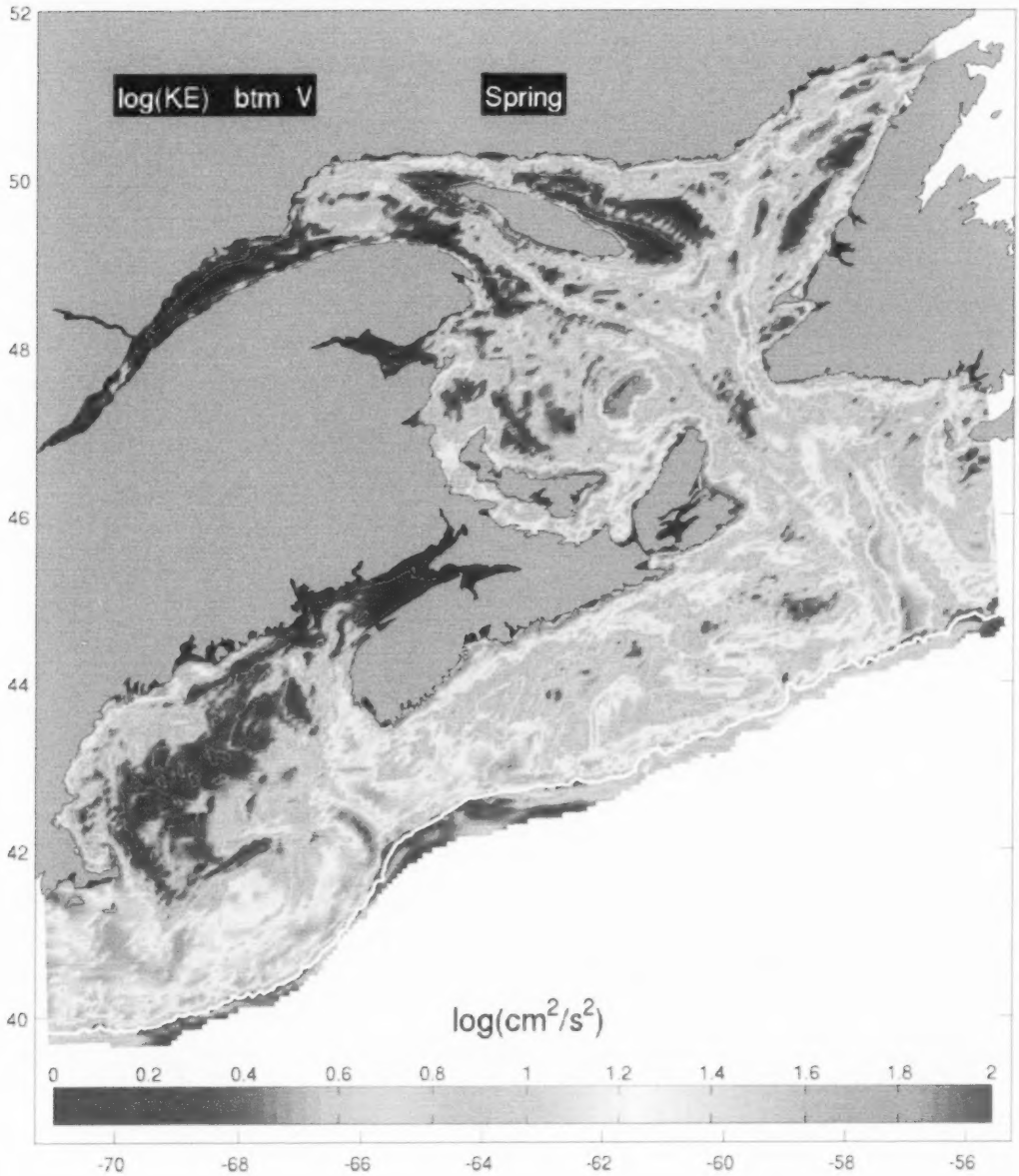

Figure 50: Spring perturbation log(kinetic energy (cm^2/s^2)) for the bottom layer velocity.

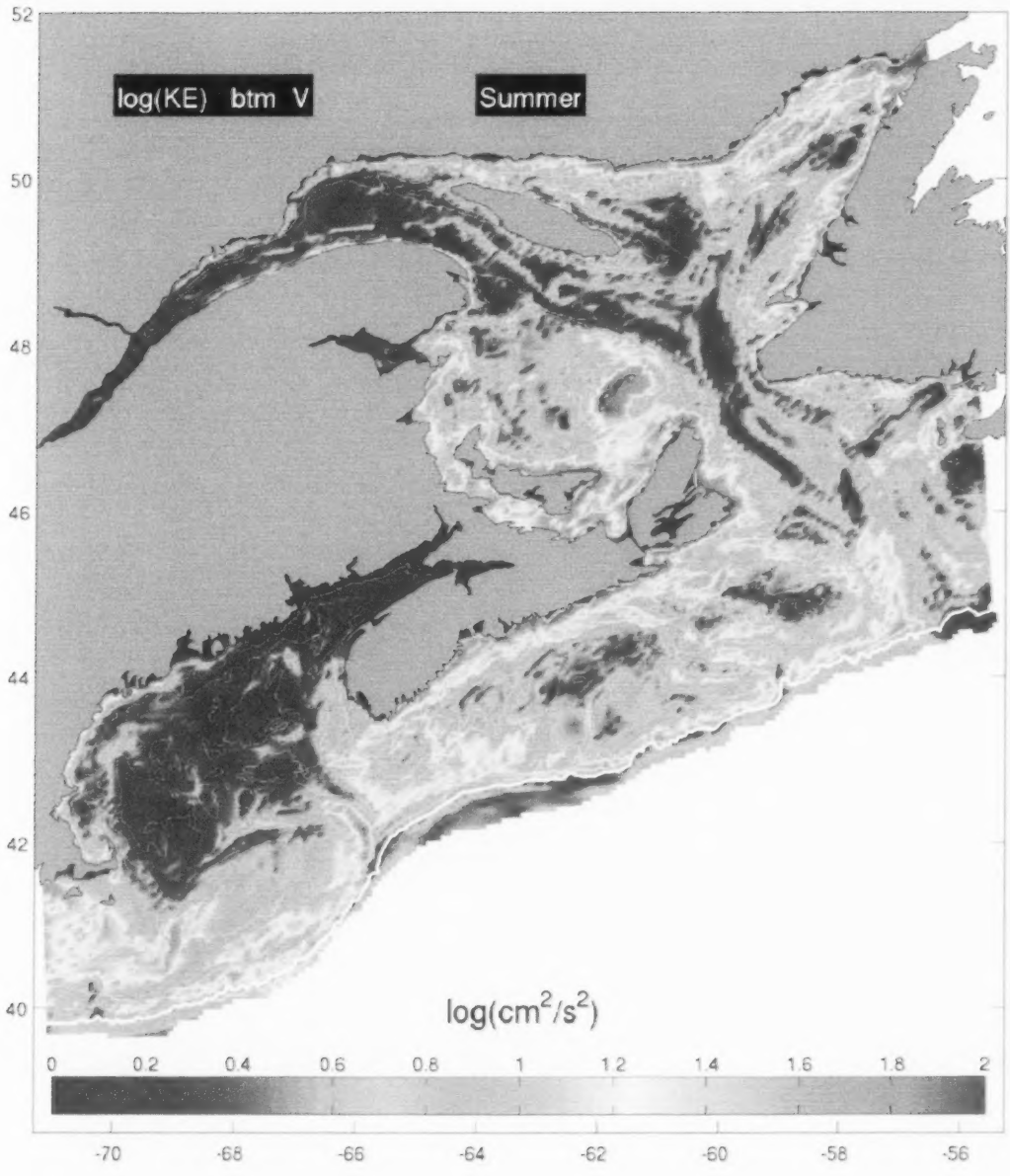

Figure 51: Summer perturbation log(kinetic energy (cm^2/s^2)) for the bottom layer velocity.

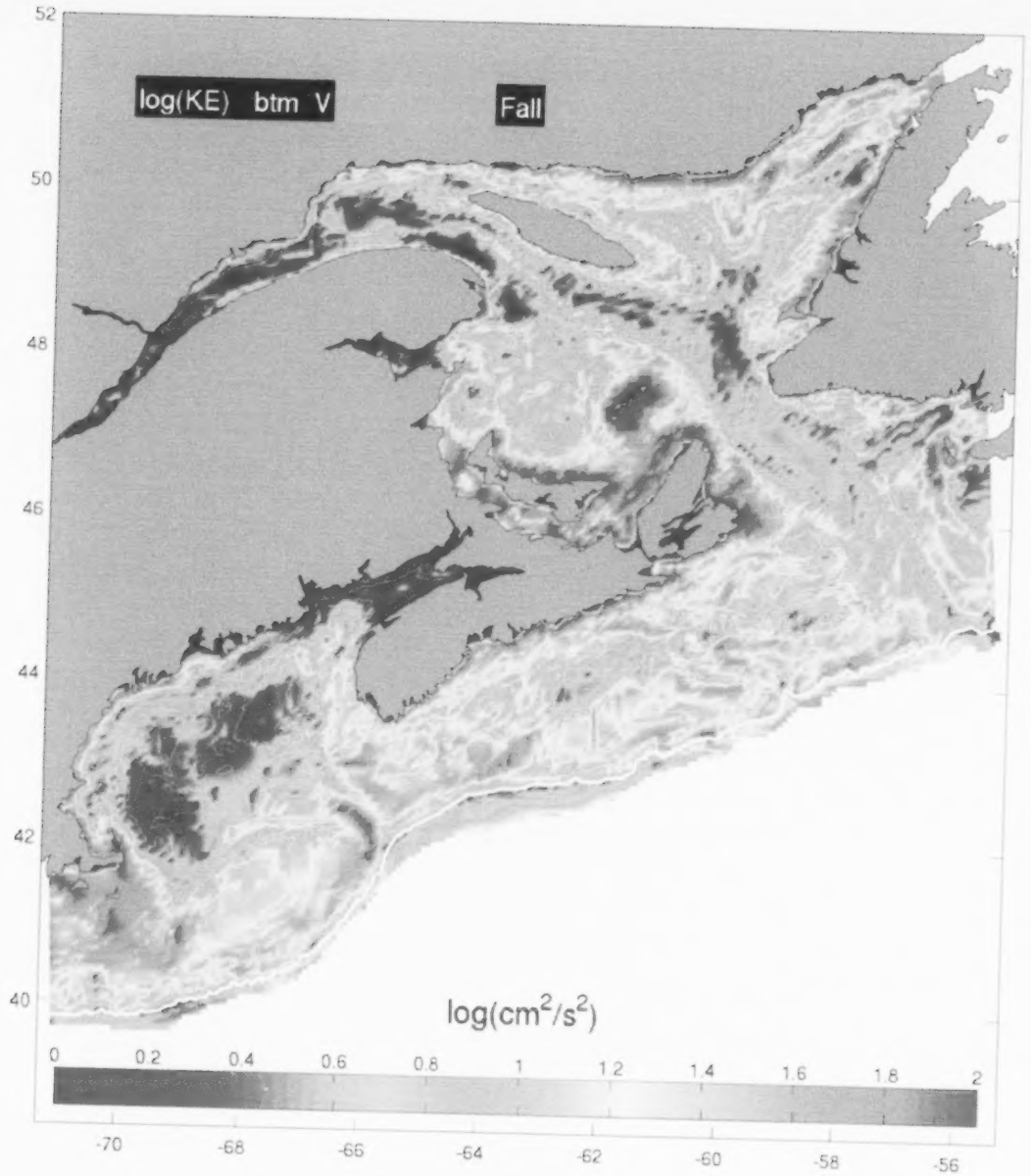

Figure 52: Fall perturbation log(kinetic energy (cm^2/s^2)) for the bottom layer velocity.

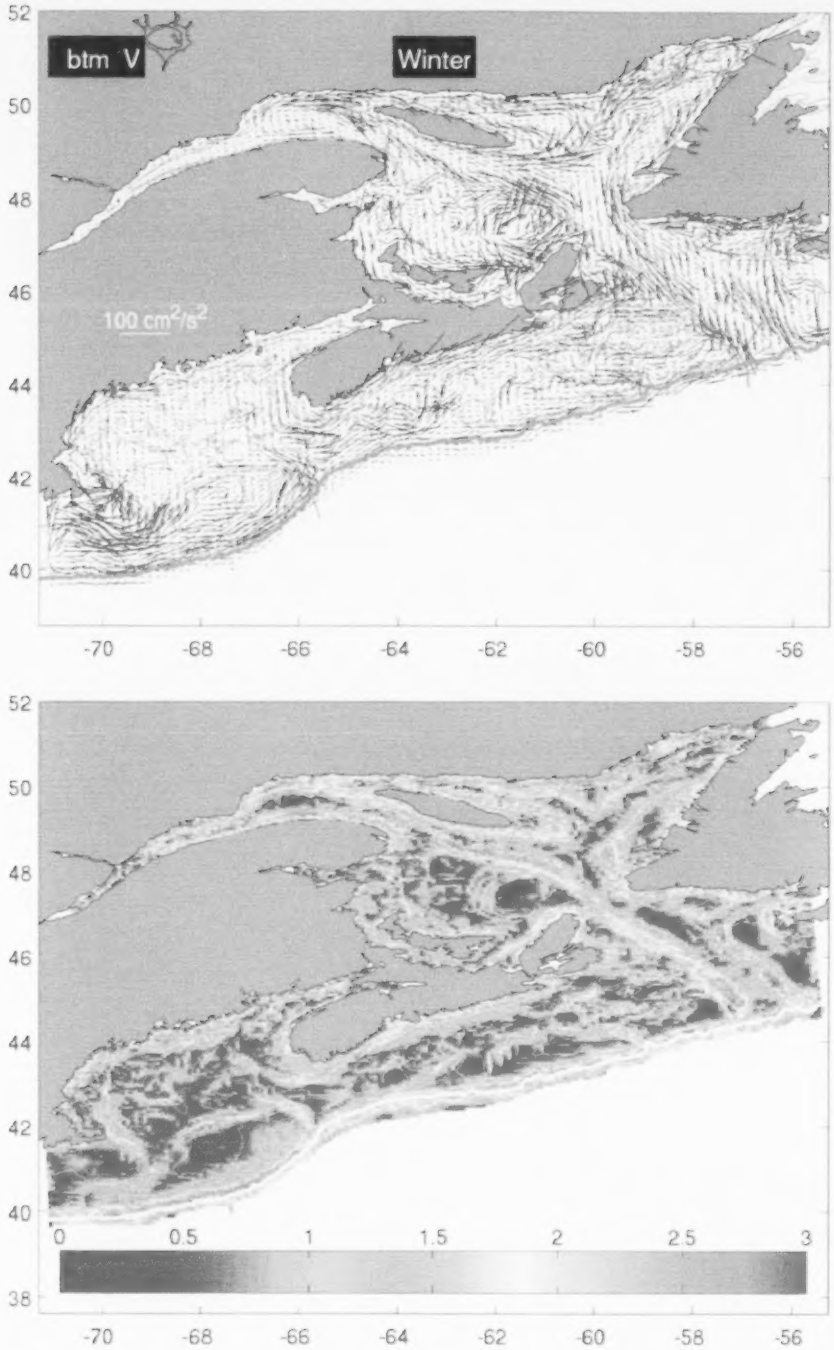

Figure 53: Winter major axes of variation (cm^2/s^2, top) and log{(energy in major axis) / (energy in minor axis)} (btm), for the bottom layer velocity.

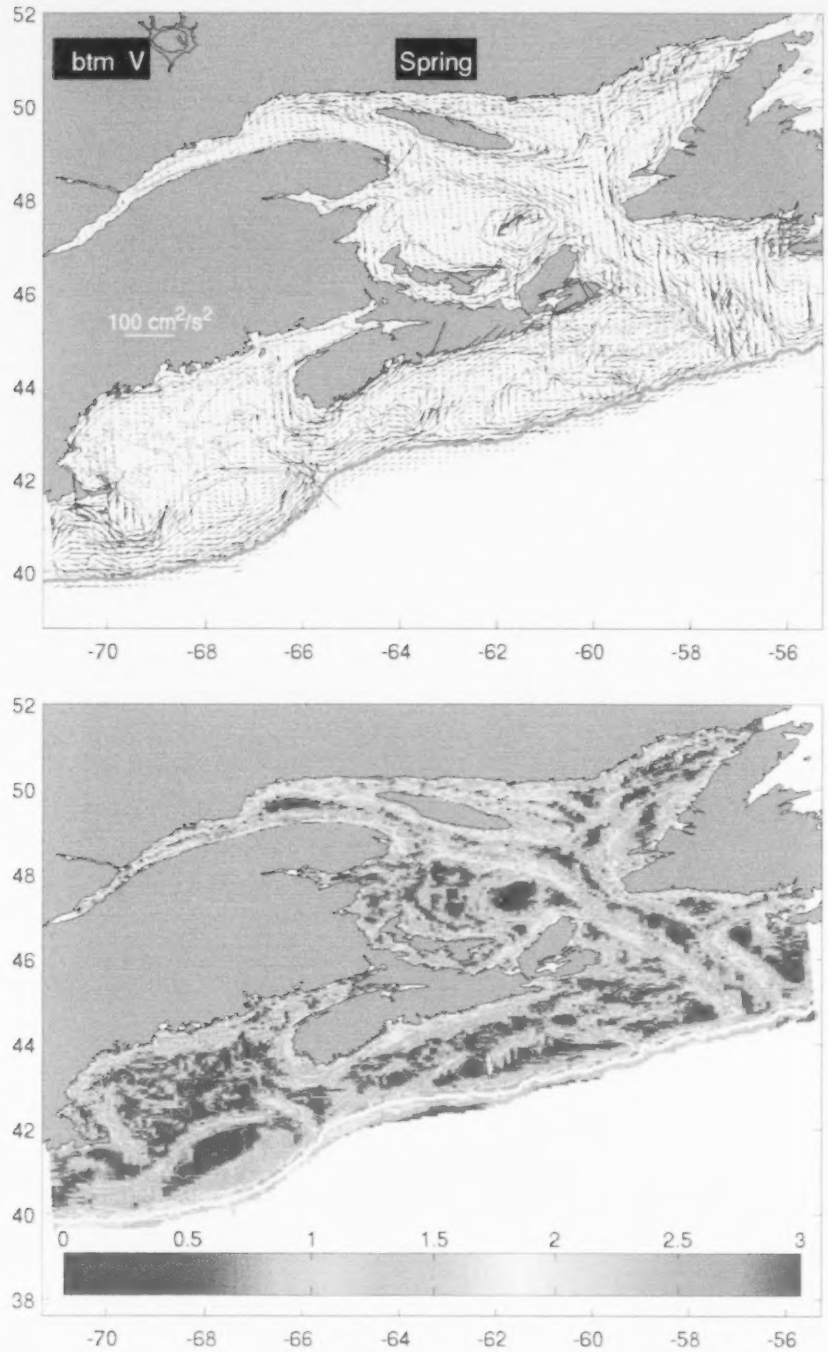

Figure 54: Spring major axes of variation (cm^2/s^2, top) and log{(energy in major axis) / (energy in minor axis)} (btm), for the bottom layer velocity.

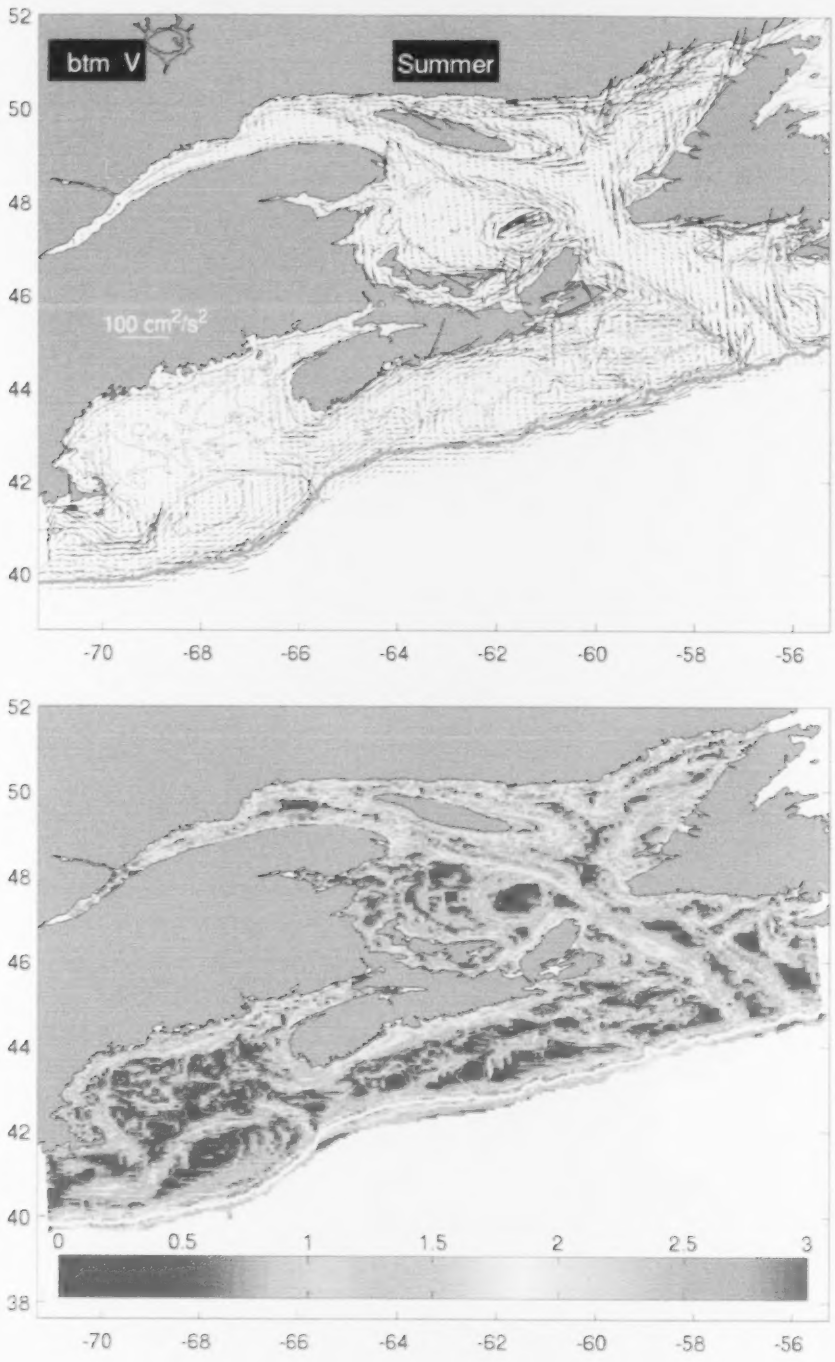

Figure 55: Summer major axes of variation (cm^2/s^2, top) and log{(energy in major axis) / (energy in minor axis)} (btm), for the bottom layer velocity.

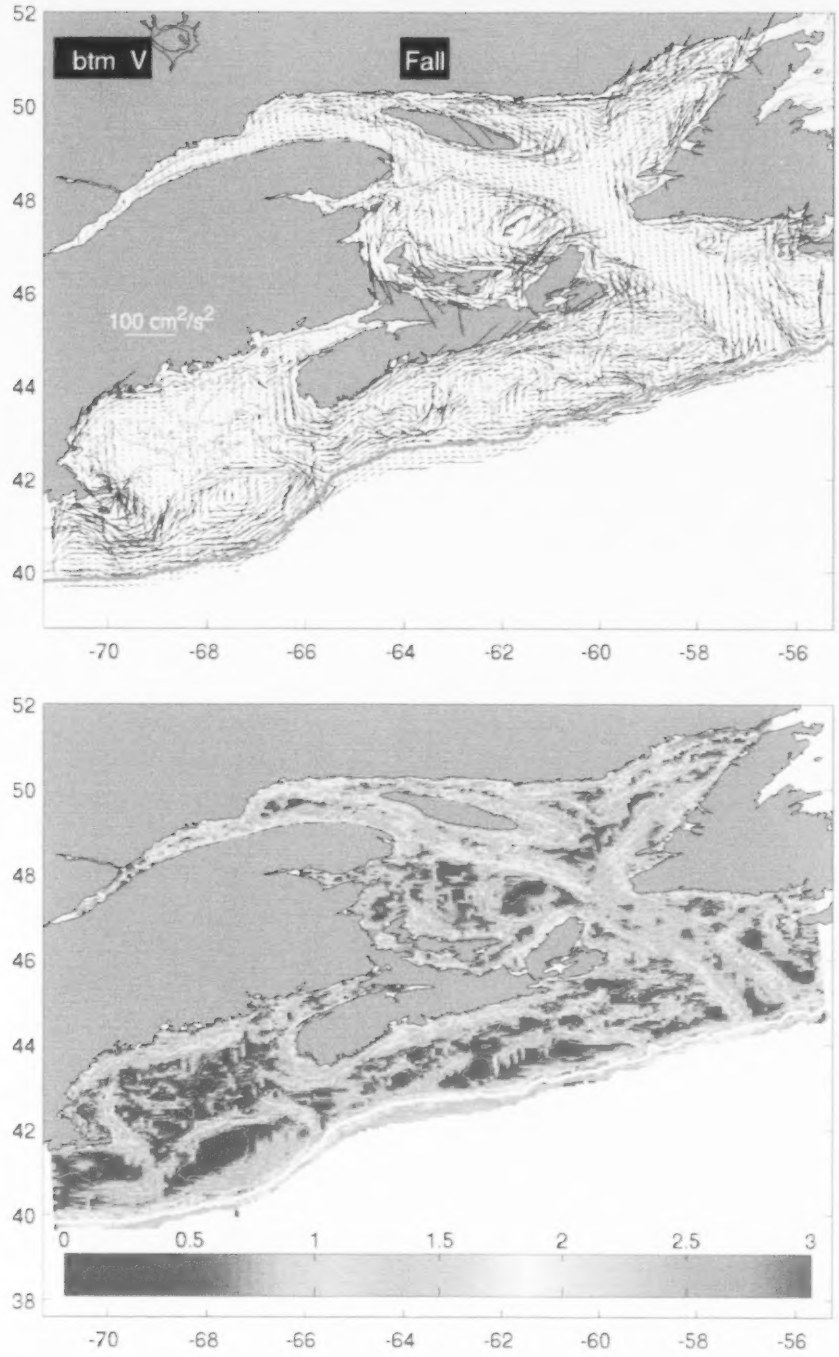

Figure 56: Fall major axes of variation (cm^2/s^2, top) and log{(energy in major axis) / (energy in minor axis)} (btm), for the bottom layer velocity.